POST-SYNTHETIC DNA-FUNCTIONALIZATION BASED ON DNA-TEMPLATED DYNAMIC CHEMISTRY

Dissertation

zur Erlangung des mathematisch-naturwissenschaftlichen Doktorgrades
"Doctor rerum naturalium"
der Georg-August-Universität Göttingen

im Promotionsprogramm: CaSuS
der Georg-August University School of Science (GAUSS)

vorgelegt von
Zeynep Kanlidere
aus Ankara

Göttingen, 2015

Betreuungsausschuss

Prof. Dr. Ulf Diederichsen	*Institut für Organische und Biomolekulare Chemie Georg-August-Universität Göttingen*
Prof. Dr. Lutz Ackermann	*Institut für Organische und Biomolekulare Chemie Georg-August-Universität Göttingen*
Prof. Dr. Philipp Vana	*Institut für Organische und Biomolekulare Chemie Georg-August-Universität Göttingen*

Mitglieder der Prüfungskommission

Referent

Prof. Dr. Ulf Diederichsen	*Institut für Organische und Biomolekulare Chemie Georg-August-Universität Göttingen*

Korreferent

Prof. Dr. Lutz Ackermann	*Institut für Organische und Biomolekulare Chemie Georg-August-Universität Göttingen*

Weitere Mitglieder der Prüfungskommission

Prof. Dr. Claudia Höbartner	*Institut für Organische und Biomolekulare Chemie Georg-August-Universität Göttingen*
Prof. Dr. Hartmut Laatsch	*Institut für Organische und Biomolekulare Chemie Georg-August-Universität Göttingen*
Dr. Alexander Breder	*Institut für Organische und Biomolekulare Chemie Georg-August-Universität Göttingen*
Prof. Dr. Philipp Vana	*Institut für Organische und Biomolekulare Chemie Georg-August-Universität Göttingen*

Tag der mündlichen Prüfung: 15.04.2015

This work was supported by the *Ministry for Science and Culture of the State of Lower Saxony* via the International PhD program Catalysis for Sustainable Synthesis (CaSuS) at the Georg-August-University Goettingen.

The work described in this doctoral thesis has been carried out under the guidance and supervision of Prof. Dr. Ulf Diederichsen at the Institute for Organic and Biomolecular Chemistry of the Georg-August-University Goettingen between October 2010 and April 2015.

I like to thank Prof. Dr. Ulf Diederichsen for the opportunity to work on interesting research topics within his group, his generous support and guidance as well as the freedom of research.

to my family

CONTENTS

1 FUNCTIONAL DNA IN SCIENTIFIC RESEARCH

DNA (deoxyribonucleic acid) besides being the genetic material of living organisms has arisen as a very important macromolecule in various fields of science due to its noteworthy properties. The reason for using DNA in applications lies in its self-assembly potential through hydrogen bonding between nucleobases and its well-defined, predictable topology. The preparation of DNA for scientific purposes requires chemical modifications on its native structure. The ability to rapidly synthesize any desired DNA sequence by automated solid-phase methods makes it possible to prepare chemically modified oligonucleotides. This chapter gives firstly an overview of the structure and properties of natural DNA followed by outlining the application of DNA as a versatile molecule in different fields of science. Finally, the possible chemical modifications in order to bring new functions to DNA are discussed. The modifications on the backbone of the oligonucleotides are extensively emphasized.

1.1 THE STRUCTURE AND FUNCTION OF DNA

The structure of DNA was discovered and published in 1953 with a great impact in biology by R. FRANKLIN, M. WILKINS, J. WATSON and F. CRICK.[1] This pioneering work led using DNA in various applications, more importantly in the field of molecular biology in initial phase. The defined structure of DNA is composed of two heteropolymer strands which are coiled around a common axis in an antiparallel fashion in the form of a double helix. Individual single strands consist of four different monomeric units which are termed as nucleotides. Each nucleotidic unit is composed of a sugar, a heterocyclic base and a phosphate group (Fig. 1a). Furthermore, the heterocyclic bases can be classified into pyrimidine derivatives (thymine **T** and cytosine **C**) and purine derivatives (adenine **A** and guanine **G**) (Fig. 1b). The nucleotide monomers are linked to each other by phosphodiester bonds between 3'- hydroxyl group (3'- OH) of the one nucleotide and 5'- hydroxyl group (5'- OH) of the adjacent one to form the sugar-phosphate backbone. The sugar-phosphate backbone is on the outside and the bases lie on the inside of the helix. The two single strands of the double helix are held together through hydrogen bonding between nucleobases and π-π stacking interactions between base-pairs.

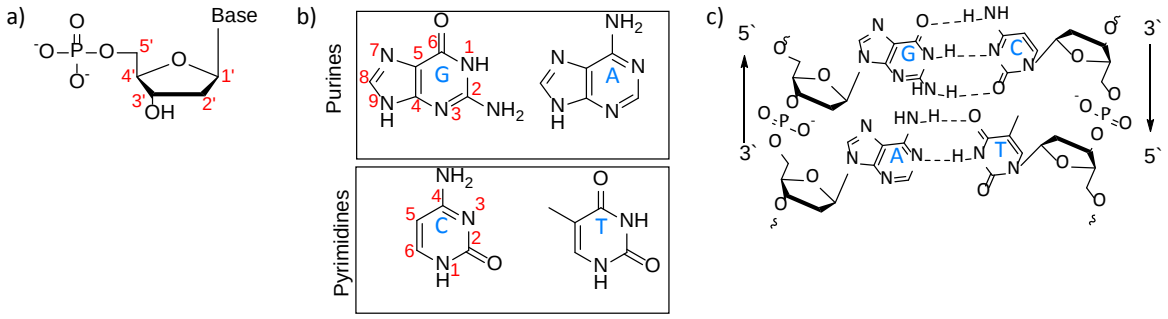

Figure 1: Building blocks of nucleic acid. a) Structure of the nucleotide monomers, 2'-deoxyguanosine **dG**, 2'-deoxyadenosine **dA**, 2'-deoxythymidine **dT**, 2'-deoxycytidine **dC**. b) Structure of four natural DNA nucleobases, Guanine **G**, adenine **A**, thymine **T**, cytosine **C**. c) Watson-Crick base-pairing in an antiparallel fashion.

The hydrogen bonded base-pairs that stabilize DNA double helix is termed as Watson-Crick base-pairing. The base-pairing process occurs in a specific manner such that the guanine residue on one strand always pairs with cytosine on the other strand and likewise the adenine residue always pairs with the thymine residue. There are three hydrogen bonds in GC base-pairs and two hydrogen bonds in AT base-pairs (Fig. 1c). This pairing of nucleobases is known as complementary base-pairing and the two single strands are complementary to each other. Thus, Watson-Crick paring is specific, predictable and enables self-assembly of complementary strands.

Apart from hydrogen bonding, the double helix is largely stabilized by stacking interactions between π-orbitals of the planar aromatic rings of the bases.[2,3] Hydrophobic and electrostatic interactions lead to the stacking interactions. The overall stability of the double helix is significantly conserved by stacking. The factors behind stacking such as hydrophobicity, stacking area, polarisability of the bases, overall dipole moment and overlap between bases contribute to an increase in the double helix stability.[4–6]

1.1.1 Replication and Protein Synthesis as DNA-Templated Reactions

The DNA macromolecule is the carrier of the genetic information in all living cells. The genetic information is coded in the sequence of the heterocyclic bases. Before cell division, DNA transfers this information to a copy of itself in a process known as DNA replication. The mechanism for this great task is provided by its highly ordered double helix structure. After the discovery of the DNA double helix it was realized that the process of DNA replication involves a templated synthesis. During DNA replication, the double helix structure is unzipped and unwound. This provides two partially single strands where the bases are exposed to the surroundings. The both unwound strands act as template for the preparation of two new daughter strands. Each incoming free deoxynucleotide triphosphate (dNTP) pairs through hydrogen bonding with its complementary base on the original unwound template strand (Fig. 2). As the dNTP pairs with its complementary base, its nucleophilic 3'-OH group reacts with the 5'-(α) phosphate of an incoming dNTP and the DNA chain grows. An enzyme, *DNA polymerase*, catalyzes the phosphodiester formation reaction but only if the base of the incoming dNTP is complementary to the base on the template strand.

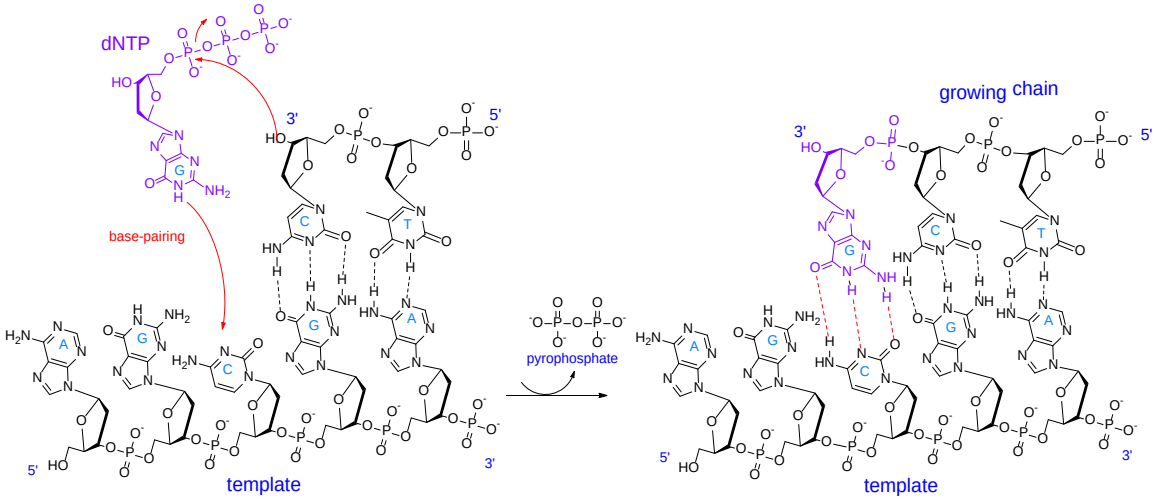

Figure 2: Model representation of DNA replication. Nucleotide triphosphates (dNTP) are monomers of DNA polymerization reaction and compose of a deoxyribose sugar, three phosphates and one of the four nucleobases. Each nucleotide is selected through base-pairing and joined together from 5'- to 3'- direction as shown on the upper strand.

Thus, DNA polymerase is a template-directed enzyme that synthesizes a product with a base sequence complementary to that of the template. The new strands are synthesized in 5'- to 3'-direction.[7]

Template-directed reaction also takes place in protein synthesis which is the second fundamental task of DNA. There are two main stages in the production of proteins; transcription and translation. Transcription is responsible for transferring the genetic information coded in DNA into an RNA molecule. In the transcription process part of the DNA double helix is unzipped which is aided by an enzyme. Once the DNA is unwound, the bases are exposed and can be used as a template for the formation of mRNA, analogous to DNA replication process. Once the DNA bases are exposed, free ribonucleotide triphosphates (rNTP) can bind to the exposed DNA bases by complementary base-pairing. RNA polymerase catalyses the formation of hydrogen bonds between the complementary DNA-RNA bases, as well as catalysing the growth of the RNA strand. The free rNTP are converted to ribonucleotide monophospates (rNMP) as they are added to the growing RNA molecule. The pyrophosphate side product is again formed during mRNA formation. The second stage of protein synthesis translates the genetic code contained in mRNA to build amino acid chains which are subsequently used in the formation of proteins.

1.2 USING DNA IN SCIENCE AND TECHNOLOGY

Beside its traditional importance in life, DNA has become an attractive macromolecule in scientific research due to its outstanding properties. (*i*) *Self-assembly*: Two single stranded oligonucleotides (both complementary to each other) in solution assemble spontaneously into double helical structure through specific base-pairing. (*ii*) *Geometry and Topology*: DNA has a very predictable geometry and well-stacked antiparallel double helix structure due to base-pairing rule. The outer diameter of the helical structure of B-DNA (the width of DNA) is 2 nm. The individual base-pairs are stacked with a distance of 0.34 nm and one helical turn is 3.4-3.6 nm.[8,9] Geometry of double helix depends on the properties of the solution such as salt and organic solvent concentration. The DNA double helix can form conformations other than B-DNA such as A- or Z-DNA. Besides forming a double helix, DNA assembles to more complex tertiary structures as well. DNA is able to fold into three-dimensional structures. For instance a single stranded DNA after 150 bp starts to behave as a worm-like polymer chain. If its ends come to close proximity, they can bond together and form circular supercoiled DNA. The geometry and topology of DNA is controllable and programmable which is an useful tool for the construction of two- and three- dimensional nanostructures.[10]

DNA is initially used in biological applications such as hybridization probes, DNA linkers, primers for PCR technique, antisense or antigene therapy and fluorescent labeling.[11–14] It is also used for many interesting nonbiological applications. It has become a versatile molecule, particularly attractive in nanotechnology. This field of science aims to use self-assembly potential of DNA not only for formation of double helix but also for construction of highly structured materials from DNA.[8,15,16] Well-defined double helical structure can be precisely controlled and programmed for the design of DNA-based architectures. Applications of DNA as scaffold for preparing supramolecular arrays as sensors, computational element, molecular switches, nano-wires, nano-pictures have been reported elsewhere.[17,18] Apart from its applications in biology and nanotechnology scientists have recognized the potential of DNA in chemical applications.[19] Task of DNA in chemical reactions could be as a template or as a direct/indirect catalyst.[20–22]

The use of DNA for all above mentioned applications often requires changes in the chemical structure of natural DNA. If some functional organic or inorganic molecules are incorporated into DNA with fluorescent,[23] electrical and magnetic[24,25] and/or metal ion binding properties, it might adopt a completely new structure and new function beyond its limits. In this manner functionalized DNA exhibit novel properties such as fluorescence emission, catalytic activity

and/or ability to carry metal ions. The utilization of DNA in a various fields of science has increased significantly with the development of automated DNA synthesis.

1.2.1 The Chemical Synthesis of Oligonucleotides

To synthesize oligonucleotides basically two different approaches are feasible: the enzymatic incorporation by DNA polymerases and the automated synthesis by DNA synthesizers (Fig. 3).

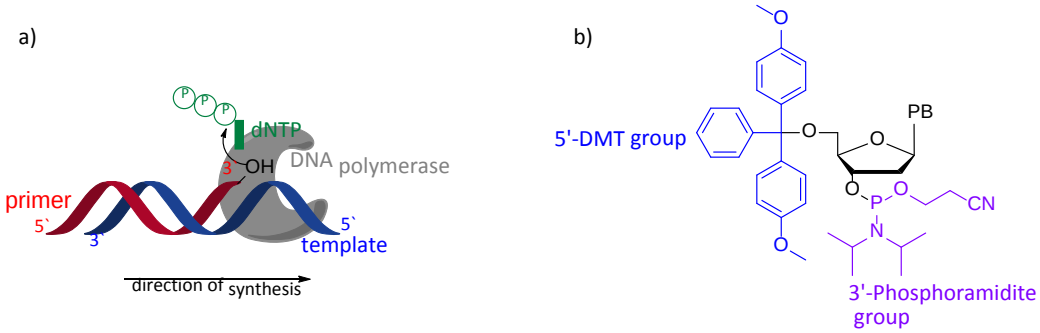

Figure 3: a) Schematic representation of polymerase chain reaction (or primer extension reaction). b) DMT-Protected phosphoramidite monomer which is necessary for the synthesis of oligonucleotides through automated DNA synthesizer. PB = Protected Base.

Enzymatic DNA synthesis by DNA polymerases

The enzymatic synthesis of DNA is termed as polymerase chain reactions.[26] In this process, the nucleotide monomers are applied as 5'-triphosphate derivatives. The DNA polymerase catalyses the template-directed elongation of the primer DNA strand by incorporation of nucleotides (Fig. 3a).

Automated DNA Synthesis by DNA Synthesizers

Nowadays it is possible to synthesize any desired sequence of oligonucleotide (up to approximately 100-nt) with or without modifications in moderate time and yield through DNA synthesizer. By DNA synthesizer, principally, the nucleoside monomers are sequentially coupled through phosphodiester linkage by elongating the oligonucleotide polymer which is bound on a solid support. For the synthesis of the oligonucleotides, first the monomeric building blocks are chemically synthesized and then the monomers are coupled via DNA synthesizer.

The natural nucleosides are not sufficiently reactive for a coupling reaction between two monomers to form a phosphodiester linkage. Therefore, the more reactive 3'- phosphoramidite derivatives (Fig. 3b) are used as building blocks for automated solid phase oligonucleotide synthesis.[27] 3'-OH of the nucleosides are converted to the more reactive *N*,*N*-diisopropylphosphoramidite group where the 5'-OH of the same nucleoside is protected by

using the acid labile 4,4'-dimethoxytrityl (DMT) group to prevent undesired reactions during the synthesis. Furthermore, exocyclic amino groups present on the nucleobases should also be protected; examples are acetyl (Ac) for cytosine, benzoyl (Bz) for adenine, dimethylformamide (Dmf) for guanine. Phosphoramidite monomers of unmodified natural nucleosides are commercially available whereas the nucleosides carrying the modifications need to be chemically synthesized.

Once the phosphoramidite derivative of the desired nucleoside with or without modifications is ready, it could be incorporated into the oligonucleotide through the automated DNA synthesizer.

1.3 CHEMICAL MODIFICATIONS OF DNA

Chemical modification of DNA represents the attachment of new functional molecules such as fluorescent dyes, intercalating agents, metal complexes or a displaceable leaving group at an appropriate section of the oligonucleotide. In initial studies, functional molecules were tethered to the 3'- or more commonly 5'- backbone ends.[28–33] In addition to 3'- and 5'- ends, the functional molecules can also be introduced within the strand.[34] A monomeric unit of an oligonucleotide composed of a sugar, a nucleobase and a phosphate backbone, each of these parts could be used for modification (Fig. 4).[35–38]

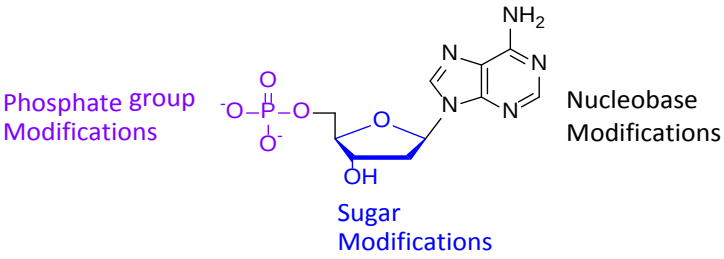

Figure 4: Chemical modification sites of a nucleotide monomer; on nucleobase, on sugar moiety or on phosphate groups.

1.3.1 MODIFICATIONS ON NUCLEOBASES

The modifications on nucleobases can be placed at pre-determined positions in helically structured duplexes. When the functional molecule is aimed to be placed in the major groove of the double helix C-5 of a pyrimidine base or C-8 of a purine base are sites of choice (Fig. 5a, b).[39,40] C-7 Modified 7-deazapurine analogs are also possible for modifications pointing towards the major groove. (Fig. 5c).[41] Modifications at these positions do not disturb Watson-Crick base-pairing. Modification is not only the attachment but also can be removal of a complete nucleobase moiety. Nucleobase moieties have been replaced with unnatural molecules such as simple heterocycles, hydrocarbons, metal-binding ligands or shape mimics of nucleobases, as shown in Figure 5d.[42]

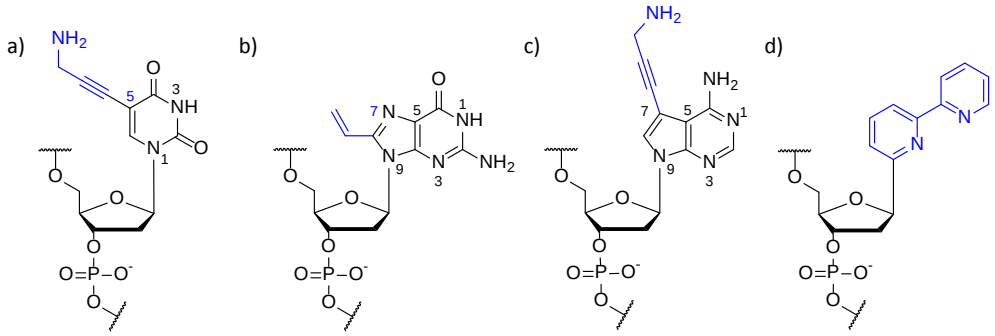

Figure 5 : Selected modifications on different labeling positions on nucleobases for internal modifications. a) Thymidine analog with new functional group on nucleobase C-5 position.[39] b) Guanosine analogue with new functional group on nucleobase C-8 position.[40] c) 7-Deaza adenosine analogue with new functional group on nucleobase C-7 position.[41] d) Ligandoside where nucleobase moiety is completely replaced with a metal-binding ligand.[42]

1.3.2 Modifications on Sugar Moiety

Modifications on the sugar moiety by varying the substituents generate oligomers which are containing sugars other than deoxyribose. There are different possibilities for covalent modifications of the sugar. The ribose ring has a free site at C-2' position at which different moieties can be attached (Fig. 6a). C-2' Position of the sugar moiety is suitable when a structural modification in the minor groove is desired.[34,43] The utilization of ribose instead of deoxyribose is easier for modification at C-2'.[44–47] Substitution of the oxygen in the ribose ring with sulfur and nitrogen or use of a hexose instead of pentose as sugar portion are examples for modifications to sugar moiety (Fig. 6b and c).[48]

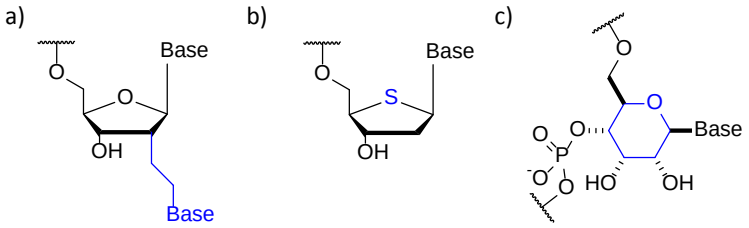

Figure 6: Selected modifications on sugar moieties by varying the substituents b) Modifications on C-2` position of a ribose which carry two bases.[46] b) Substitution of the oxygen atom on the ribose with a sulfur atom.[49] c) Use of a hexose instead of pentose as modifications.[48]

1.3.3 Modifications on Phosphate Group

Chemical modifications on the backbone can be performed by varying the substituent of the phosphate group of the nucleotide. Modification of the phosphodiester linkage is possible through automated DNA synthesis.[50] The phosphate group can be modified by replacing one of the oxygens with a different substituent (Fig. 7). The first chemically synthesized

oligonucleotides were methylphosphonates where the non-bridging oxygen was replaced with a methyl group at each phosphorous atom on the oligonucleotide chain (Fig. 7a). Although those oligonucleotides are highly stable in biological systems, the absence of charge on the backbone reduces its solubility. Methylphosphonate linkages are also inherently helix-destabilizing. Phosphorothioates where the non-bridging oxygen atom was replaced with a sulfur atom, are most widely used modified oligonucleotides because of their nuclease stability and their ease of synthesis (Fig. 7b). Another example of modifications on the phosphodiester linkage is the replacement of the oxygen at the 3' position on the ribose by an amine group for the formation of N3´→ P5´ oligonucleotides (Fig. 7d).

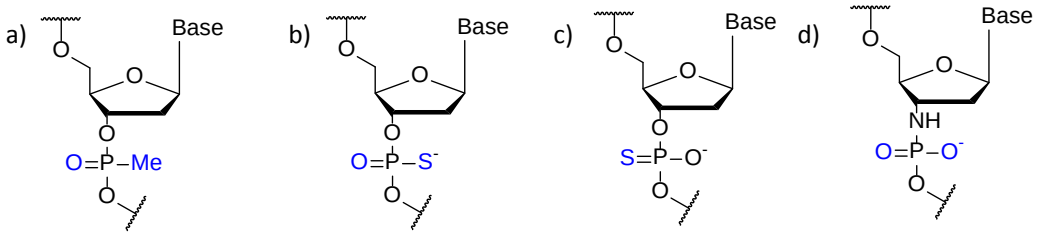

Figure 7: Selected modifications on phosphate group by varying the substituents. a) Metylphosphonate oligonucleotides.[51] b, c) Phosphorothioate oligonucleotides.[52] d) N3´→ P5´ oligonucleotides. [53]

1.4 Replacing the Sugar-Phoshate Backbone with Acyclic Scaffolds

Natural DNA has a D-(deoxy)-ribose phosphodiester backbone. The oligonucleotide modifications by varying the substituents on the sugar moiety or phosphodiester linkage have been mentioned in Chapter 1.4. The other approach for the modification on the backbone is altering the backbone topology through acyclic scaffolds in order to create novel informational oligomers with a completely new artificial backbone (Fig. 8).

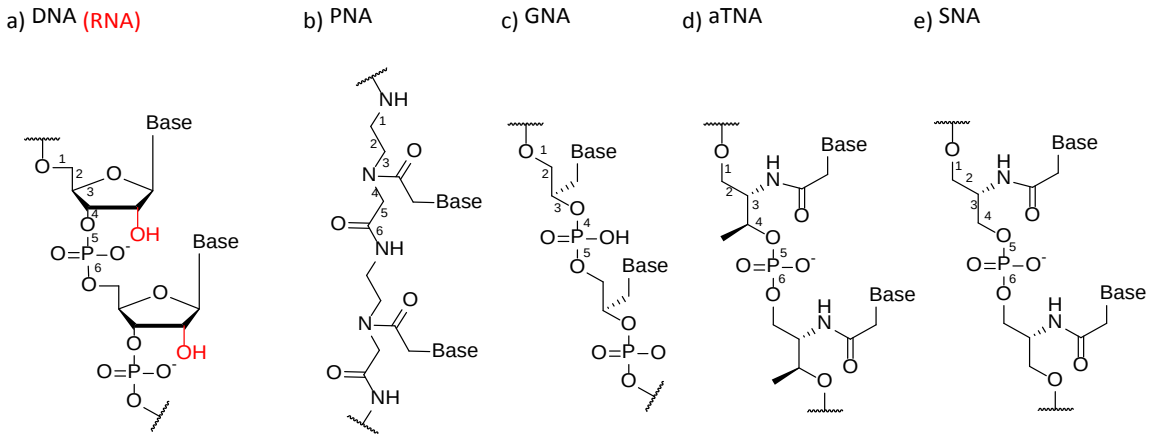

Figure 8: Chemical structures of nucleic acid analogs synthesized from acyclic scaffolds. a) Deoxyribonucleic acid **DNA**; b) Peptide nucleic acid **PNA**; c) Glycol nucleic acid **GNA**;[54] d) Acyclic threoninol nucleic acid **aTNA**;[55] e) Serinol nucleic acid **SNA**.[56] Numbers were assigned in order to show six bonds in the backbone for one repeat of **DNA**, **PNA**, **aTNA** and **SNA**; five bonds in the backbone for **GNA**.

The sugar-phosphate backbone can be completely replaced with a non-natural acyclic linker for example a peptide linker while keeping the nucleobases in the case of peptide nucleic acids (PNAs).[57] PNAs are artificial nucleic acids with an acyclic and uncharged backbone. The sugar-phosphate backbone was replaced by a *N*-(2-aminoethyl) glycine unit (Fig. 8b). The extremely high stabilities of PNA/PNA, PNA/DNA and PNA/RNA duplexes are due to the absence of electrostatic repulsion between the two strands because PNA has a neutral backbone.

Apart from PNA, the backbone of oligonucleotides can be altered by replacing the ribose unit with a non-natural acyclic linker but keeping the phosphate group (Fig. 8c,d,e).[58–61] The chemical structure of completely artificial oligonucleotides, glycol nucleic acids (GNA), acyclic threoninol nucleic acids (aTNA) and serinol nucleic acid (SNA) are shown in Figure 8. Acyclic scaffolds are alkyl-based diol linkers. Various acyclic scaffolds have been used so far which can be termed as C_2-, C_3- or C_n- scaffolds due to the number of carbon atoms between two hydroxyl groups (Fig. 9).[62–66] Amongst acyclic scaffolds, glycerol, serinol and threoninol as C_3-scaffold are

most frequently used ones because they possess three carbon atoms between two hydroxyl groups as in the D-ribose between 3'- and 5'- hydroxyl groups (Fig. 9).[61]

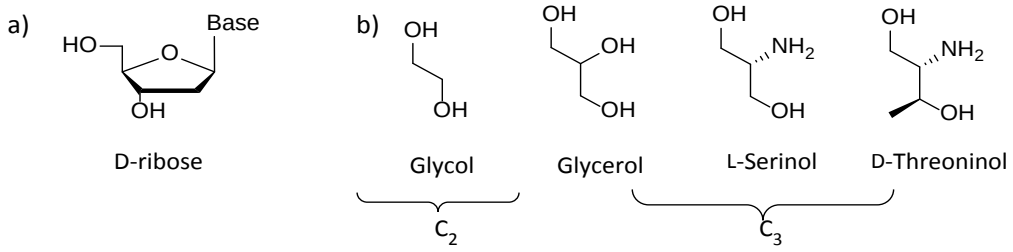

Figure 9: a) The native nucleoside is given for a better comparison. b) Acyclic diol linkers used in oligonucleotide backbone modifications. Glycol has two carbon atoms between its two hydroxyl groups (C_2-scaffold), whereas glycerol, serinol and threoninol have three carbon atoms similar to ribose of a native nucleoside (C_3-scaffold).

An acyclic glycol linker is used in order to synthesize GNA.[54,65] Nucleobases are tethered on the glycol linker and the two hydroxyl groups are converted into a phosphoramidite monomer which is compatible for utilization in an automated DNA synthesis. Likewise, aTNA is synthesized by using acyclic D-threoninol and SNA by using L-serinol as linear backbone.[56,67,68] Those oligonucleotide analogs have different solubility properties due to their individual backbone topology. They can recognize base-pairs with their complementary strands and have stacking abilities to form the double helical structure and some are more stable than natural DNA.[55] Although the glycol linker is more flexible than D-ribose, the GNA homoduplex found to be more stable than a DNA and RNA duplex.[55] Similarly homoduplexes of aTNA and SNA are more stable than DNA and RNA duplexes. The stabilities of homoduplexes are in the order of aTNA > PNA ≈ GNA ≥ SNA > RNA > DNA.[55]

The presence of two hydroxyl groups in acyclic scaffolds makes it possible for their conversion into the phosphoramidite monomer, thus they can be easily coupled to each other or to natural nucleotides using a DNA synthesizer. After any functional molecule or nucleobase is attached on the acyclic linker, this scaffold can be introduced at any position in the oligonucleotide sequence through the corresponding phosphoramidite monomer. By using more than one acyclic modification in the same strand, the introduction of different kinds of functional molecules in the sequence is also possible. The utilization of acyclic scaffolds lies not only in the preparation of completely modified backbones but also in selective modification at desired position. Figure 10 shows the backbone modifications as a result of incorporation of acyclic C_2-, C_3- or C_n- scaffolds in order to create a ribose-free site on the backbone. The ribose-free site can carry either a natural nucleobase or an unnatural functional molecule.

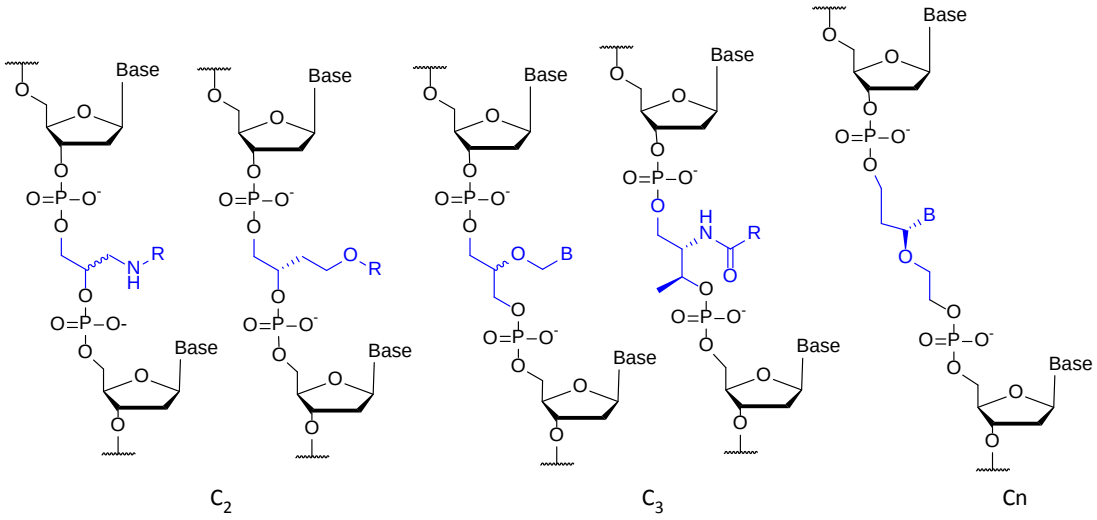

Figure 10: Backbone modified oligonucleotides with an acyclic scaffold. B: Nucleobase; R: Functional molecule.[61]

There are some advantages of utilizing acyclic scaffolds in comparison to utilizing nucleoside scaffolds in order to incorporate functional molecules into oligonucleotides. The corresponding phosphoramidite of acyclic scaffolds are easily accessible compared to nucleoside scaffolds. In some cases the ribose ring of nucleoside scaffolds is not suitable for attaching some functional molecules that would sterically hinder the formation of the desired modification and destabilize the duplex. Particularly in these cases, acyclic scaffolds are an efficient choice when there are synthetic obstacles to attach functional molecules on natural nucleoside.

1.5 POST-SYNTHETIC FUNCTIONALIZATION OF DNA

Modifications can be incorporated into oligonucleotides by DNA synthesis mainly by two approaches; direct incorporation and post-synthetic incorporation. With the direct approach the functional molecule is attached to the desired position of the nucleotide scaffold and then incorporated into DNA directly through the synthetic cycle as already described. Sometimes there are synthetic difficulties to prepare the corresponding phosphoramidite monomer of the unnatural molecule which is desired to be introduced into DNA. In this case the post-synthetic method is usually used. Furthermore, in some cases the incorporation of some functional molecules is incompatible with the oxidation step in DNA synthesis. In a post-synthetic approach, firstly, a nucleophilic reactive group is incorporated into oligonucleotide through the direct modification and then this reactive group is further functionalized with the desired molecule post-synthetically. The conventional reactive groups introduced before the post-synthetic approach are amines and thiol groups. Other approaches that have most widely used for post-synthetic functionalizations are Diels-Alder reaction[69], click chemistry[70] and Staudinger ligation[38].

The acyclic threoninol linker (Fig. 9, Chapter 1.4) is an efficient choice in order to incorporate amino or thiol functional groups into oligonucleotides. The presence of an amino or thiol group on the oligonucleotide enables the post-synthetic modifications. Threoninol whose amine is protected with an appropriate protecting group such as Fmoc or Alloc, can be introduced into oligonucleotides through the corresponding phosphoramidite monomer. After selective deprotection of the protecting group, a functional group with a carboxyl group or aldehyde group can be attached on the amine site of the oligonucleotide.[59] Likewise, a functional thiol group can be introduced into oligonucleotides as well, through the substitution of the amine group of threoninol with a thiol group.[71] Threoninol, carrying the protected thiol group, can be introduced into oligonucleotides through the phosphoramidite monomer. The formation of the reactive thiol group enables the post-synthetic modifications of oligonucleotides.

2 POST-SYNTHETIC FUNCTIONALIZATION OF DNA THROUGH DYNAMIC COMBINATORIAL CHEMISTRY

Two informational processes are fundamental to biological evolution. Firstly, the replication of the genetic information and secondly, transferring the information into functional molecules. These processes use DNA- or RNA-templates as source of information to encode its information into a new biopolymer. The desire to apply a similar process as Nature, chemists used DNA with templating property as an informational macromolecule for chemical synthesis of nonnatural nucleic acids in a process known as polymerase chain reaction (PCR). In Nature and in the PCR process, template-directed selection of nucleobase-carrying monomers and amplification for the generation of new oligonucleotides require the use of an enzyme. An alternative approach to translating the information into a new oligonucleotide analog relies on non-enzymatic template-directed polymerization. Recently, dynamic combinatorial chemistry (DCC) has been used in non-enzymatic template-directed reactions for the reversible assembling of new adaptive oligonucleotide analogs.[72] *Furthermore, DCC enables the formation of informational oligomers with backbones other than phosphodiester backbone.*

In this chapter firstly, the principles of DCC concept will be outlined and followed by a brief discussion on previous scientific studies related to template-directed synthesis of oligonucleotides and their analogs. The combination of template-directed reactions with dynamic combinatorial chemistry (DCC) for reversible functionalization of oligonucleotides is discussed. Finally, the approach of this study is given.

2.1 PRINCIPLES OF DYNAMIC COMBINATORIAL CHEMISTRY

Combinatorial chemistry (CC) is a useful tool particularly for drug discovery as well as in the development of new catalysts.[73,74] In contrast to conventional synthesis where starting materials **A** and **B** react to obtain one product **AB**, in combinatorial synthesis different variants of **A** (for example ten variants of A_1-A_{10}) react with different variants of **B** (B_1-B_{10}). Each substance reacts with all other reactants such that in a single synthesis step it is possible to prepare a large number of products. For example, ten reagents of **A** react with ten reagents of **B** to generate a library with hundreds of variants of product **AB** in a single combinatorial library (CL).[75] Whilst CC is a rapid synthesis method, much time and effort is necessary for the purification and analysis of individual products in the library. Each product in the library needs to be synthesized independently in order to identify and isolate a selected product. Although high-throughput screening techniques can accelerate these processes, still obstacles remain in combinatorial synthesis.[76]

Dynamic combinatorial chemistry (DCC) is a subset of CC that aims to simplify the screeining process by generating self-screening libraries. In contrast to CC, DCC uses reversible reactions between building blocks carrying the functional groups for the generation of the library (or dynamic combinatorial library, DCL).[77–79] Through the reversible reaction, there is a continuous exchange of building blocks and interconversion of library members. The composition of the library is determined by thermodynamic stability of each member. If a template molecule is added into the library that will bind to a specific member through noncovalent interactions and remove it from the pool. The ability of the template to select the specific product will greatly simplify the screening process. Furthermore, during the selection process, the product distribution of the library would undergo a change in order to adapt itself. The schematic representation of the concept behind DCC is shown in Figure 11.[77,80] The design of DCC represents three basic requirements: *(i)* The preparation of the initial building blocks, *(ii)* Generation of dynamic combinatorial library (DCL), *(iii)* Selection and Amplification**.**

Figure 11: The schematic representation of dynamic combinatorial chemistry (DCC). a) Initial building blocks carrying the functional groups; b) Dynamic combinatorial library (DCL) containing the all possible products formed by reversible reaction; c) The selection of the best-bound product through the template.(redrawn from [80])

2.1.1 THE PREPARATION OF THE INITIAL BUILDING BLOCKS

Design of building blocks needs to fulfill some important features. Firstly, they must carry appropriate functional groups such as an amine, thiol or aldehyde for a reversible exchange. The rest of the molecule should not carry other functional groups that will interfere with the chosen exchange reaction. Secondly, they should possess functionalities to aid molecular recognition with the template. The geometry of the building blocks must fit in potential target sites.

2.1.2 GENERATION OF DYNAMIC COMBINATORIAL LIBRARY (DCL)

The DCC process is based on a reversible exchange reaction. Exchange reactions used in DCL could include covalent reactions, noncovalent interactions and metal-ligand coordination. Reversible covalent reactions, although slower, form more stable products and are easier to analyze and isolate. An applied reversible reaction has to be compatible with the experimental conditions, such as pH, solvent and/or temperature at a defined time of the experiment. Various types of reversible reactions have been used so far for the covalent binding of initial building blocks in aqueous media including imine, thioester, acetal, disulphide, acylhydrazone formation.[77,81] Initial building blocks must be prepared with appropriate functional groups (such as aldehydes, amines, thiols) which allows the reversible exchange with one another due to the chosen reversible reaction. In a reversible DCC process there is a continuous formation and breaking of covalent bonds between the initial building blocks until the equilibrium is reached.[77,78,82,83] Once the equilibrium is reached all possible products of the system generate a dynamic combinatorial library (DCL).

Due to its reversibility, the dynamic library has an adaptive behavior against any change in the reaction conditions. The equilibrium can respond to external changes that results in

reorganization between the building blocks of the library in order to minimize the total free energy of the system. Thus, the proportions of the library members can be controlled by adjusting the reaction conditions and the equilibrium can be shifted towards the desired product. This flexible and adaptive nature of the dynamic library is the advantage over its static library.

The external changes can include altering the pH, temperature, electric field or adding/removing reactants, but the most exploited one is the addition of a template to encourage the formation of a particular product. The addition of a template into the reaction mixture, or so-called template-directed reactions, with the intention of selecting one specific product relies on molecular recognitions between the template and initial building blocks. Molecular recognition results from reversible non-covalent forces such as hydrogen bonding, electrostatic interactions, metal coordination, donor-acceptor interactions, and π-π stacking interactions. Behind molecular recognition there is also a dynamic character, reversible assembly/disassembly process. It is equilibrium-controlled and generates the thermodynamically most stable assembly.[84] Thus DCC is a combination of non-covalent self-assembly processes and reversible covalent formation. DNA has an important place as a template, due to the self-assembly and recognition potential through hydrogen bonding.

2.1.3 Selection and Amplification of the Best-binder

In a dynamic library at equilibrium, the addition of a template which binds selectively to one of the products (through molecular recognition) will result in a shift of the equilibrium towards this product. The concentration of this best bound product will be increased at the expense of the others. The desired molecule will be stabilized once trapped by the template, whereas the rest of the unbound products continue to be exchanged. That is a self-screening process and makes the isolation and identification of the desired molecule easier for DCC. One advantage of DCC over CC is the combination of the library generation and screening process in a single step. Furthermore, in order to obtain the desired product in high efficiency, the parameters of DCC can be changed such as the introduction of the right template, which is fitting to the structural properties of the desired product. Finally, all the possible products in the library must be separable by some spectroscopic or spectrometric technique.

2.2 DCC THROUGH REVERSIBLE IMINE FORMATION

Among the various reversible covalent reactions imine formation through condensation of aldehydes with amines has special interest because of its role in biological processes (Fig. 12). Imine bonds are ideal for DCLs because their formation are fast and reversible under physiological conditions.

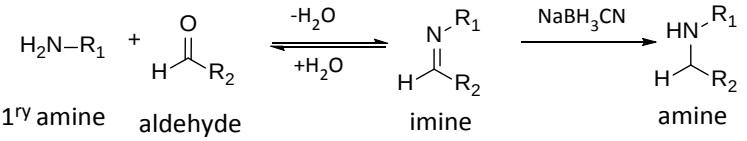

Figure 12: Reversible formation of imines from primary amines and aldehydes followed by the reduction of imines to amines by addition of sodium cyanoborhydride.

Imine bond formation involves the loss of H_2O so the addition of water to the imine product leads to hydrolysis and drives the equilibrium to the other direction leading to the formation of starting materials.[84] Most imine formation reactions are carried out in organic solvents in order to shift the reversible imine formation towards the condensation product. During imine formation water removal is necessary with diaryl or arylalkyl ketones, but aldehydes can usually be condensed with amines without removing water from reaction mixture.[83] Although the general features of imine formation are well understood, imine formation in water is limited.[85] Imine formation in the field of dynamic combinatorial chemistry is usually performed in aqueous organic mixtures[86] or aqueous solutions because reversibility is necessary for the generation of libraries of dynamic compounds.[87,88] Furthermore, the instability of imines in aqueous solution causes analytical and isolation problems within the DCC concept. The solution for this obstacle is the reduction of imine to amine by addition of sodium cyanoborhydride (Fig. 12).[89] Reductive amination is known to be compatible with templated synthesis and DCC in aqueous media.[90]

2.3 Application of DCC for Functionalization of Oligonucleotide Analogs

Dynamic combinatorial chemistry is mostly used as a tool for drug discovery processes in the search of new bioactive molecules with an affinity to biomacromolecules.[79,81,83,91–94] Recently, the DCC approach has been extended to the generation of new adaptive oligonucleotide analogs.[95] Oligomers of this type have been prepared by reversible coupling of monomeric units in the presence of a DNA (RNA or PNA as well) template. The selection of monomeric units (monomeric nucleotides or nucleobases) is directed by base-pairing between the template and the monomers. The transfer of the information coded in the nucleobase sequence of the template into the new assembled oligonucleotide analog represents a simple model to DNA replication. In contrast to Nature and enzymatic DNA polymerization in the PCR process, the templated replication using DCC is reversible, therefore, allows for error correction.

Template-directed synthesis of oligonucleotide analogs can be designed in two ways; backbone ligation and base-filling approaches.[21,96] (*i*) *Backbone ligation;* is the construction of the backbone of the oligomer from combination of either monomeric nucleotides or of short oligonucleotides (Fig. 13a). The coupling of suitably functionalized monomeric nucleotides can generate a new backbone other than native DNA backbone. (*ii*) *Base-filling*; is the addition of monomeric nucleobases to a pre-formed abasic backbone (Fig. 13b). The attachment of the nucleobases on the pre-formed backbone creates a new oligonucleotide analog.

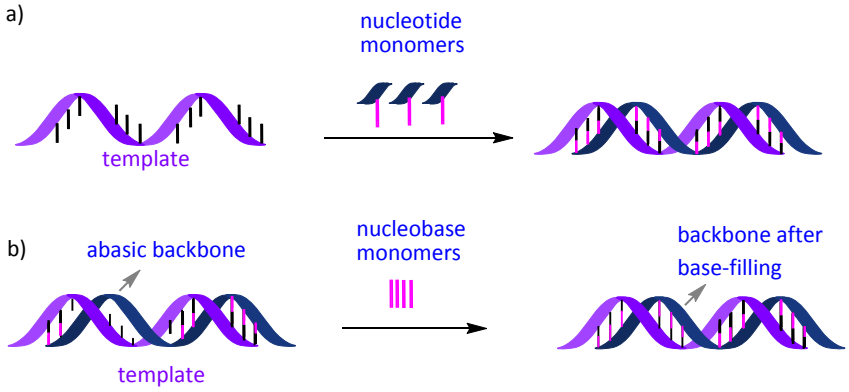

Figure 13: Two strategies for templated synthesis of oligonucleotides illustrated in the example of DNA backbone. a) Templated oligonucleotide synthesis by backbone ligation; b) Templated oligonucleotide synthesis by base-filling.(redrawn from [97])

If the backbone ligation or base-filling processes are performed by using a reversible reaction under thermodynamic control, the new synthetic informational oligomer would be responsive to a selection pressure. The attachment of nucleobases can be continuously and reversibly exchanged as a result of the addition of a new template strand with different sequence.

2.3.1 BACKBONE LIGATION

Early attempts for template-directed oligonucleotide synthesis focused on backbone ligation through a coupling reaction between two monomeric nucleotides or short oligonucleotides by joining backbone functional groups where DNA, RNA or PNA was used as template.[98–105] The first application of backbone ligation used an irreversible reaction to form phosphodiester bond.[106] Short oligonucleotides were bound to their complementary sites along a template through hydrogen-bonding. The adjacent monomers on the template, one of them was carrying hydroxyl group at 3'-end and the other one was carrying a phosphate group at 5'-end, are coupled forming a phosphodiester bond in presence of a suitable activator (Fig 14a). The macromolecular template directs the reaction by bringing the reactive species in close proximity and hence, increasing the effective molarity of the reactive groups.[107] In addition to the phosphodiester backbone formation other reactions such as amine acylation, amide formation, phosphothioester and phosphoseleno formation could be performed to generate oligomers of DNA analogs by using backbone modified nucleotides with the required appropriate reactive groups at the 3'-and 5'-terminals.[108–110]

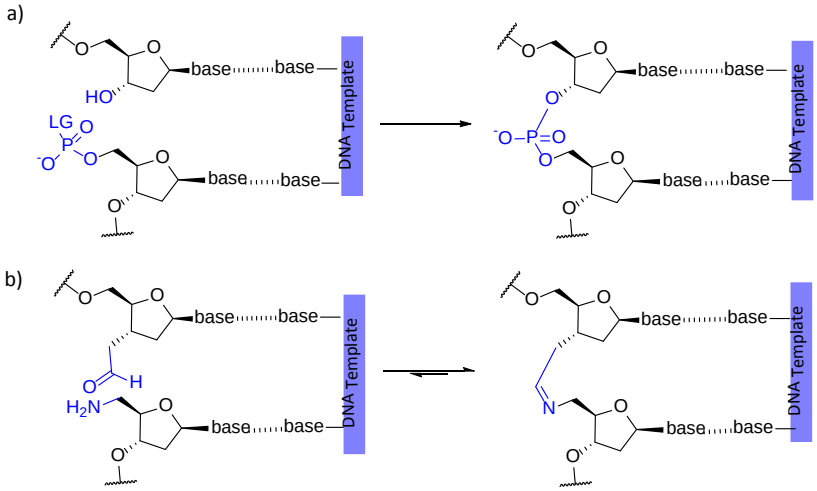

Figure 14: a) Representative DNA-templated phosphodiester formation through backbone ligation of short oligonucleotides. Two nucleotides were coupled to form the native phosphodiester backbone.[106] LG: Leaving group. b) Representative DNA-templated imine formation through backbone ligation of short oligonucleotides.[108]

In order to synthesize oligonucleotide analogs on a template, a reversible reaction could be employed as well. The introduction of a reversible step enhances thermodynamic control in the template-directed synthesis.[108] As shown in Figure 14b, incubation of 5'-amino and 3'-aldehyde functionalized DNA oligonucleotides with a complementary DNA template result in formation of double-stranded oligonucleotides. The template brings the two oligonucleotides carrying the

functional groups in close proximity and formation of an imine-linked new oligonucleotide can be observed.[111]

The above given examples show the formation of a single imine bond without generating a DCL by reversible coupling of two short oligonucleotides on the template. This concept can be extended to the *sequence-specific polymerization* of nucleic acids in presence of a DCL.[105] Non-enzymatic polymerization typically uses one DNA (RNA or PNA) template and a pool of nucleotide monomers (G, C, T, A) for coupling along the template. Nucleotide monomers are selected from the pool by template strand. One of the nucleobase monomers from the pool, the one complementary to the template strand´s nucleobase should be selected. In this manner, information on the template strand could be transferred from template to the new synthesized strand. The new synthesized strand could carry an imine bond function (or amine by reduction of the imine bond) on its backbone if the nucleotides bear an amino function at one end and an aldehyde at the other end (Fig. 15). In this manner, monomers containing a nonnatural backbone could generate DNA or RNA mimicking oligomers containing ribose unit on the backbone but replacing the phosphate with amine.[101]

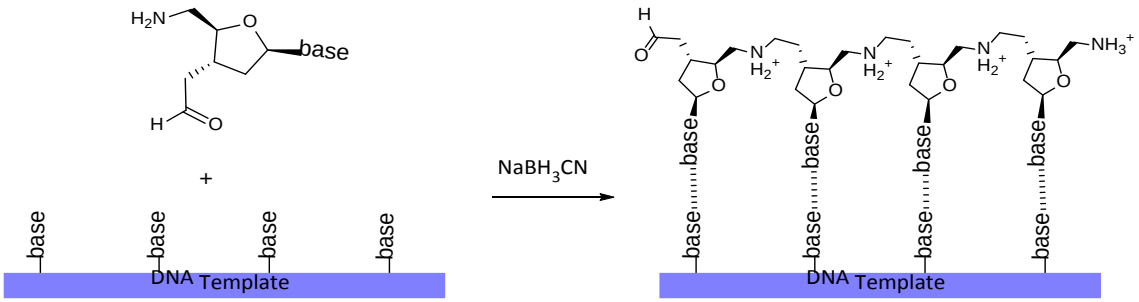

Figure 15: Schematic representation of a DNA-templated polymerization through backbone ligation used in the work of LYNN and co-workers.[101]

2.3.2 BASE-FILLING REACTIONS

Sequence-selective base-filling approach is an alternative route to non-enzymatic nucleic acid synthesis and considers the addition of individual monomeric nucleobases to a pre-formed abasic backbone. Initial attempts used an abasic ribose-phosphate backbone for the attachment of nucleobases on the abasic site through the formation of a *N*-glycosidic bond. However, the formation of a *N*-glycosidic bond between a ribose unit and a nucleobase in water is a challenging work (Fig. 16).[96,112,113]

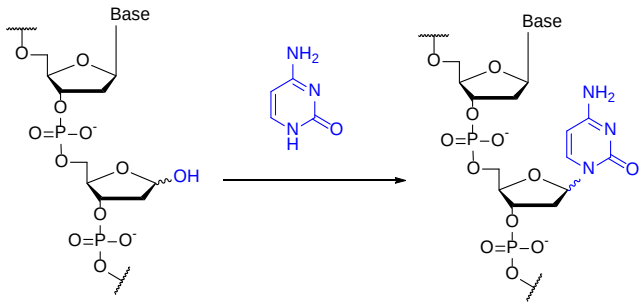

Figure 16: Schematic representation of a base-filling process on an abasic site of DNA backbone by *N*-glycosidic bond formation.

Since the *N*-glycosidic bond formation without catalyst is unfavorable, LIU and co-workers have used, a nucleic acid variant, PNA backbone for base-filling reactions instead of using a DNA backbone.[97] PNA is a good candidate for base-filling reactions because its abasic site is a versatile secondary amine. This amine site on the backbone would be filled more favorable than *N*-glycosidic bond formation through amine acylation or reductive amination by modifying the nucleobase monomers with appropriate functional groups (Fig. 17, `blank site´ is dashed boxed). Therefore, the individual nucleobase monomers (A, G, C, T) are prepared with carboxylic acid or aldehyde groups that can react with amine group on the backbone. The PNA with abasic site is pre-annealed to its complementary PNA strand. In the presence of all nucleobase monomers in the reaction mixture, the proper monomer is selectively bound on the pre-annealed PNA duplex. The tethered nucleobase is selected among all other nucleobases through the recognition of the complementary nucleobase on the template opposite to the blank site. In Figure 17 the selection of a guanine nucleobase through templating of PNA carrying cytosine in its sequence is shown. Base-filling of PNA by amine acylation generates native PNA and by reductive amination generates artificial PNA with a new backbone so-called deoxyPNA. For base-filling, both a reversible reaction through reductive amination and an irreversible acylation reaction were reported and both of them show sequence selectivity. However, better yields and selectivities are obtained by reductive amination. Dynamic iminium formation allows for error correction by reversing the formation of mistemplated products.

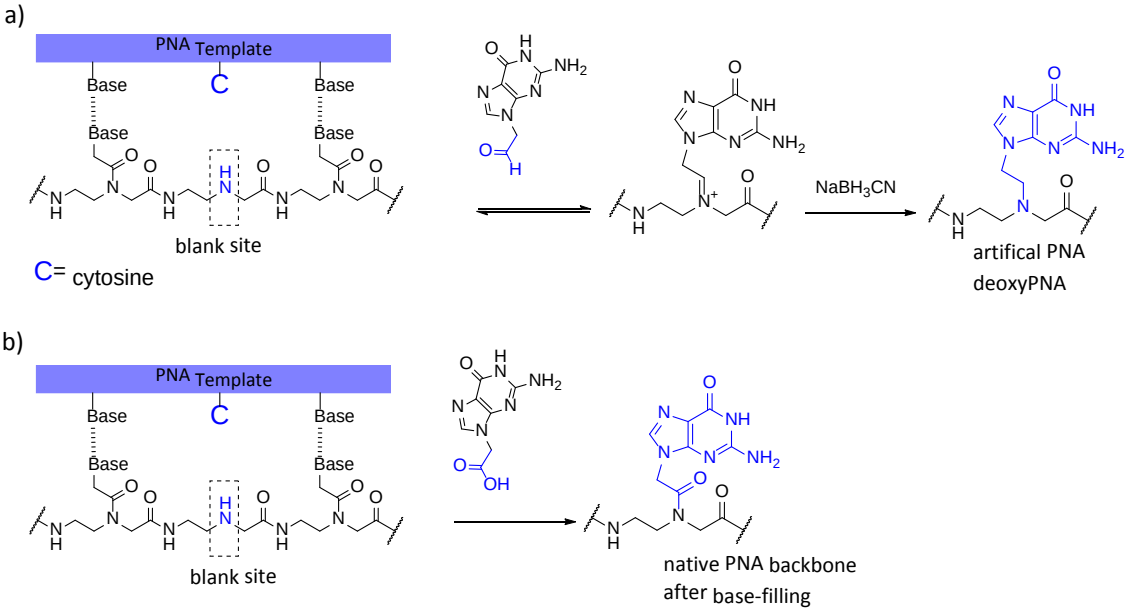

Figure 17: Base-filling chemistry on a PNA backbone used in the work of LUI and co-workers.[114] The selective incorporation of a guanine nucleobase is shown. a) The base-filling reaction for incorporation of nucleobase monomers through reductive amination to generate native PNA. b) The base-filling reaction for incorporation of nucleobase monomers through amine acylation to generate deoxyPNA.

A similar work for base-filling reactions by using a PNA backbone was performed by BRADLEY and co-workers.[115] Reversible imine exchange reaction was used in order to incorporate aldehyde modified nucleobase monomers on a single abasic site (a secondary amine) of the PNA. In this concept, the PNA with abasic blank site was hybridized to a DNA template. The correct nucleobase was selectively incorporated to fill the abasic site which could be then identified by MALDI mass spectrometry. Thus, the blank site on PNA was used to read out the unknown nucleotide of the DNA template. The nucleobase which was selectively bound on the blank site was used to identify the unknown site on the DNA strand.

Recently GHADIRI and co-workers used a regular peptide backbone for the reversible attachment of nucleobases on that backbone.[72] This work shows the application of *dynamic combinatorial chemistry* for synthesizing an artificial oligomer with a peptide backbone carrying nucleobases on its amino acid side chains. This regular peptide consists of a cysteine moiety as every second amino acid in its sequence. Thioester exchange reaction is used for the reversible attachment of modified nucleobases onto the peptide backbone (Fig. 18). By addition of nucleobases with thioester-linkage at cysteines of the backbone, a new PNA-like oligomer carrying nucleobase recognition units is created and denoted as thioester PNA (tPNA). The selection process of the best-binding one among all four nucleobases is directed by a DNA template. The nucleobase sequence of the template decides the incorporation of the right nucleobase through base-pairing. In Figure 18, the selection of an adenine nucleobase through templating of DNA

including thymine in its sequence is shown. tPNA oligomers are the first example of reversible artificial informational oligomers. Sequence of tPNA would adapt itself to any change of nucleobase sequence in the template strand. The reversible nature of a new adaptive and sequence-specific oligomer enables for any error correction.[95]

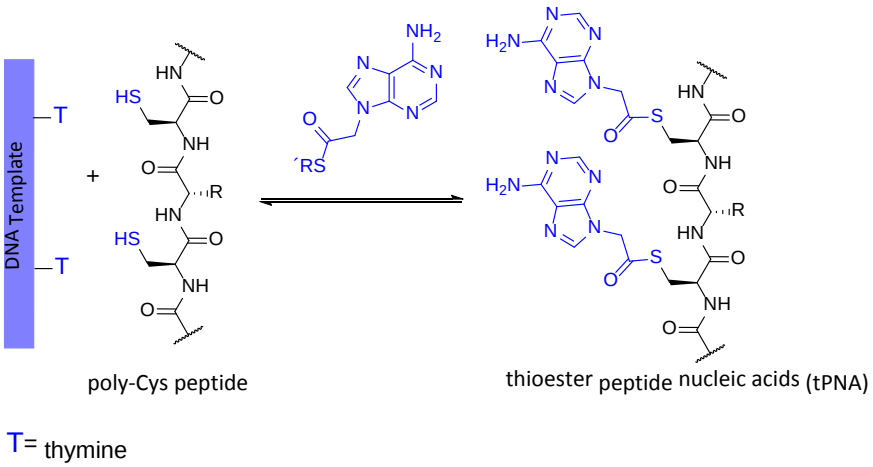

Figure 18: The schematic representation of transesterification exchange mechanism used in the work of GHADIRI and co-workers showed the formation of thioester peptide nucleic acids (tPNA) by reversibly attaching of the nucleobases.[72]

2.4 THE APPROACH OF THIS STUDY

Several classes of nucleic acid analogs varying in backbone structure have been reported.[116] The idea for modification of the native nucleic acid by replacing the ribose unit of the backbone with an acyclic linker was inspired from ASANUMA and co-workers.[61] This work includes the incorporation of a D-threoninol-based acylic linker into the oligonucleotide strand in order to generate a ribose free (acyclic) site in the backbone which lacks the nucleobase. The use of D-threoninol within the strand not only introduces an abasic ribose free site but also results in the introduction of an amine group on the backbone (Fig. 19). The presence of the reactive amine group enables further functionalization of the oligonucleotide by filling this abasic site with appropriate functional molecules. Various functional molecules of interest can be tethered irreversibly with a carboxyl group or reversibly with an aldehyde group to the amine group post-synthetically such as functional molecules fluorophores, metal ligands or the natural nucleobase monomers. The incorporation of nucleobases at the abasic site would be a post-functionalization approach for the non-enzymatic synthesis of informational oligomers. Dynamic Combinatorial Chemistry (DCC) can be applied for the post-synthetic functionalization of the backbone modified oligonucleotides with an acyclic and abasic site.

The idea to attach nucleobase monomers reversibly to the backbone of a linear oligomer in order to obtain new informational oligomers was inspired from GHADIRI. The use of peptide nucleic acid (PNA) carrying abasic sites on its linear backbone or regular linear peptide backbone are good candidates to attach nucleobase monomers on the abasic sites through dynamic chemistry approach. However, none of the abasic DNA backbones have been used for nucleobase filling approach due to the difficulties faced during the attachment of nucleobases directly on the ribose unit. The presence of ribose free site carrying a reactive amine group on the backbone of oligonucleotides synthesized while working on this thesis makes DNA also a good candidate for the reversible attachment of nucleobase monomers on the backbone.

The aim of this work is the utilization of modified abasic and acyclic oligonucleotides for the non-enzymatic sequence-specific attachment of nucleobase monomers on the abasic site (Fig. 19).

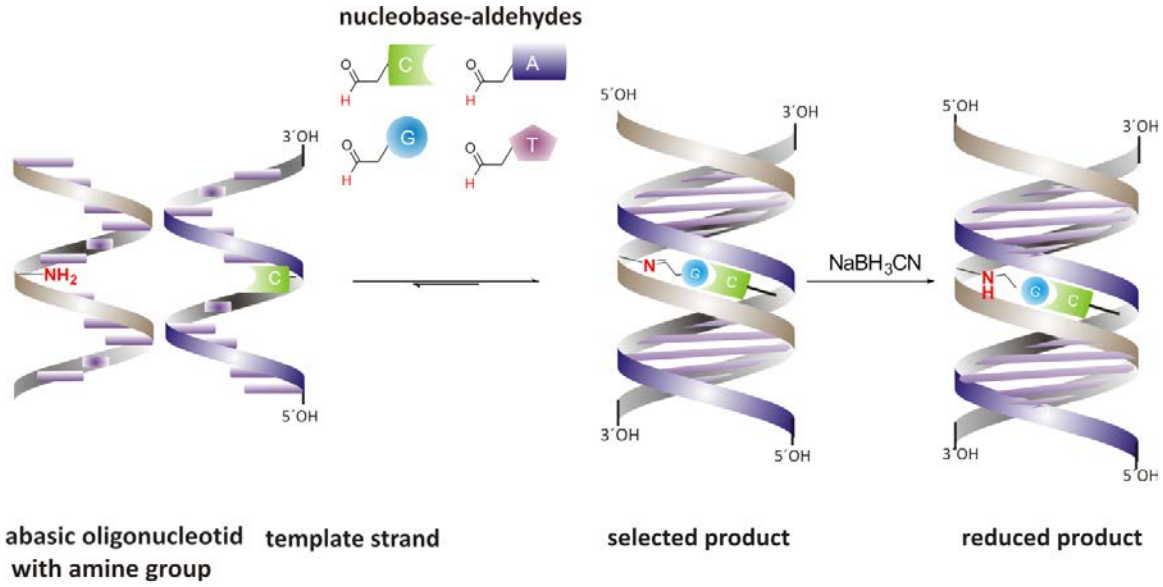

Figure 19: Schematic representation of the model system used in this work in order to functionalize the backbone modified oligonucleotide through dynamic chemistry approach.

If all four nucleobases are prepared with an aldehyde group, the imine formation reaction can be used for filling the blank abasic position through reversible reaction of aldehyde nucleobases with a primary amine on the backbone. The attachment of nucleobase monomers on the backbone sites could be only achieved in the presence of complementary strand as a template to provide the required recognition and effective molarity for the reaction. The addition of a DNA template into the reaction may selectively choose the best binding nucleobase monomer to fill the blank position and direct the formation of thermodynamically most stable product through sequence specific recognition. This work represents the non-enzymatic encoding of a DNA-template and sequence-specific formation of new informational oligonucleotide analogs.

3 DESIGNING DYNAMIC COMBINATORIAL MODEL SYSTEM

In this chapter the design of a model dynamic system for DNA-templated base-filling reactions on a DNA backbone is shown. The investigations for the selective incorporation of nucleobase monomers on the abasic site of a pre-formed acyclic DNA backbone is discussed.

Firstly, the synthetic routes for the building blocks, which are backbone modified DNA and aldehyde modified nucleobases, is given. Secondly, library (DCL) generation conditions through imine exchange reaction and simultaneous selection of the desired product by introduction of the DNA-template are provided. The questions related to the selectivity that could be obtained by introduction of the right template are answered. Finally analysis of the DCL through HPLC and ESI-MS will be given.

3.1 Synthesis of Initial Building Blocks of a Dynamic Library

The building blocks for the DCL are the modified oligonucleotide with an amine group on the backbone (Fig. 20a) and four nucleobases carrying an aldehyde group (Fig. 20b). The incorporation of D-threoninol-based acyclic scaffold results in the formation of a functional amine group on the backbone of the oligonucleotide which required the modifications of nucleobases with aldehyde groups in order to fill the abasic site through a reversible imine exchange reaction. Apart from canonical nucleobases, 1,10-phenantroline ligand was also functionalized with an aldehyde in order to test it in reversible imine exchange reactions (Fig. 20c).

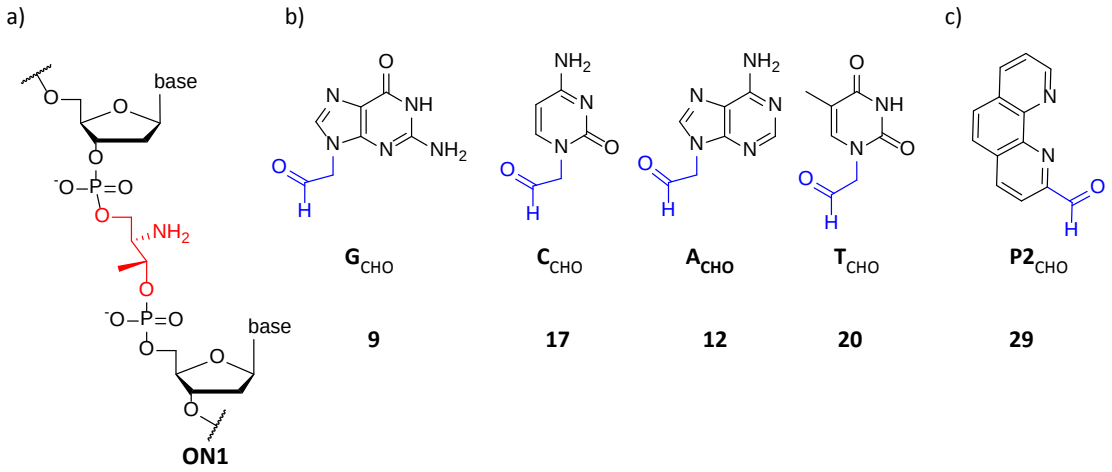

Figure 20: The initial building blocks of the dynamic combinatorial model system applied in this work. Building blocks should be prepared with appropriate amine and aldehyde functionalities due to the imine exchange reaction used to generate DCL. a) Modified oligonucleotide with an amino group, **ON1**; b) A set of aldehyde modified nucleobases, $\mathbf{G}_{CHO}$, $\mathbf{C}_{CHO}$, $\mathbf{A}_{CHO}$ and $\mathbf{T}_{CHO}$. c) Aldehyde substituted phenantroline, $\mathbf{P2}_{CHO}$.

3.1.1 Synthesis of Modified Oligonucleotides Based on D-Threoninol

3.1.1.1 Use of The Threoninol as Acyclic Scaffold

Threoninol (2-amino-1,3-butanediol) is a very efficient and most frequently used C_3-scaffold for the introduction of functional molecules into oligonucleotides.[61] The same number of carbon atoms between two alcohol groups on threoninol makes its structure similar to natural DNA backbone (carbon atoms between two phosphodiester) (Fig. 21). Unlike other C_3-scaffolds as glycerol and serinol, there are two chiral carbon atoms available with respect to the methyl

group on the threoninol. Threoninol which can be synthesized from threonine is commercially available in both the L- and D-stereoisomers (Fig. 21).

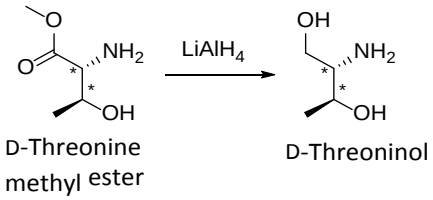

Figure 21: Synthesis of D-threoninol through reduction of D-threonine methyl ester.

In this work, the use of D-threoninol instead of L-threoninol for the backbone modification of oligonucleotides was important because the incorporation of D-threoninol was known to stabilize the DNA duplex much more than the use of L-threoninol.[117–121] ASANUMA and co-workers investigated the introduction of azobenzene moiety into DNA through the use of both D-threoninol and L-threoninol scaffolds for the photoregulation of duplex formation.[120] When azobenzene was attached to D-threoninol, the photoregulation function was higher than L-threoninol as a result of its winding property. Since both the natural DNA and D-threoninol prefer clockwise winding, the incorporation of azobenzene through D-threoninol was much more stable than its enantiomer L-threoninol.[61]

The D-threoninol scaffold can be incorporated into oligonucleotides via its corresponding phosphoramidite monomer which is suitable for automated DNA synthesis. In the conversion route of threoninol into the phosphoramidite monomer, the first step usually includes the attachment of a base-surrogate (a functional molecule or a nucleobase) mostly carrying a carboxyl group to the primary amine of threoninol through amide bond. After attachment of base-surrogates, it is easily converted to phosphoramidite monomers by using the two hydroxyl groups (Fig. 22). Thus, a functional molecule on threoninol scaffold can be introduced at any position in the sequence using a DNA synthesizer.

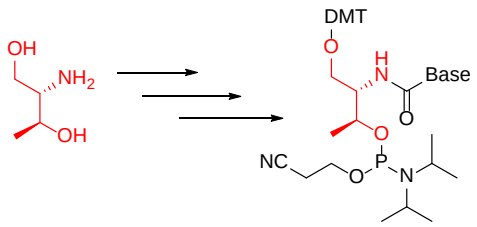

Figure 22: Conversion of D-threoninol derivative into phosphoramidite monomer.

The primary amine of threoninol might or might not carry base-surrogates. The incorporation of a threoninol linker (with free amine group, no base-surrogate) into oligonucleotides would change the backbone structure and lower the duplex stability because of the distortion in the backbone.[122] However attachment of base-surrogates on amine group can compensate for instability particularly if those base-surrogates are aromatic planar molecules. Incorporation of base-surrogates into oligonucleotides offers a variety of duplex designs (Fig. 23). Base-surrogates on the threoninol linker can pair with itself or with a natural/modified nucleobase on the complementary strand (Fig. 23a, b). A wedge-type insertion means that the base-surrogate attached on the amine group of threoninol has nothing to pair opposite of its complementary strand (Fig. 23c).[61]

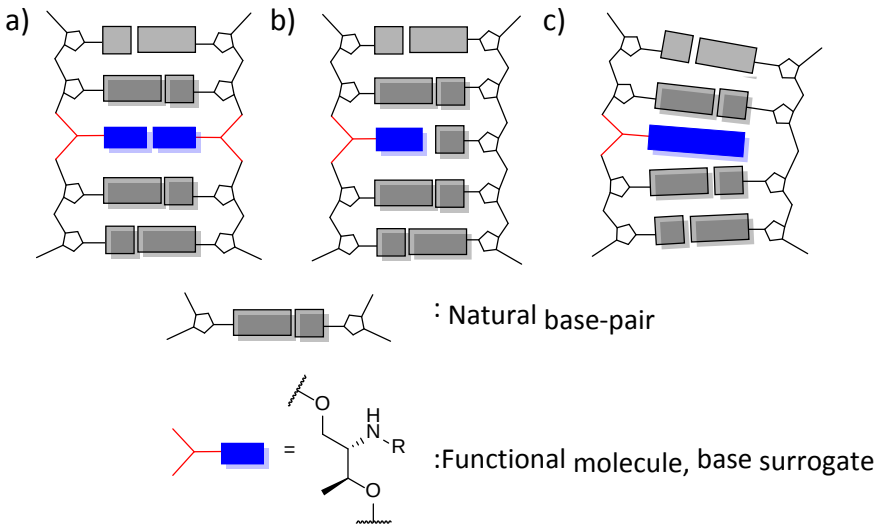

Figure 23: The possible sequence designs for the incorporation of acyclic scaffolds into the oligonucleotides. a) Two base surrogates can be pairing in a duplex; b) One base-surrogate can pair In a mismatch pattern with a natural or modified nucleobase; c) Wedge-type insertion of base-surrogate that has nothing to pair opposite of its complementary abasic strand.(adapted from [71])

Wedge-type insertion of threoninol scaffolds carrying moieties such as psoralen, acridine, azobenzene, dyes or natural bases into natural DNA can fairly stabilize the duplex even when more than one threoninol is inserted. The planar structure of these molecules acts as an intercalator and stabilizes the duplex by stacking interactions. The melting temperature (T_m) of the duplex containing Wedge-type inserted dyes was found to be higher than the native duplex. In contrast incorporation of the same dyes opposite of a natural nucleotide to form an dye-nucleobase mismatch destabilizes the duplex because of steric hindrance.[61] However, not all intercalated planar molecules stabilize the duplex. Molecular size of the tethered functional molecule is also an important factor for generating stable duplex. Since the length of the

Watson-Crick base-pair is around 11 Å, intercalated functional molecules of similar length fit the internal space between adjacent base-pairs and stabilize the duplex. The functional molecules with length higher than 11 Å lower the duplex stability as they are too long to intercalate due to the steric hindrance. Destabilization also occurs when a smaller sized intercalator is tethered to threoninol because of insufficient stacking interactions.[61]

3.1.1.2 Synthesis of the D-Threoninol-Based Phosphoramidite Monomer

For the work employed in this thesis no functional molecule but a reactive amino group on the oligonucleotide backbone was necessary (Fig. 20a, Chapter 3.1). Therefore, from the commercially purchased D-threoninol (**1**), a phosphoramidite monomer (**4**) was synthesized in three facile steps (Fig. 24). In the initial step the primary amine of D-threoninol (**1**) was protected with a suitable, base labile 9-fluorenyl-methylcarbonyl (Fmoc) group in 90% yield in order to prevent the side reactions. The Fmoc group can be easily removed in the subsequent steps after the incorporation of phosphoramidite monomer into oligonucleotide strands by using the DNA synthesizer.

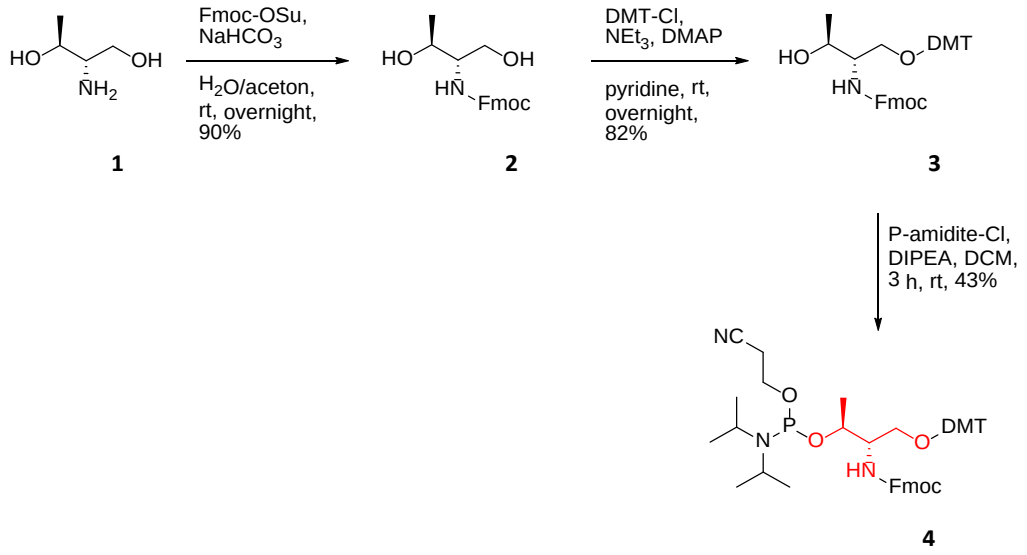

Figure 24: Synthetic route for phosphoramidite monomer (**4**) from commercially available D-threoninol (**1**).

After protection of the amino group, the primary hydroxyl group of the D-threoninol (**1**) was protected with a DMT group and the secondary hydroxyl group was converted into the phosphoramidite. Since DMT selectively reacts with the primary alcohol, the presence of an additional methyl group on the threoninol brings selectivity for the protection of the primary hydroxyl group. The primary alcohol was protected regioselectively with the acid labile DMT

group in the presence of triethylamine in dry pyridine under argon. The presence of 4-(dimethylamino)-pyridine (DMAP) also catalyzes the selective tritylation of the primary alcohol to give the derivative **3** in 82% yield. During the purification of derivative **3** by flash column chromatography, small amounts of triethylamine were added into the eluent. This was necessary due to the fact that silica gel was known to be acidic. Prior to the reaction, the co-evaporation of the Fmoc-D-threoninol (**2**) with dry prydine resulted in better yields of derivative **3**.

The third step is the phosphitylation of the secondary hydroxyl group. It was achieved by treating derivative **3** with 2-cyanoethyl *N,N*-diisopropylchlorophosphoramidite and *N,N*-diisopropylethylamine (DIPEA) in dry dichloromethane under argon for three hours. Purification by flash column chromatography and precipitation into cold hexane afforded derivative **4** in 43% yield. The phosphoramidite monomer was characterized by ^{31}P NMR spectroscopy which shows two diastereomers with two peaks at 147.92 and 148.18 ppm. The (P^{III}) of the phosphoramidite is air and moisture sensitive. For this reason it had to be prepared under strictly anhydrous conditions using argon.

3.1.1.3 INCORPORATION INTO OLIGONUCLEOTIDES

The phosphoramidite monomer **4** was incorporated into oligonucleotides via automated solid phase DNA synthesis. The synthetis cycle for the elongation of the oligonucleotide chain performed in the DNA synthesizer is shown in Figure 25.

The oligonucleotide chain was synthesized on a controlled pore glass (CPG) from 3'- to 5'-end. For every step, anhydrous acetonitrile was used as the solvent. The cycle started with the detritylation of the starting nucleoside by treatment with 3% dichloroacetic acid in toluene on the solid support. Following the detritylation, the support-bound nucleoside was coupled with the next nucleoside phosphoramidite monomer which was activated with 5-benzylmercaptotetrazole by protonating the diisopropylamino group. The attack of the 5'-OH group of the support-bound nucleoside to the phosphorus atom of activated phosphoramidite created a support-bound phosphite-triester. The unreacted 5'-OH groups on the resin-bound nucleoside were capped with acetyl groups to avoid them to participate to next reaction steps. The unstable phosphite-triester (P^{III}) intermediate formed in the coupling step was converted to a stable (P^{V}) species prior to the next detritylation step. The oxidation of (P^{III}) was achieved by 0.02 M Iodine in THF/pyridine. The resultant phosphotriester gave a DNA backbone protected with a 2-cyanoethyl group. The 2-cyanoethyl group prevents undesirable reactions at phosphorus during subsequent steps.

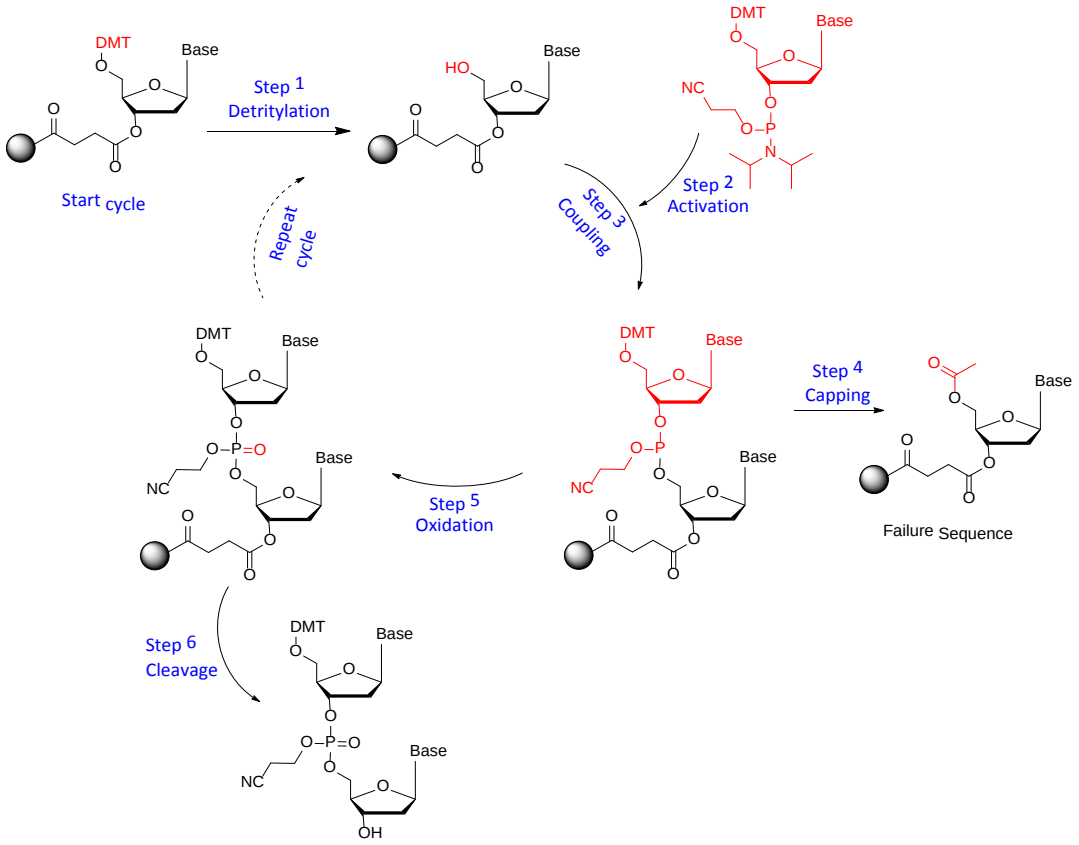

Figure 25: Oligonucleotide synthesis cycle on a solid support by using an automated DNA synthesizer.

The last step was detritylation of the 5'-end group on the newly synthesized strand. After detritylation, a new synthetic cycle can start to introduce the next nucleoside until the desired sequence/length is obtained.

After completion of the full length sequence, the synthesized strand was cleaved from the support while the last nucleotide of the sequence was still carrying the 5'-DMT group. The cleavage from the CPG support was performed manually. This was done by ammonium hydroxide at 50 °C for overnight. Under these conditions the protecting groups on the heterocyclic bases, 2-cyanoethyl groups on the phosphate groups and Fmoc groups on the primary amine were all removed (Fig. 26). After the cleavage process, the obtained solution was filtered and the product was further purified by preparative RP-HPLC. The collected fractions were lyophilized.

The 5'-DMT group on the synthesized oligonucleotides were manually removed. The detritylation of 5'-DMT group was done by a treatment with 80% acetic acid at room temperature for one hour. During the cleavage of the trityl moiety from the oligonucleotide chain, an orange colour was observed caused by the trityl cation. The obtained solution was

passed through *Sep-Pak®* cartridges in order to avoid from the trityl cation. The analysis of the oligonucleotides was done by mass spectrometry (ESI-MS).

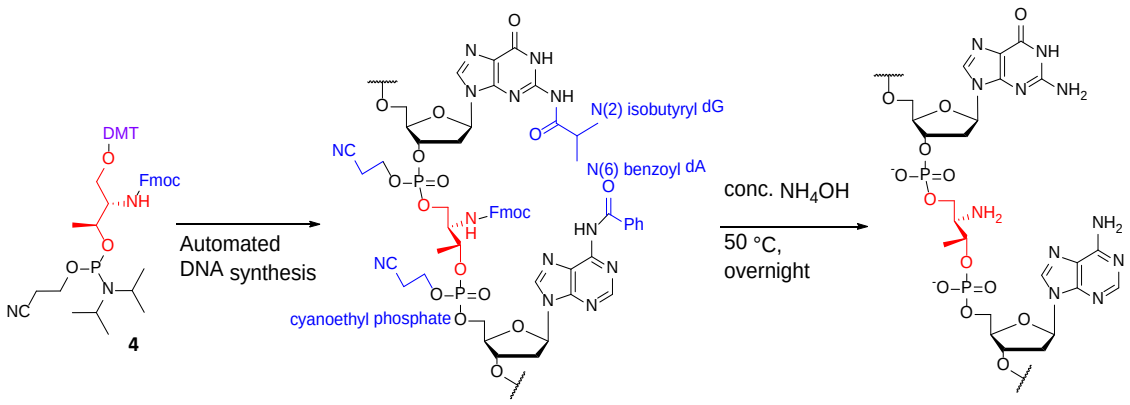

Figure 26: Phosphoramidite monomer was incorporated into oligonucleotide via automated synthesis on a solid support. DMT-ON synthesis was performed. The protection groups on nucleobases, on phosphate groups and Fmoc group were removed using ammonium hydroxide.

The free amine functionality was built on the backbone of the synthesized oligonucleotides through the use of phosphoramidite monomer **4**. The phosphoramidite monomer **4** was incorporated into non-self-complementary 13mer oligonucleotides. The sequences of the synthesized oligonucleotides are shown in Table 1. Singly modified oligonucleotides, carrying the acyclic site in the middle (**ON1**) and at the end (**ON3**) of the sequence were prepared. The incorporation was achieved at both places in the same sequence as well (**ON2**). In natural DNA backbone the distance between 5'- hydroxy groups of two adjacent nucleotides is length of 6-bonds. Substitution of D-threoninol in the backbone fulfills the requirement of length of 6-bonds.

Table 1 The sequences of the modified oligonucleotides synthesized in this work.

ON	Sequence (5'-3') [a]	Mass (*m/z*)
1	CGCTAT**X**TATCGC [b]	3761.67
2	CG**X**TAT**X**TATCGC	3639.66
3	GC**X**CATTTTACCG	3761.67

[a] ***'X'*** represents the abasic site with amino group.

[b] **ON1** was used in further studies in the dynamic base-filling reactions.

3.1.1.4 MELTING TEMPERATURE STUDIES

In order to investigate if threoninol sites in the oligonucleotide backbone disturb hybridization with their complementary DNA strands, the duplex melting temperatures (T_m) were measured for probes **ON1-2,** carrying one and two threoninol sites respectively. A series of melting temperature experiments were conducted for **ON1**, 5'-d(CGCTAT**X**TATCGC) (**X** = threoninol site) with its four complementary strands 5'-d(GCGATA**Y**ATAGCG) (**Y** = dG; **Y** = dC; **Y** = dA; **Y** = dT) containing the guanine, cytosine, adenine and thymine residue opposite to the threoninol site. These results were compared with the corresponding natural DNA-DNA duplex 5'-d(CGCTAT**X**TATCGC) · 5'-d(GCGATA**Y**ATAGCG) where **X** = dG, **Y** = dC; **X** = dC, **Y** = dG; **X** = dA, **Y** = dT; **X** = dT, **Y** = dA (Fig. 27).

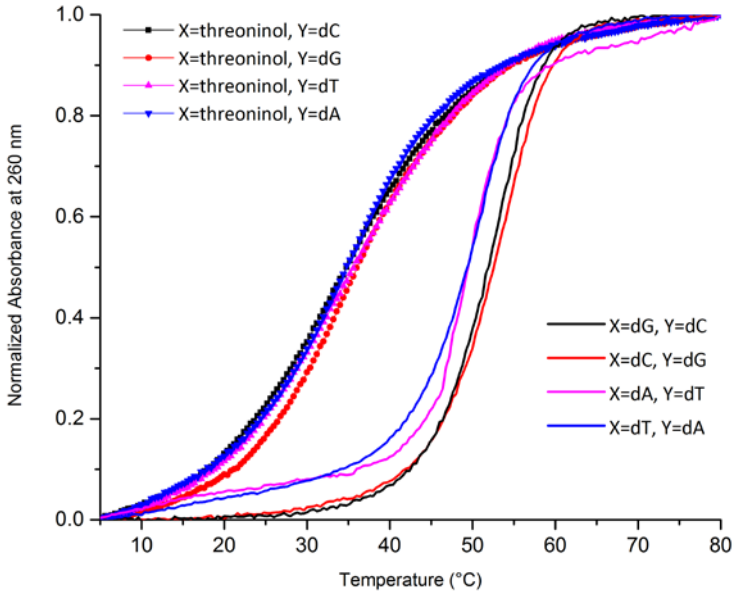

Figure 27: Comparison of melting curves for the duplex formation for **ON1** with its complementary strands, 5'-d(CGCTAT**X**TATCGC)-3'·5'-d(GCGATA**Y**ATAGCG)-3' (**X** = threoninol, **Y** = dG; **Y** = dC; **Y** = dA; **Y** = dT) (up) and for natural DNA·DNA duplexes, 5'-d(CGCTAT**X**TATCGC)-3'·5'-d(GCGATA**Y**ATAGCG)-3' (**X** = dG,**Y** = dC; **X** = dC,**Y** = dG; **X** = dA,**Y** = dT; **X** = dT, **Y** = dA). (2,5 µM ds-DNA, 10 mM sodium phosphate buffer, pH 7, 100 mM NaCl). The absorbance values have been normalized to allow better comparison.

As shown in Figure 27, the 1:1 mixture of **ON1** with its four complementary strands exhibited a typical sigmoidal curve. In comparison to its natural duplex, the incorporated threoninol site in the central position lowered the melting temperature significantly ($\Delta T_m \approx$ - 17 °C) because of the distortion in the duplex (Table 2). However, it has been reported that the incorporation of functional molecules such as dyes with planar structures and stacking interactions straightens the stability of the disturbed duplex.[61] With this in mind, the post-synthetic incorporation of the

nucleobases on the threoninol site of **ON1** for the approach of this thesis, would stabilize the duplex.

Table 2 Melting temperatures (T_m) of oligonucleotide **ON1** and its native duplex.

Duplex	T_m/°C [a]
X = threoninol, Y=dG (X=dC, Y=dG)	35.5 (54.0)
X = threoninol, Y=dC (X=dG, Y=dC)	34.1 (53.2)
X = threoninol, Y=dA (X=dT, Y=dA)	34.5 (51.1)
X = threoninol, Y=dT (X=dA, Y=dT)	33.7 (49.2)

[a] The values in brackets (blue) represents the T_m of the native duplex.

The melting temperatures were conducted for **ON2,** CG**X**TAT**X**TATCGC (X = threoninol site), which had an extra second threoninol site at the end of the strand (Fig. 28). The same complementary strands were used as for **ON1** with sequence GCGATA**Y**ATAGCG (**Y** = dG; **Y** = dC; **Y** = dA; **Y** = dT). As shown in Figure 28, the broader melting transitions were observed for **ON2** with two threoninol sites as compared to **ON1** with one threoninol site indicating that the hybridization is less cooperative. In comparison to ON1, the presence of a second threoninol site in the same strand lowered the melting temperature ($\Delta T_m \approx$ - 10 °C).

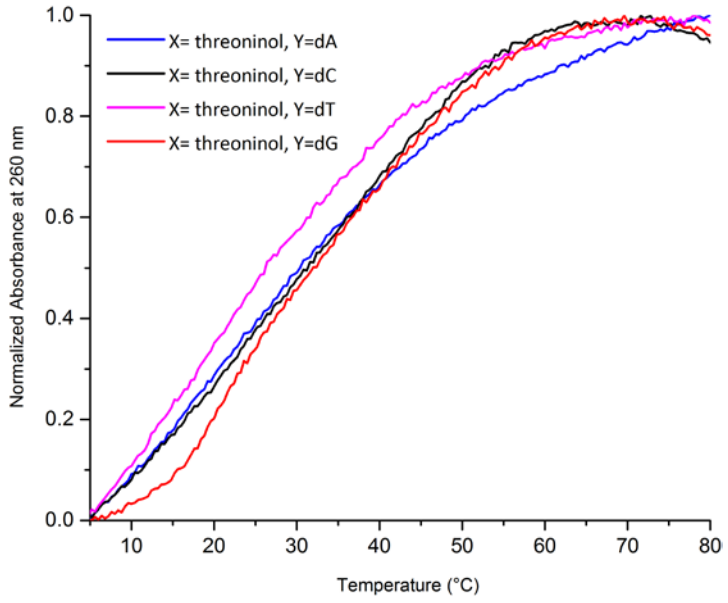

Figure 28: Melting curves for the duplex formation for **ON2**, 5'-d(CG**X**TAT**X**TATCGC)-3'·5'-d(GCGATA**Y**ATAGCG)-3'. (**Y** = dG; **Y** = dC; **Y** = dA; **Y** = dT). (2,5 µM ds-DNA, 10 mM sodium phosphate buffer, pH 7, 100 mM NaCl). The absorbance values have been normalized to allow better comparison.

3.1.2 SYNTHESIS OF ALDEHYDE-MODIFIED NUCLEOBASES

Depending on the chosen imine exchange reaction, the four nucleobase-aldehydes were prepared ($\mathbf{G}_{CHO}$, $\mathbf{C}_{CHO}$, $\mathbf{A}_{CHO}$ and $\mathbf{T}_{CHO}$; Chapter 3.1, Fig. 20). Literature known synthesis was applied; initially, nucleobases were alkylated with bromoacetaldehyde diethyl acetal at the N^1- or N^9-position of pyrimidine or purines, respectively.[123,124] Diethyl acetal nucleobases were then hydrolyzed to aldehydes in aqueous trifluoroacetic acid (TFA) through microwave radiation reactions.[125] Aldehydes of nucleobases were obtained as TFA salts of their hydrates.

In the case of guanine, 2-amino-6-chloropurine (**5**) was used as starting material which has a higher solubility and allows a selective alkylation at the N^9- over N^7-position (Fig. 29). In the first step, 2-amino-6-chloropurine (**5**) was alkylated with bromoacetaldehyde diethyl acetal in the presence of cesium carbonate in *N,N*-dimethylformamide (DMF) at 110 °C for 24 hours. Under these conditions the alkylation was directed predominantly to the N^9-position to afford the alkylated derivative **6** in 60% yield. Afterwards, substitution of the 6-chloro atom by oxygen atom was necessary in order to generate the keto group of the guanine derivative **7**. This was achieved by alkaline hydrolysis of the derivative **6** in the presence of 1,4-diazabicyclo[2.2.2]oktane (DABCO) and potassium carbonate under reflux for two hours. For deionization of the reaction mixture, the solution of products was passed through an ion-exchange column using Dowex. After deionization, derivative **7** was obtained in 60% yield. The acidic hydrolysis of derivative **7** was performed in 1 M HCl by refluxing at 95 °C for one hour to give derivative **8** in 50% yield.

In another accelerated route, the nucleophilic aromatic substitution of the chloride and acidic hydrolysis of derivative **6** was combined in a single step through the use of microwave radiation in aqueous TFA at 100 °C for 30 minutes. $\mathbf{G}_{CHO}$ (**9**) was obtained as hydrate trifluoroacetate as a blue solid in 90% yield.

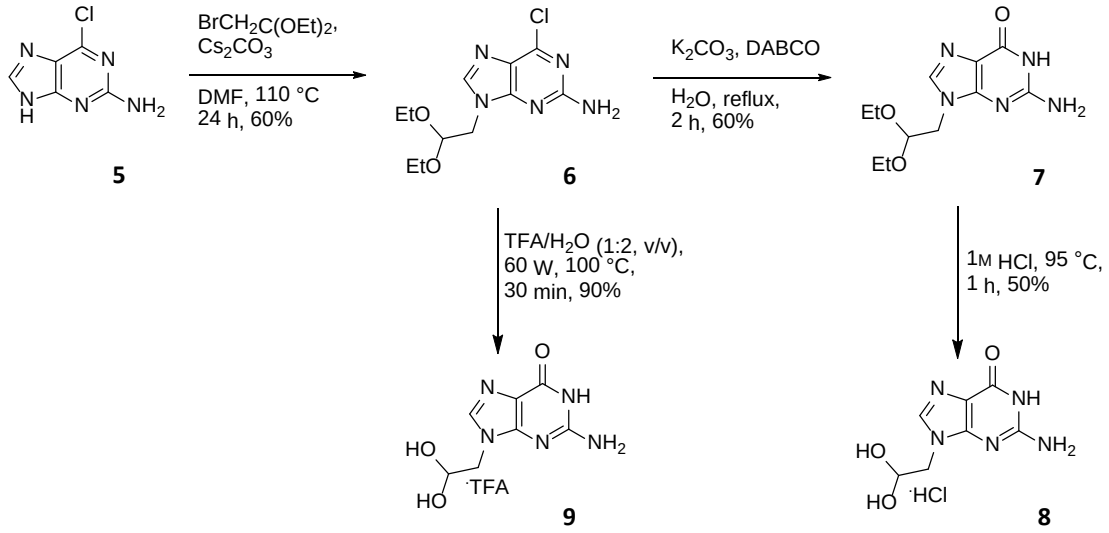

Figure 29: Synthetic route of aldehyde modified guanine nucleobase, $\mathbf{G}_{CHO}$.

Alkylation of adenine (**10**) at N^9 was performed using the same route as described for guanine (Fig. 30). Adenine was alkylated in the presence of bromoacetaldehyde diethyl acetal and potassium carbonate in DMF at 110 °C. After 24 hours acetal **11** was afforded in 60% yield. The hydrolysis of the derivative **11** in aqueous TFA in microwave at 110 °C for 30 minutes gave aldehyde $\mathbf{A}_{CHO}$ (**12**) in 90% yield as the hydrate trifluoroacetate.

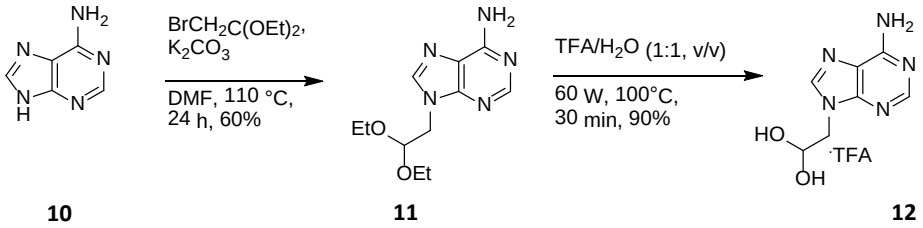

Figure 30: Synthetic route of aldehyde modified adenine nucleobase, $\mathbf{A}_{CHO}$.

Before the alkylation of cytosine, it was necessary to protect the exocyclic amine by an acyl (Ac) group (Fig. 31). Cytosine (**13**) was treated with acetic anhydride and acetic acid for 17 hours under reflux to afford the protected cytosine (**14**) in 88% yield. Following this, the derivative **14** and bromoacetaldehyde diethyl acetal was heated up to 110 °C in DMF in the presence of cesium carbonate for 24 hours to give N^1-alkylated cytosine (**15**) in 60% yield. After alkylation, the Ac protecting group was removed with methanolic ammonia to afford derivative **16**. Acidic hydrolysis of the derivative **16** in aqeous TFA gave aldehyde modified cytosine $\mathbf{C}_{CHO}$ (**17**) in 90% yield as the hydrate trifluoroacetate.

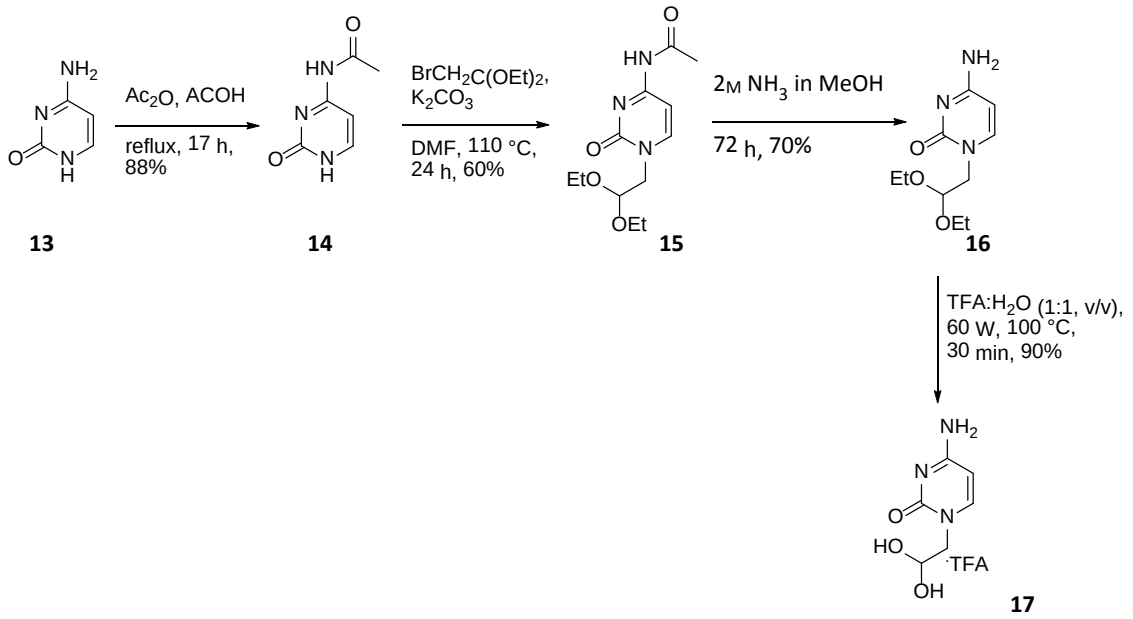

Figure 31: Synthetic route of aldehyde modified cytosine nucleobase, $\mathbf{C}_{CHO}$.

In a similar route, thymine (**18**) was alkylated at the N^1-position with bromoacetaldehyde diethyl acetal to afford derivative **19** in 55% yield which was then hydrolyzed by refluxing in aqueous TFA to afford aldehyde $\mathbf{T}_{CHO}$ (**20**) in the hydrate form in 90% yield (Fig. 32).

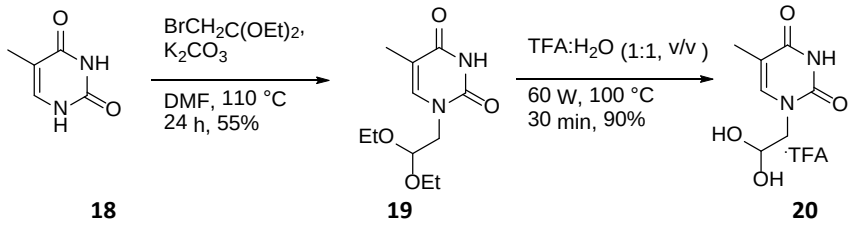

Figure 32: Synthetic route of aldehyde modified thymine nucleobase, $\mathbf{T}_{CHO}$.

3.1.3 Synthesis of Aldehyde-Modified Phenantroline

1,10-Phenantroline-based ligands are important class of chelating agents with large π-surface (Fig. 33).[126] The planar nature of 1,10-phenantroline can interact with DNA as either intercalating or groove-binding species.[127] Furthermore, covalent incorporation of non-nucleosidic, phenantroline-derived building blocks into DNA as a base surrogate without destabilizing the DNA duplex has been already reported.[128,129] The use of these base surrogates can effectively enhance the duplex stability of DNA with an abasic site. The stabilization results from the stacking interactions between the phenantroline and DNA base-pairs.

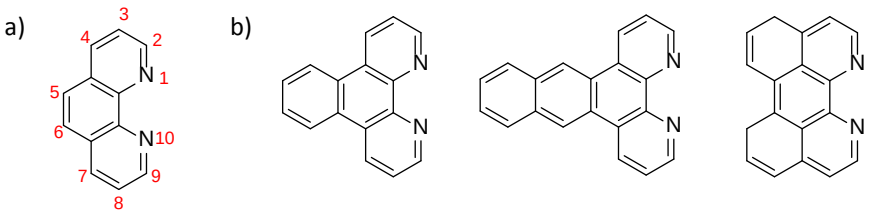

Figure 33: Schematic representation of phenantroline-based ligands. a) 1,10-phenantroline; b) Derivatives of 1,10-phenantroline with extended aromatic surfaces.

Considering these properties, the aldehyde substituted 1,10-phenantroline derivatives, 9-methyl-1,10-phenantroline-2-carbaldehyde, **P1**$_{CHO}$ (**25**, Fig. 34) and 1,10-phenantroline-2-carbaldehyde, **P2**$_{CHO}$ (**29,** Fig. 35) were synthesized in order to attach them to the amino group on the backbone of **ON1**. Apart from the incorporation of nucleobases on **ON1**, the dynamic chemistry approach could provide an aspect for its application as dynamic combinatorial catalyst formation particularly for enantioselective reactions by attaching catalytic species or metal ligands into the oligonucleotides.

In the first place, the synthesis of 9-methyl-1,10-phenantroline-2-carbaldehyde (**P1**$_{CHO}$) was initiated but afterwards, 1,10-phenantroline-2-carbaldehyde (**P2**$_{CHO}$) was noticed to be synthesized in two-steps and in better yields. The only structural difference between **P1**$_{CHO}$ and **P2**$_{CHO}$ is that **P1**$_{CHO}$ has one methyl substituent on the ring at C^9-position. **P2**$_{CHO}$ was used in further studies for its incorporation into DNA.

For the synthesis of 9-methyl-1,10-phenantroline-2-carbaldehyde (**P1**$_{CHO}$), commercially available 2,9-dimethyl-1,10-phenantroline (**21**) was chosen as starting material (Fig. 34). In order to enhance the reactivity of derivative **21**, mono-*N*-oxide derivative **22** was synthesized in quantitative yield by selective oxidation of derivative **21** with 30% hydrogen peroxide in glacial acetic acid (AcOH) at 65 °C. Acetic anhydride (Ac_2O) was added to the derivative **22** and refluxed to give **23** in 90% yield. Transesterification of the derivative **23** with anhydrous potassium carbonate in ethanol gave alcohol **24** in 87% yield. Alcohol **24** was oxidized to aldehyde **25** with oxalyl chloride under Swern conditions in 20% yield.

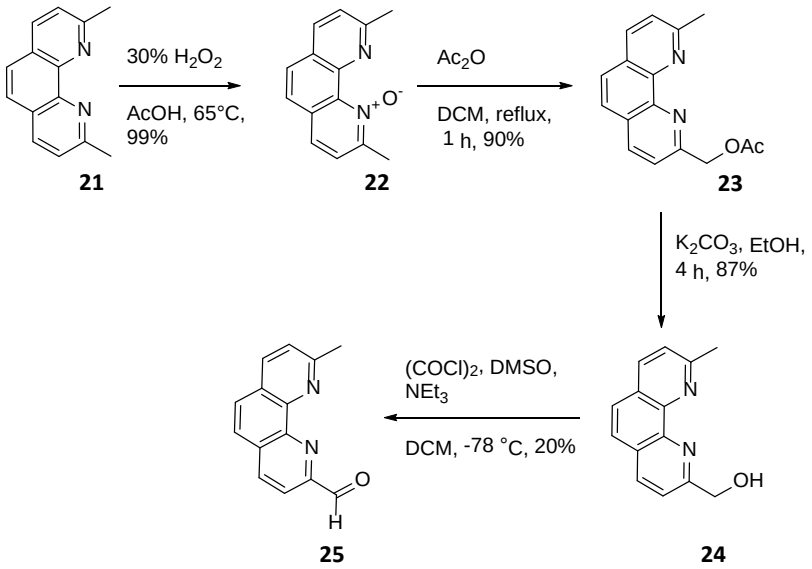

Figure 34: Synthetic route of 9-methyl-1,10-phenantroline-2-carbaldehyde, **P1**$_{CHO}$.

P2$_{CHO}$ was prepared from commercially available 8-aminoquinoline (**26**). A reaction between 8-aminoquinoline (**26**) and crotonaldehyde ((2*E*)-but-2-enal) (**27**) in 70% sulfuric acid (H_2SO_4) in the presence of sodium iodide (NaI) gave derivative **28** in 62% yield (Fig. 35). The methyl group was oxidized by selenium dioxide (SeO_2) to give the corresponding aldehyde **29** in 70% yield.

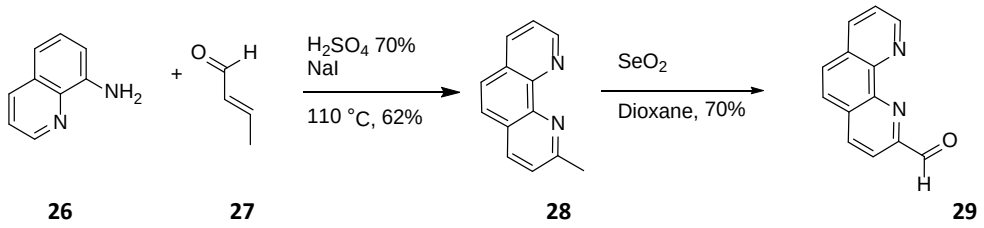

Figure 35: Synthetic route of 1,10-phenantroline-2-carbaldehyde, **P2**$_{CHO}$.

3.2 GENERATION OF THE DCL THROUGH REVERSIBLE IMINE EXCHANGE

One of the fundamental requirements for the generation of DCLs is the design of a system that involves the combination of two reversible processes; the reversible covalent bond formation and reversible non-covalent interactions. The work employed here presents implementation of the DCL concept involving a reversible imine exchange reaction between the backbone modified oligonucleotide **ON1** and a set of aldehyde modified nucleobases ($\mathbf{G}_{CHO}$, $\mathbf{C}_{CHO}$, $\mathbf{A}_{CHO}$, $\mathbf{T}_{CHO}$) as shown in Figure 36. The selection of one nucleobase to be attached to the amino group on the backbone in a higher efficiency than the rest of the nucleobases was directed by DNA-templating. The addition of a template to the reaction, with the intention of increasing the efficiency of one specific product, relies on the reversible non-covalent forces such as hydrogen bond formation.

The imine-based libraries are often generated at mildly acidic pH and at room temperature.[83] A mildly acidic pH is high enough to provide sufficient free amine to attack the carbonyl group of the aldehyde, but low enough for protonation of the carbonyl oxygen prior to the nucleophilic attack and also for protonation of the resulting tetrahedral intermediate for elimination of water. In this work, all imine exchange reactions between **ON1** and the aldehyde modified nucleobases ($\mathbf{G}_{CHO}$, $\mathbf{C}_{CHO}$, $\mathbf{A}_{CHO}$, $\mathbf{T}_{CHO}$) were performed at room temperature in 20 mM sodium phosphate buffer at pH 6 containing 1 M NaCl.

For the purpose of this work, 13mer **ON1** and one of the four 16mer complementary oligonucleotide template strands $\mathbf{T}_{C/G/T/A}$ (Table 3) were mixed in a 1:1 ratio, followed by the addition of an excess amount of all four aldehyde nucleobases $\mathbf{G}_{CHO}$, $\mathbf{C}_{CHO}$, $\mathbf{A}_{CHO}$, $\mathbf{T}_{CHO}$ in equimolar or non-equimolar concentrations. The reaction mixtures were incubated for three hours at room temperature at pH 6. The aldehydes and the amine were allowed to react reversibly to form four intermediate imine products. The four possible imine products in the dynamic library under equilibrium are shown in Figure 36b. In addition, the intermediate imine products in equilibrium were subsequently reduced to amines (Fig. 36c). Thus, irreversible formation of amines facilitated the isolation and analysis of the equilibrated DCL. Reduction was performed by adding sodium cyanoborhydride ($NaBH_3CN$) and shaking it for one hour. After reduction of the imine intermediates, there were four possible final amine products (**ON1+G**, **ON1+C**, **ON1+A**, **ON1+T**) (Fig. 36c). The proportions of imine products in the library should vary by altering the template strand, based on their affinity to the template strand. Addition of different template strands would shift the equilibrium towards the formation of one product.

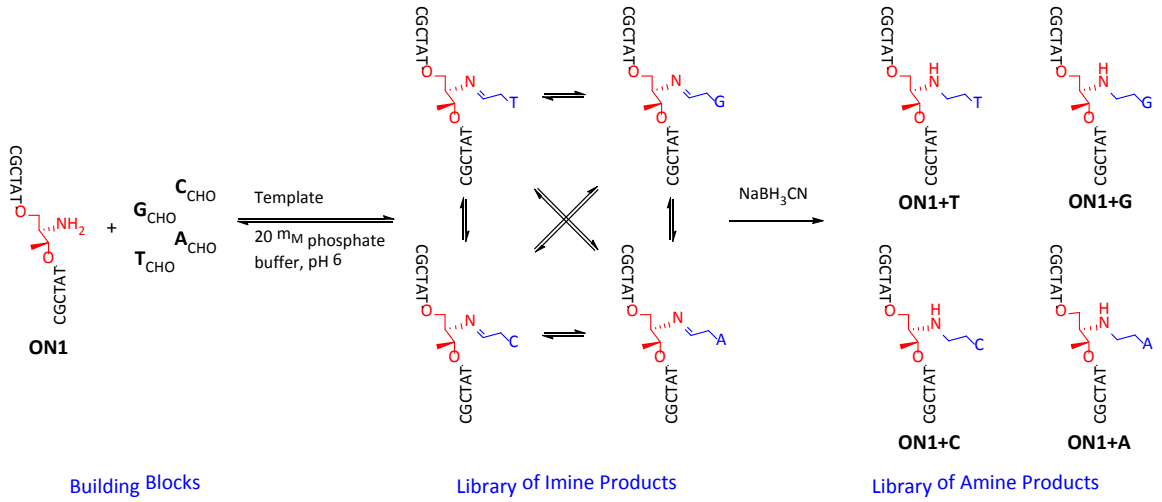

Figure 36: a) Initial building blocks; amine and aldehydes in the presence of the template. b) A dynamic combinatorial library of all possible imine products generated by reversible combinations of the starting materials. c) Library of amine products after reduction.

Four template strands ($\mathbf{T}_{C/G/T/A}$) were used which were complementary to the **ON1** but varying in their single nucleobase opposite to the amino group on **ON1** (Table 3). Here, the capital letter index of **T** stands for the cytosine, guanine, thymine and adenine nucleobase positioning opposite to the amine on **ON1**. The template strands were used as 16mers where the **ON1** was a 13mer in order to achieve better seperations through HPLC.

Table 3: Sequences of modified and the template oligonucleotides used in this work.

Oligonucleotide	Sequence (5'-3')
ON1	CGCTAT**X**TATCGC [a]
$\mathbf{T}_C$	GCGATA**C**ATAGCGGTT [b,c]
$\mathbf{T}_G$	GCGATA**G**ATAGCGGTT
$\mathbf{T}_T$	GCGATA**T**ATAGCGGTT
$\mathbf{T}_A$	GCGATA**A**ATAGCGGTT

[a] `**X**´represents the abasic site with an amino group.
[b] Nucleobases corresponding to the abasic site of the modified strand are shown in bold letters.
[c] The GTT sequence at 3'-end was added to extend the sequence to make it easier to separate through HPLC.

The efficiency and selectivity of the base incorporation were tested by altering the template strand in the reaction. Four reactions were employed in parallel, each includes one of the template strand ($\mathbf{T}_{C/G/T/A}$) under same conditions. The selectivity and the composition of the

library for each template was analyzed by anion exchange HPLC (AE-HPLC) and electrospray ionization mass spectrometry (ESI-MS).

3.3 HPLC CONDITIONS FOR THE ANALYSIS OF DCL

The challenging task of the applied DCC model system was the separation of the oligonucleotides in the library for their analysis. Prior to the analysis of the library, the reaction mixture was purified from the salts and excess of the aldehydes through gel filtration (*Centri.Pure N10*). The analysis of the purified final reaction mixture was performed by AE-HPLC with detection at 260 nm.

Early studies involved the development of a method for the chromatographic separations of oligonucleotides in the DCL. The final reaction mixture contained a mixture of six oligonucleotides: the unreacted modified strand **ON1**, one of the template strand $\mathbf{T}_{C/G/T/A}$, and the four possible reductive amination products (**ON1+G**, **ON1+C**, **ON1+A**, **ON1+T**) resulting from the base incorporation (Fig. 36, Chapter 3.2). In this mixture, the four product strands and the unreacted **ON1** were bound to the complementary template strand through hydrogen bonding. During the analysis of the reaction mixture by chromatography, it was necessary to break the hydrogen bonds in order to separate the oligonucleotides from the template strand. This could be achieved by performing the separation under denaturating conditions. There are two methods to restrict hydrogen bonding interactions between product strands and the complementary template strand; the denaturating conditions at high pH values up to 12 or at high temperatures up to 80 °C. Furthermore, the template strands were used as 16mer complementary sequences in order to elute them later than 13mer sequences. Thus, it was allowed to enlarge the distance of retention times between the oligonucleotide **ON1** and the template strand.

Besides the separation of the template strand from the rest of the oligonucleotides using denaturating conditions, the 13mer oligonucleotides had to be separated from each other. The starting sequence CGCTAT**X**TATCGC (**ON1**) and the product sequences (**ON1+G**, **ON1+C**, **ON1+A**, **ON1+T**) had the same length differing only by one nucleobase in the central position `**X**´. The starting sequence (**ON1**) had a free amino group at position `**X**´ where the base-filled products were carrying one of the four nucleobases attached with an ethyl linker on the amino group. Since the oligonucleotides in the library had the identical length, their separation with the length-based reverse phase HPLC method was not suitable. When analyzing single stranded oligonucleotides of identical length, anion exchange chromatography is the method of choice to resolve the components based on interactions with hydrophobic bases. Thus, elution is influenced by the base composition of the same-length oligonucleotides. Since the

oligonucleotides (**ON1, ON1+G**, **ON1+C**, **ON1+A**, **ON1+T**) differed in one nucleobase, the one positioning on `**X**´ would influence the elution order.

During the anion exchange chromatographic seperations in this work, either elevated temperatures or elevated pH were used as denaturating conditions. The resolution of the peaks and the elution order of oligonucleotides were influenced by pH or temperature as well. For example, at pH 12 each G or T base contributes a negative charge from the deprotonated oxygen atoms and is eluted later than A and C bases. This could be an advantage for the elution of **ON1+G** and **ON1+T**. However, better resolution of the peaks for **ON1**, **ON1+C** and **ON1+A** was obtained when a high temperature was used. Elution conditions for each individual chromatogram are given individually after each experiment in Chapter 3.4.

ESI-MS was employed for the characterization of the reaction products after their separation through HPLC. Desalting of the oligonucleotide was crucial for the ESI-MS analysis. The multiple adducts on the phosphate backbone of the oligonucleotide dramatically decreased the sensitivity and complicated the interpretation of the spectra. Desalting was performed manually through *Sep-Pak®* cartridges in order to avoid an excess of salts.

3.4 ANALYSIS OF THE DCL

3.4.1 EFFECT OF THE TEMPLATE

In preliminary experiments, the attachment of a single nucleobase onto **ON1** was investigated under reductive amination conditions. In order to investigate the effect of the template on the formation of the product, the guanine-aldehyde ($\mathbf{G_{CHO}}$) (1.3 mM) was added to a 1:1 mixture of **ON1** (32 μM) and $\mathbf{T}_C$ (32 μM) in phosphate buffer at pH 6. The reaction mixture was stirred for three hours at room temperature and then for reduction $NaBH_3CN$ (160 mM) was added and the mixture was further shaken for one hour. This reaction was repeated in the absence of the template strand ($\mathbf{T}_C$). This time, instead of the template strand, the same volume of phosphate buffer was added into the reaction in order to keep the reactions in same volume for a better comparison. After removal of the inorganic salts by gel filtration, reactions were analyzed with AE-HPLC under denaturating conditions at pH 12. HPLC profiles of the experiments in absence and in presence of the template strand $\mathbf{T}_C$ are given in Figure 37. Comparison of the two chromatograms clearly indicated that in absence of a template strand, the peak for **ON1** (8.5 min) was not diminished and no new (or very tiny amounts) product formation was observed under the applied conditions (Fig. 37a). When the template strand ($\mathbf{T}_C$) was added, **ON1** was completely consumed and a new peak gave rise corresponding to the mass of the guanine incorporated product (**ON1+G**) (10.9 min) (Fig. 37b). These results shows the strong influence of the template strand on the reaction. **ON1+G** was eluted later than **ON1** because at pH 12 guanine has an additional negative charge on its oxygen atom. Furthermore, the separation of all three peaks (**ON1, ON1+G** and $\mathbf{T}_C$) was achieved by denaturation. The use of a complementary template longer than **ON1** resulted in its elution at high retention times.

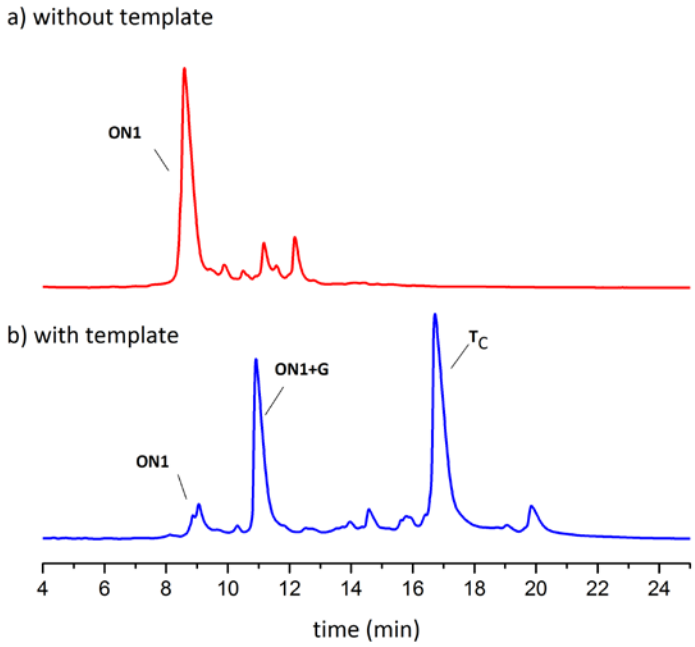

Figure 37: Representative HPLC profiles after reductive amination between $\mathbf{G}_{CHO}$ and **ON1** in absence of the template strand ($\mathbf{T}_C$) (red) and in presence of the template strand ($\mathbf{T}_C$) (blue). Solvent system (A3) 10 mM NaOH, pH 12; (B3) 10 mM NaOH, 1.25 M NaCl, pH 12. Gradient 35-70% B3. Final concentrations in a 310 µL reaction volume (20 mM sodium phosphate buffer, 1 M NaCl, pH 6): 32 µM in **ON1** and $\mathbf{T}_C$; 1.3 mM in $\mathbf{G}_{CHO}$; 160 mM in $NaBH_3CN$.

The same reaction of **ON1** (32 µM) with $\mathbf{G_{CHO}}$ (1.3 mM) in the presence of the template $\mathbf{T}_C$ (32 µM) was repeated in three *Eppendorf* caps in parallel. The reaction mixtures were incubated at room temperature for one hour, two hours and three hours, respectively, before addition of $NaBH_3CN$. After a cleaning process, the reaction mixtures were analyzed by AE-HPLC (Fig. 38). The formation of the guanine incorporated product (**ON1+G**) was observed after one hour but was not fully achieved. After three hours, the **ON1** was completely converted into **ON1+G**. Hereafter, all further experiments for DNA-templated reductive amination were performed with an incubation time of three hours.

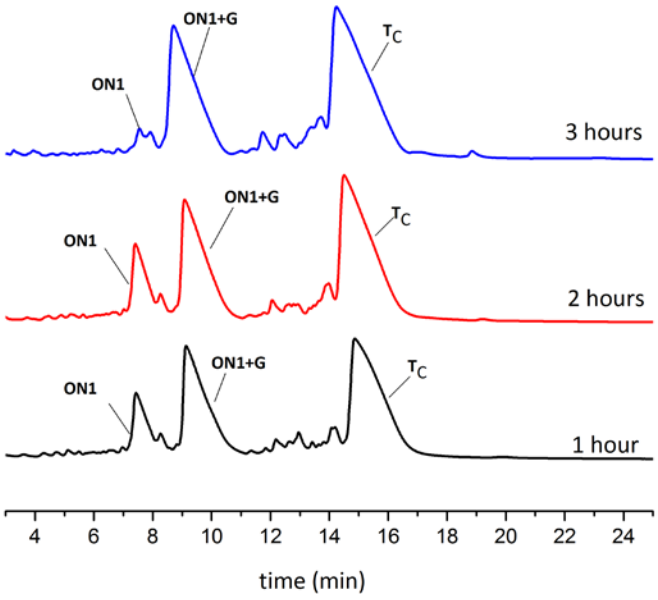

Figure 38: Representative HPLC profiles after DNA-templated reductive amination between **ON1** and $\mathbf{G}_{CHO}$ with an incubation time of 1 hour (black), 2 hours (red) and 3 hours (blue). Solvent system (A3) 10 mM NaOH, pH 12; (B3) 10 mM NaOH, 1.25 M NaCl, pH 12. Gradient 35-70% B3. Final concentrations in a 310 µL reaction volume (20 mM sodium phosphate buffer, 1 M NaCl, pH 6): 32 µM in **ON1** and $\mathbf{T}_C$; 1.3 mM in $\mathbf{G}_{CHO}$; 160 mM in $NaBH_3CN$.

3.4.2 Base-Filling in Presence of One Nucleobase

Having shown that guanine-aldehyde was efficiently bound to **ON1** via reductive amination, the capacity of dynamic binding was tested also for cytosine, adenine and thymine aldehydes individually in the presence of the template strand. Four reactions were performed in parallel and in each **ON1** (32 µM) was allowed to react with one of the four nucleobases $\mathbf{G}_{CHO}$, $\mathbf{C}_{CHO}$, $\mathbf{A}_{CHO}$ or $\mathbf{T}_{CHO}$ (1.3 mM). To each of these mixtures, an appropriate template strand $\mathbf{T}_C$, $\mathbf{T}_G$, $\mathbf{T}_T$ or $\mathbf{T}_A$ (32 µM) was added, respectively. As a template strand, one of the complementary strands of **ON1** was used, the one which has the complementary base of the added nucleobase-aldehyde opposite to the blank **X** position of **ON1**. In this way, the use of $\mathbf{T}_C$ with cytosine as its templating base would direct the formation of guanine incorporation, likewise $\mathbf{T}_G$ of cytosine incorporation, $\mathbf{T}_T$ of adenine incorporation and $\mathbf{T}_A$ would direct the formation of thymine incorporation.

AE-HPLC analyses were performed under denaturating conditions using high pH in order to break any hydrogen bonding between the template and library members. As shown in each chromatogram in Figure 39, 16mer templates were eluted at high retention times. It was possible to fully resolve the guanine and thymine incorporated products (**ON1+G**, **ON1+T**) from **ON1** because at pH 12 these both nucleobases were negatively charged due to the deprotonated oxygen and they were eluted at high retention times compared to **ON1** (Fig. 39a and d). However, in the case of cytosine and adenine incorporation, the products **ON1+C** and

ON1+A were not clearly resolved and were eluted together with **ON1** since cytosine and adenine contribute no additional negative charge due to the absence of deprotonated oxygen (Fig. 39b and c). However, the formation of the products **ON1+C** and **ON1+A** were proven by ESI-MS.

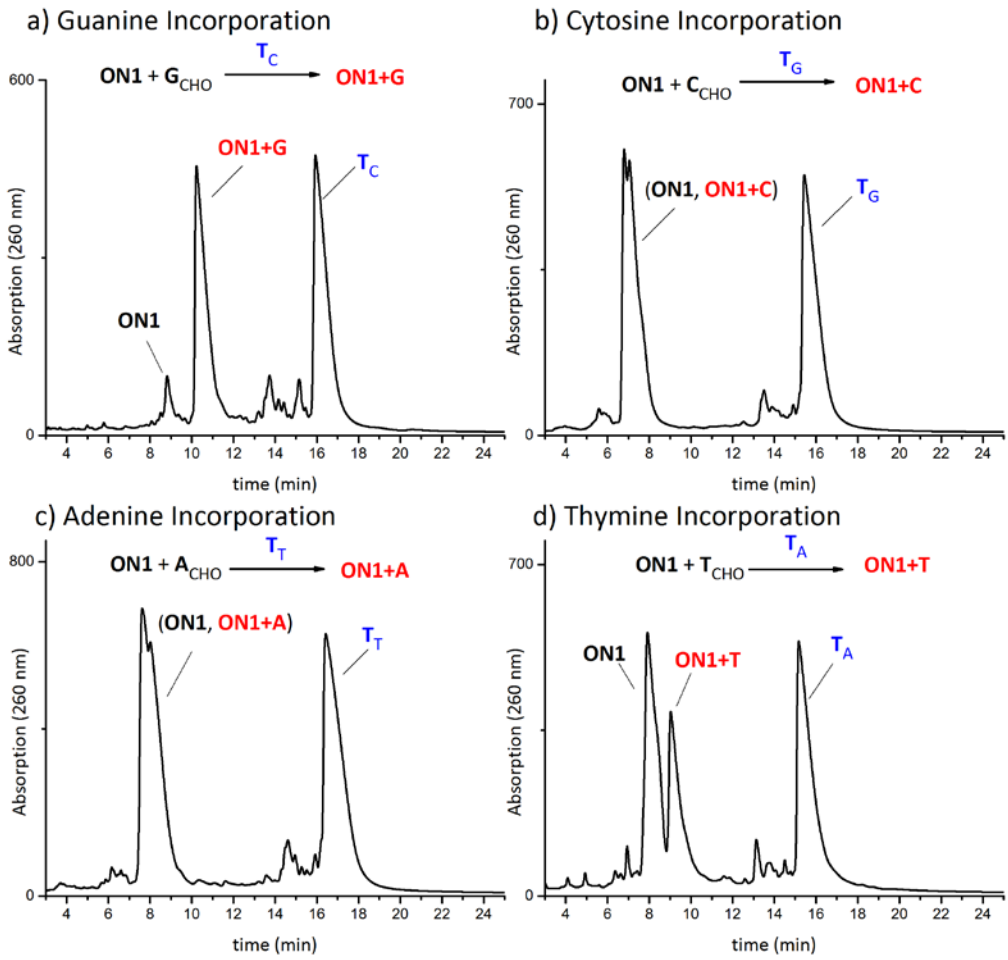

Figure 39: Representative AE-HPLC (at pH 12) profiles after DNA-templated reductive amination. Solvent system (A3) 10 mM NaOH, pH 12; (B3) 10 mM NaOH, 1.25 M NaCl, pH 12. Gradient 35-70% B3. a) Reductive amination between **ON1** and $\mathbf{G}_{CHO}$ in the presence of $\mathbf{T}_C$; b) Redutive amination between **ON1** and $\mathbf{C}_{CHO}$ in the presence of $\mathbf{T}_G$; c) Reductive amination between **ON1** and $\mathbf{A}_{CHO}$ in the presence of $\mathbf{T}_T$; d) Reductive amination between **ON1** and $\mathbf{T}_{CHO}$ in the presence of $\mathbf{T}_A$. Final concentrations in a 310 µL reaction volume: 20 mM sodium phosphate buffer, pH 6; 32 µM in **ON1** and template strand; 1.3 mM in nucleobase aldehyde; 320 mM in $NaBH_3CN$.

As it is described in Chapter 3.3, pH and temperature have different influence on the elution of the oligonucleotides through anion exchange chromatography. In order to accomplish better elution for **ON1+C** and **ON1+A**, the HPLC elution conditions were changed. Therefore, elevated temperature (80 °C) was tried as elution conditions instead of elevated pH in order to break the hydrogen bonding with the template strand. At high temperature, better resolution of peaks was obtained than in the case of using elevated pH. Under these conditions, **ON1** was eluted and

separated effectively from all four product sequences (Fig. 40). Furthermore, the elution of **ON1+C** and **ON1+A** was efficiently achieved. The elution order due to increasing retention times of oligonucleotides was found to be as followed: **ON1** < **ON1+C** < **ON1+A** < **ON1+T** < **ON1+G**.

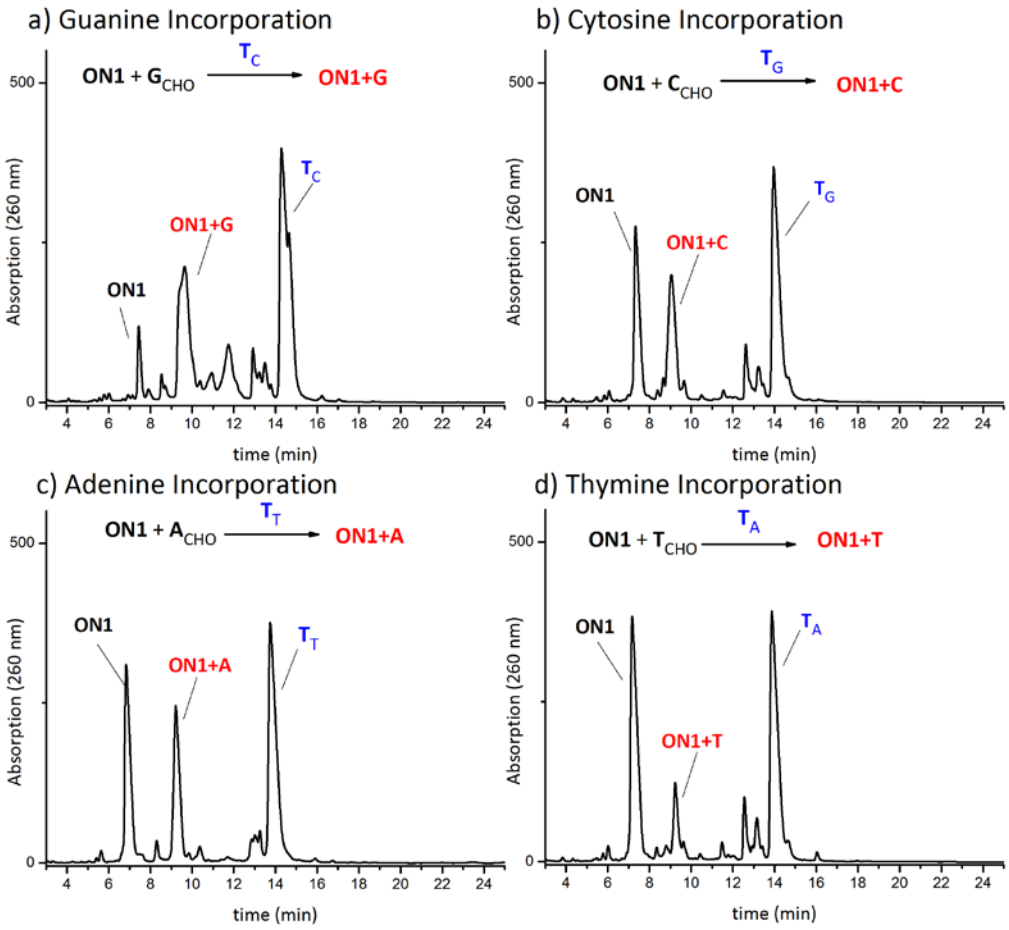

Figure 40: Representative AE-HPLC profiles (at 80 °C) after DNA-templated reductive amination for base-filling in the presence of a single nucleobase. Solvent system (A2) 20 mM Tris-Cl, pH 8; (B2) 20 mM Tris-Cl, 1.25 M NaCl, pH 8. Gradient 25-60% B2. a) Reductive amination between **ON1** and $\mathbf{G}_{CHO}$ in the presence of $\mathbf{T}_C$; b) Reductive amination between **ON1** and $\mathbf{C}_{CHO}$ in the presence of $\mathbf{T}_G$; c) Reductive amination between **ON1** and $\mathbf{A}_{CHO}$ in the presence of $\mathbf{T}_T$; d) Reductive amination between **ON1** and $\mathbf{T}_{CHO}$ in the presence of $\mathbf{T}_A$. Final concentrations in a 310 µL reaction volume: 20 mM sodium phosphate buffer, pH 6; 32 µM in **ON1** and template strand; 1.3 mM in nucleobase aldehyde; 320 mM in $NaBH_3CN$.

Conversion of **ON1** into products was determined by a comparison of the HPLC peak areas of the product and the starting material (Table 4). The most successful incorporation was detected from the reaction between $\mathbf{G}_{CHO}$ and **ON1**, where **ON1** was nearly completely converted into the guanine incorporated product (**ON1+G**) (Fig. 40a). 6:1 ratio of the product to starting material **ON1** was obtained (Table 4)**.** Cytosine and adenine were incorporated in comparable but lower yields than the incorporation of guanine. When the thymine aldehyde was allowed to react with **ON1**, the formation of product **ON1+T** was observed but with the lowest efficiency (Fig. 40d).

Based on these results, guanine was incorporated with higher yield due to its three hydrogen bonding capacity and higher π-stacking interactions.

Table 4: Ratio of HPLC peak areas resulted from base-filling through DNA-Templated reductive amination.

Figure 35	Reaction	Templating Base	Product	Product:ON1
A	**ON1**+$\mathbf{G}_{CHO}$	C	**ON1+G**	6:1
B	**ON1**+$\mathbf{C}_{CHO}$	G	**ON1+C**	1:1
C	**ON1**+$\mathbf{A}_{CHO}$	T	**ON1+A**	1:1
D	**ON1**+$\mathbf{T}_{CHO}$	A	**ON1+T**	1:4

In terms of these results, the four possible components of the library (**ON1+C** , **ON1+A** , **ON1+T**, **ON1+G**) were synthesized separately and their retention times were determined on AE-HPLC. The identification of each product individiually were helpful for the understanding of further experiments in the presence of all four nucleobases in same reaction vessel.

3.4.3 Base-Filling in Presence of Four Nucleobases

The approach was further explored by including all four nucleobases in the same reaction vessel. Four reactions were performed in parallel and in each **ON1** (32 µM) was allowed to react simultaneously with four nucleobase-aldehydes in equimolar concentrations: $\mathbf{G}_{CHO}$ (1.3 mM), $\mathbf{C}_{CHO}$ (1.3 mM), $\mathbf{A}_{CHO}$ (1.3 mM), $\mathbf{T}_{CHO}$ (1.3 mM). To each of these four mixtures one of the four template strands was added ($\mathbf{T}_C$, $\mathbf{T}_G$, $\mathbf{T}_T$ or $\mathbf{T}_A$; each in 32 µM). The reaction mixtures were incubated at room temperature for three hours for the formation of the library of imine products. After three hours, the imines were reduced to the amines by addition of $NaBH_3CN$. The composition of each library was analyzed by AE-HPLC. The effect of the template on the proportions of products in the amine-based library was investigated. The efficiency and selectivity of base incorporation in the presence of different templates was analyzed.

With regard to previous results (Chapter 3.4.2), AE-HPLC was performed using a high temperature (80 °C) in order to achieve better resolution. High temperature allowed the elution of **ON1** from the rest of the product strands which was not possible at high pH. As shown in Figure 41, in each case **ON1** was eluted earlier than the rest, whereas templates were eluted at longest retention times. The presence of different templates gave different conversion of **ON1**. In presence of template $\mathbf{T}_C$, oligonucleotide **ON1** was completely consumed and the highest conversion of **ON1** was observed as predicted from the previous results.

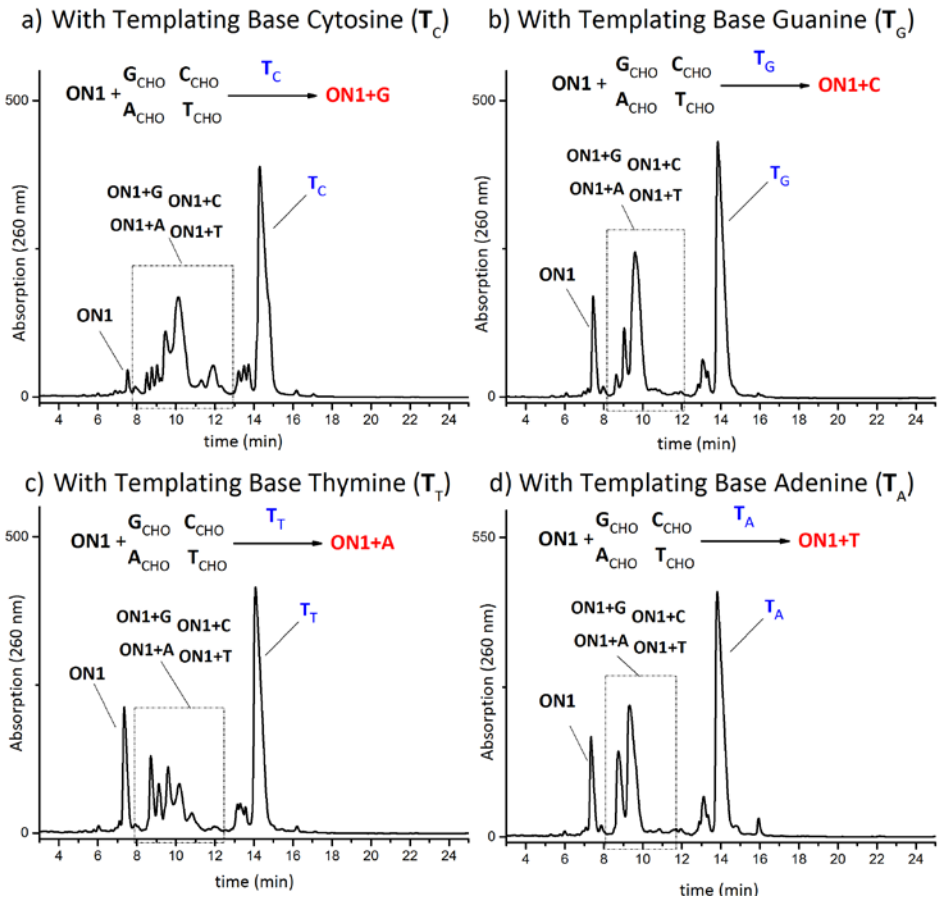

Figure 41: Representative AE-HPLC profiles (at 80 °C) after DNA-templated reductive amination for base-filling in the presence of all four nucleobases. Solvent system (A2) 20 mM Tris-Cl, pH 8; (B2) 20 mM Tris-Cl, 1.25 M NaCl, pH 8. Gradient 25-60% B2. a) In the presence of $\mathbf{T}_C$; b) In the presence of $\mathbf{T}_G$; c) In the presence of $\mathbf{T}_T$; d) In the presence of $\mathbf{T}_A$. Final concentrations in a 310 µL reaction volume: 20 mM sodium phosphate buffer, pH 6; 32 µM in **ON1** and template; $\mathbf{G}_{CHO}$ (1.3 mM), $\mathbf{C}_{CHO}$ (1.3 mM), A_{CHO} (1.3 mM), $\mathbf{T}_{CHO}$ (1.3 mM); 160 mM in $NaBH_3CN$**.**

All four products were eluted as a mixture of **ON1** and the template. Although **ON1** was efficiently separated, a second purification step was necessary for the separation of this mixture of products. Therefore, the mixture of the products (shown in Fig. 41 in a dot dashed rectangle) was collected and emposed to a second purification step by AE-HPLC but this time applying elevated pH as the method of denaturation. At high pH, the deprotonated oxygens of guanine and thymine were an advantage and better separation of the mixture into the four products was observed (Fig. 42).

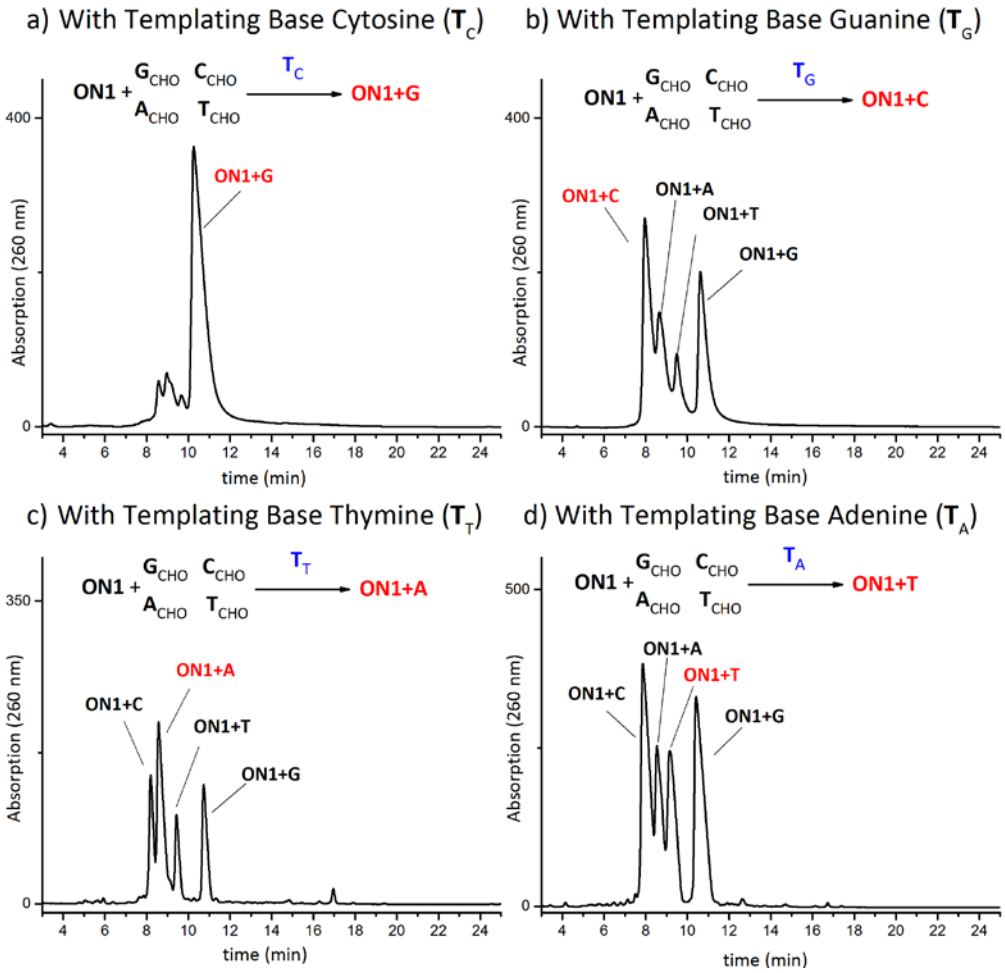

Figure 42: Representative AE-HPLC profiles (at pH 12) after DNA-templated reductive amination for base-filling in the presence of all four nucleobases. Solvent system (A3) 10 mM NaOH, pH 12; (B3) 10 mM NaOH, 1.25 M NaCl, pH 12. Gradient 35-70% B3. a) In the presence of $\mathbf{T}_C$; b) In the presence of $\mathbf{T}_G$; c) In the presence of $\mathbf{T}_T$; d) In the presence of $\mathbf{T}_A$. Final concentrations in a 310 µL reaction volume: 20 mM sodium phosphate buffer, pH 6; 32 µM in **ON1** and template strand; G_{CHO} (1.3 mM), C_{CHO} (1.3 mM), A_{CHO} (1.3 mM), T_{CHO} (1.3 mM); 160 mM in $NaBH_3CN$.

In presence of the template $\mathbf{T}_C$ (Fig. 42a), the peak which was corresponding to the mass of guanine incorporated product (**ON1+G**) was afforded. Only small amounts of other possible products were formed in comparison to **ON1+G**. This suggests that only one of the nucleobase amongst the four nucleobases was selectively incorporated into the oligonucleotide **ON1** that stabilizes the duplex formed with complementary $\mathbf{T}_C$. Upon addition of template strand $\mathbf{T}_G$, rising of a new peak was observed containing the mass of the cytosine incorporated product **ON1+C**. $\mathbf{T}_G$ induced the formation of cytosine incorporated product **ON1+C**. However, the selectivity of the cytosine incorporation was not as efficient as in case of guanine incorporation. In addition to the peak for **ON1+C**, the peaks for other mistemplated products were also identified. Amongst the mistemplated products, the guanine incorporated one (**ON1+G**) was obtained in higher ratios. Similar results were observed for adenine incorporation with template $\mathbf{T}_T$ where the peak

for product **ON1+A** was resolved as the most favorable one. A reaction in which the templating base was replaced with $\mathbf{T}_A$, HPLC results showed that the formation of thymine incorporated product **ON1+T** was the least selective one. Even the formation of mistemplated cytosine and guanine products were more favorable than the formation of **ON1+T**. Based upon this data, it can be concluded that when a new template was added, the library reorganized itself by amplifying the most stable product at the expense of others. The product which had the strongest binding to the template was dominant in the library. However, the composition of the library does not necessarily consist of only the strongest bound product, but rather reflects a combination of products by arranging the whole system to the lowest energy. Thus, except selective incorporation of guanine through $\mathbf{T}_C$ (Fig. 42a), in addition to the incorporation of the correct nucleobase, mistemplated products were also observed. However, in absence of a template no product formation was observed.

Concisely, in the presence of a suitable template, guanine was incorporated more selectively than cytosine, adenine and thymine. The efficiency of the thymine incorporation was the lowest amongst all four nucleobases. Because of the elution of the peaks with a close distance, a comparison between adenine and cytosine in their efficiency and selectivity could not be determined. However, a better selectivity of cytosine than adenine can be predicted due to the higher numbers of hydrogen bonds of cytosine and guanine compared to adenine and thymine. Furthermore, due to higher π-stacking, guanine incorporation was more efficient than cytosine and likewise, adenine incorporation was more efficient than thymine.

In order to have a better understanding of the reasons behind the selectivity, the duplex stabilities for **ON1+G**, **ON1+C**, **ON1+A** were investigated (unfortunately, **ON1+T** was excluded from this experiment because of not having enough sample). A series of melting temperature experiments were conducted for duplexes of **ON1+G**, **ON1+C**, **ON1+A** with their complementary template strands $\mathbf{T}_C$, $\mathbf{T}_G$ and $\mathbf{T}_T$ respectively (Fig. 43).

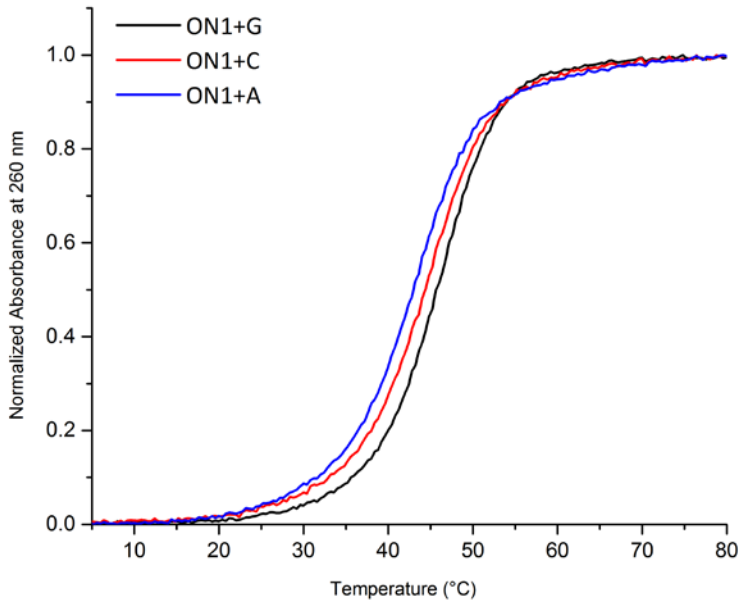

Figure 43: Melting curves for the duplex formation for the products **ON1+G**, **ON1+C**, **ON1+A** with their complementary strands $\mathbf{T}_C$, $\mathbf{T}_G$, $\mathbf{T}_T$. (2,5 µM ds-DNA, 10 mM sodium phosphate buffer, pH 7, 100 mM NaCl).

It can be apparently seen that, the highest melting temperature was obtained for **ON1+G** followed by **ON1+C** and **ON1+A**, respectively. This provides further confirmation of the selectivities observed for the nucleobases.

Table 5: Melting temperatures of the products **ON1+G**, **ON1+C**, **ON1+A** with their complementary strands $\mathbf{T}_C$, $\mathbf{T}_G$, $\mathbf{T}_T$.

Duplex	Sequence[a, b]	T_m/°C [c]
ON1+G·T$_C$	5'-d(CGCTAT**X**$_G$TATCGC)-3'· 5'-d(GCGATA**C**ATAGCG)-3'	46.2 (34.1)
ON1+C·T$_G$	5'-d(CGCTAT**X**$_C$TATCGC)-3'· 5'-d(GCGATA**G**ATAGCG)-3'	44.7 (35.5)
ON1+A·T$_T$	5'-d(CGCTAT**X**$_A$TATCGC)-3'· 5'-d(GCGATA**T**ATAGCG)-3'	42.9 (33.7)

[a] Herein the capital letter under **X** stands for the guanine, cytosine and adenine incorporated products.

[b] The GTT sequence at 3'-end was removed from the templates $\mathbf{T}_C$, $\mathbf{T}_G$ and $\mathbf{T}_T$ for melting temperature experiments.

[c] The values in brackets (blue) represents the T_m of the ON1 from Table 2 in Chapter 3.1.1.3.

Prior to that, the duplex melting temperature of **ON1** with its complementary strands was measured and the results specified (Table 2, Chapter 3.1.1.3) the insertion of a threoninol linker within the oligonucleotide lowering the duplex stability because the formation of an acyclic and

abasic site disturbed the backbone. However, the filling of the abasic site with one of the nucleobase raised the T_m about 10 °C higher than the **ON1**.

3.4.4 Base-Filling in Presence of Non-equimolar Amounts of Nucleobases

According to Le Chatelier's principle, changing the starting concentrations of the nucleobase-aldehydes would change the composition of the products in the dynamic library. In order to increase the selectivity of the nucleobases which were incorporated in lower yields under equimolar conditions, the initial concentrations of those nucleobase-aldehydes were increased. **ON1** (32 μM) was allowed to react with four nucleobase-aldehydes in concentrations $\mathbf{G}_{CHO}$ (1.3 mM), $\mathbf{C}_{CHO}$ (1.7 mM), $\mathbf{A}_{CHO}$ (2.3 mM), $\mathbf{T}_{CHO}$ (4.3 mM).

The change in the starting concentrations of the nucleobase-aldehydes resulted in a change in the proportions of the products in the library (Fig. 44). The peak for the favourable product had the highest intensity in each case. However, an increase in the concentration of the nucleobase-aldehydes resulted in an increase in the formation of the mistemplated products as well.

Guanine incorporation was still selective even in the presence of excess concentrations of the other nucleobase-aldehydes (Fig. 44a). Although the formation of the favourable products for cytosine and adenine incorporation was observed, the formation of mistemplated products was unavoidable. Due to the high concentration of thymine-aldehyde, the efficiency in the formation of thymine incorporated product in the presence of $\mathbf{T}_A$ was increased in comparison to the same reaction in less concentration of thymine (Fig. 44d).

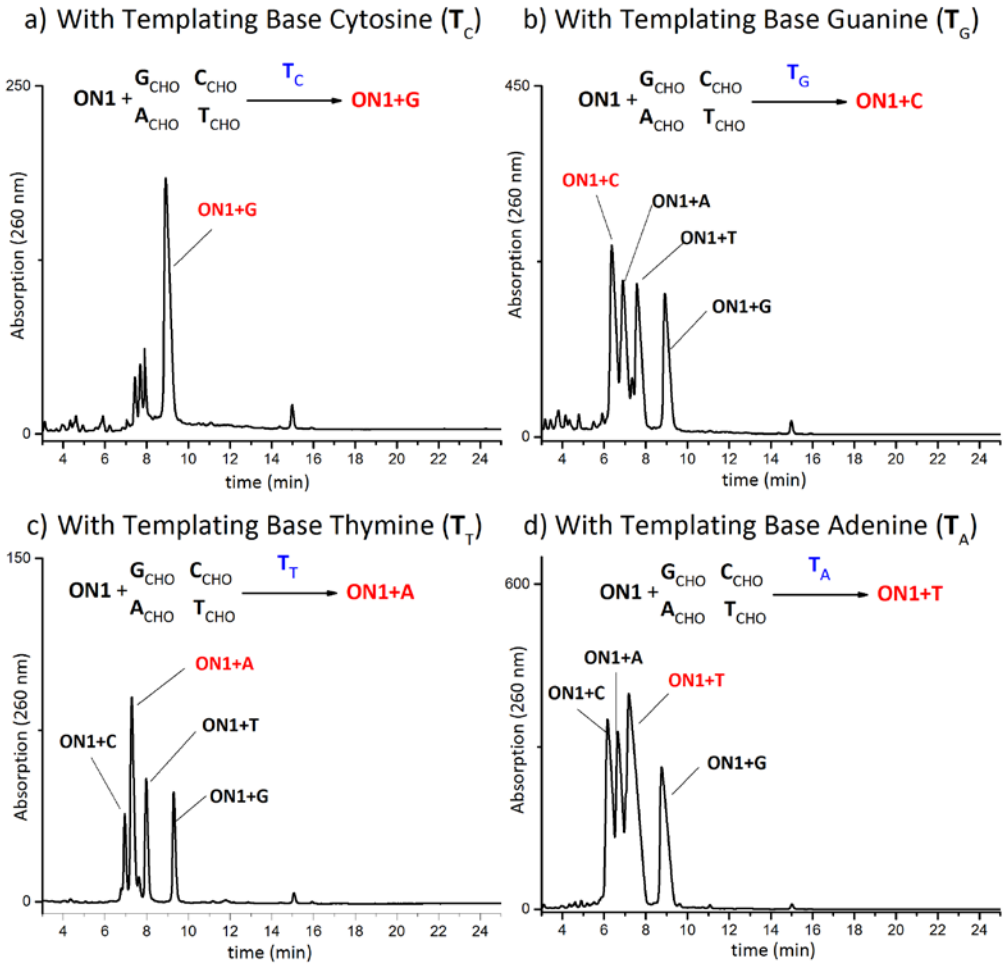

Figure 44: Representative AE-HPLC profiles (pH 12) after DNA-templated reductive amination for base-filling in the presence of all four nucleobases. Solvent system (A3) 10 mM NaOH, pH 12; (B3) 10 mM NaOH, 1.25 M NaCl, pH 12. Gradient 35-70% B3. a) In the presence of $\mathbf{T}_C$; b) In the presence of $\mathbf{T}_G$; c) In the presence of $\mathbf{T}_T$; d) In the presence of $\mathbf{T}_A$. Final concentrations in a 310 µL reaction volume: Final concentrations in a 310 µL reaction volume: 20 mM sodium phosphate buffer, pH 6; 32 µM in **ON1** and template strand; G_{CHO} (1.3 mM), C_{CHO} (1.7 mM), A_{CHO} (2.3 mM), T_{CHO} (4.3 mM); 160 mM in $NaBH_3CN$.

3.4.5 Test of Reversibility

In order to investigate the reversibility of the nucleobase incorporation, in the absence of the guanine-aldehyde ($\mathbf{G}_{CHO}$), the cytosine-, adenine- and thymine-aldehydes ($\mathbf{C}_{CHO}$, $\mathbf{A}_{CHO}$ and $\mathbf{T}_{CHO}$) (1.3 mM) were added to a 1:1 mixture of **ON1** (32 µM) and $\mathbf{T_C}$ (32 µM). Reaction mixture was stirred for three hours at room temperature and $\mathbf{G}_{CHO}$ was added into this reaction mixture immediately before reduction which was then further shaken for one hour.

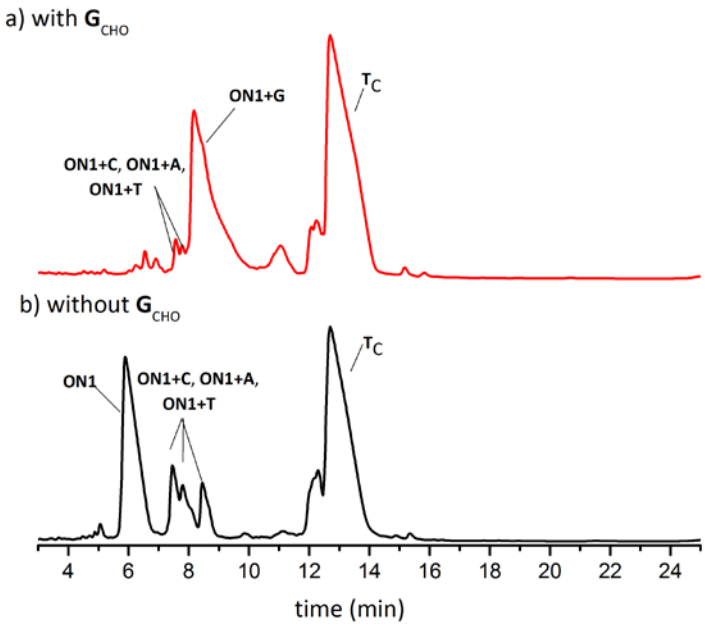

Figure 45: Representative AE-HPLC profiles after DNA-templated reductive amination for base-filling in the presence of $\mathbf{G}_{CHO}$ (red) and in the absence of $\mathbf{G}_{CHO}$ (black). Solvent system (A2) 20 mM Tris-Cl, pH 8; (B2) 20 mM Tris-Cl, 1.25 M NaCl, pH 8. Gradient 25-60% B2.

Reaction in the absence of guanine-aldehyde resulted in the formation of cytosine, adenine and thymine incorporated products (Fig. 45b). Upon addition of the $\mathbf{G}_{CHO}$, the incorrect products were corrected through the formation of guanine incorporated product (**ON1+G**) (Fig.45a). This result indicated the adaptive and flexible nature of the dynamic library and the reversibility of the selection process.

3.4.6 ABASIC TEMPLATING

Abasic sugar sites are common type of lesion in DNA.[130] Due to its biological importance, there is a strong investigation for recognizing the abasic sites in DNA for diagnostic applications.[131] As a part of those investigations, the use of aromatic residues with large π-surfaces opposite to the abasic site in order to stabilize the duplex DNA has been reported.[132,133] An abasic site in an oligonucleotide duplex causes a distortion because of lack of continuity of the base stacking.[131] It has been reported that a complemantary oligonucleotide with flat, aromatic residues opposite to the abasic site can be used to stabilize the oligonucleotide duplex.[129] The aromatic residues can compensate the missing nucleobase by providing the aromatic stacking within the duplex. Thus, nucleosides carrying pyrene and other polyaromatic hydrocarbons have been used in order to compensate the missing nucleobase.[134] Furthermore, the use of non-nucleosidic phenanthrene and phenantrolines as base surrogates has been reported to stabilize the abasic sites in a DNA duplex.[128]

By taking this into consideration, ,10-phenantroline-2-carbaldehyde (**P2**$_{CHO}$) was used in dynamic incorporation reactions in order to investigate the effect of an abasic site in the template strand. A DNA template (**T**$_P$) which had an abasic ribose moiety opposite to the acyclic site of **ON1** was used in the dynamic incorporation reactions (Fig. 46).

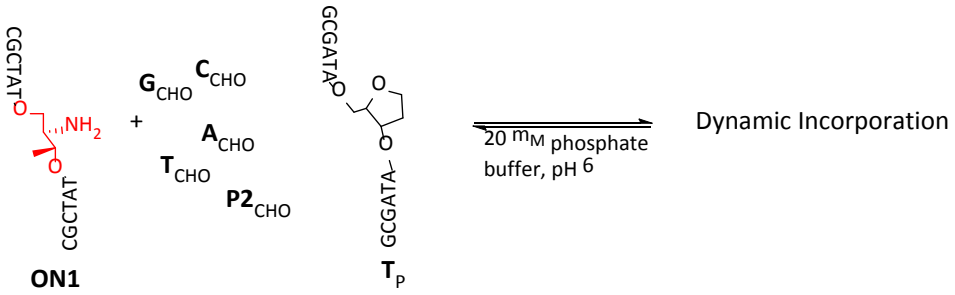

Figure 46: The use of abasic DNA template for the reversible incorporation of nucleobase-aldehydes, **G**$_{CHO}$, **C**$_{CHO}$, **A**$_{CHO}$ and **T**$_{CHO}$ and phenantroline-aldehyde **P2**$_{CHO}$.

In a reaction where the **P2**$_{CHO}$ together with **G**$_{CHO}$, **C**$_{CHO}$, **A**$_{CHO}$ and **T**$_{CHO}$ (each in 1.3 mM) were added into a 1:1 mixture of **ON1** (32 µM) and the abasic template **T**$_P$ (32 µM) showed the selective incorporation of **P2**$_{CHO}$ (Fig. 47).

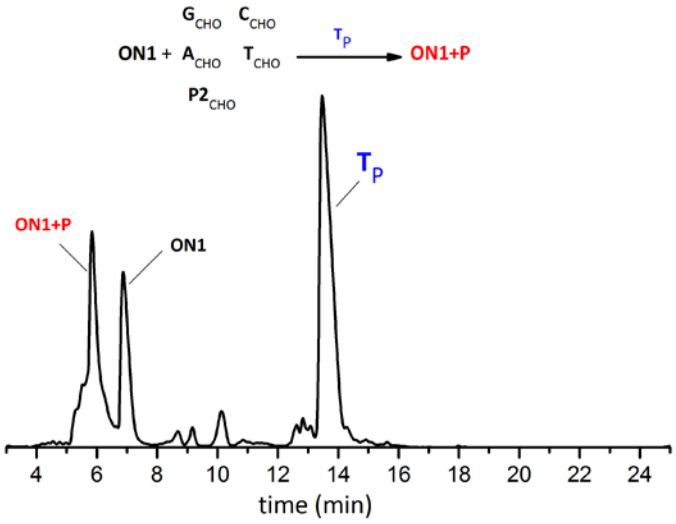

Figure 47: Representative AE-HPLC profiles after DNA-templated reductive amination for base-filling in the presence of **P2**$_{CHO}$. Solvent system (A2) 20 mM Tris-Cl, pH 8; (B2) 20 mM Tris-Cl, 1.25 M NaCl, pH 8. Gradient 25-60% B2.

Phenantroline incorporated product (**ON1+P**) eluted in shorter retention times than **ON1**. The analysis of the peak of **ON1+P** by ESI-MS showed a mass difference of a *m/z* = +60. That might be a result of copper ion coordination. Therefore oligonucleotide (**ON1+P**) was passed through a

Chelex®-100 resin in order to remove all metal residues coordinated during the synthesis and purification steps. The ESI-MS analysis after this process showed the expected mass for (**ON1+P**).

3.5 DISCUSSION

The dynamic imine library between the primary amine on a pre-formed DNA backbone and a pool of monomeric nucleobase-aldehydes was established in presence of a complementary DNA template. The four possible products, which resulted from the incorporation of the four nucleobases, in the imine library were analyzed after their subsequent reduction to an amine library. As analysis method anion exchange-HPLC and ESI-MS was chosen. The combination of these two techniques enabled the separation of the species in the library followed by their identification. The separation by HPLC gave convenient information about the number of different products present in the library. The subsequent analysis of the HPLC output by ESI-MS identified each of the detected species. In order to discuss the relative amounts of each product in the library, the ideal HPLC seperations should include better resolution of the peaks. If this prerequisite could be fulfilled, ratio of the composition of any library member could be quantified by a comparison of the peak areas. If the relative amounts of each product could have been obtained, a better discussion on the selectivity for each nucleobase could be given. For all that, with the analysis method applied in this thesis, any change in the proportion of the products could be successfully proven from the peak intensities. In short, the advantage of DCC is in that it allows an easy synthesis of a large range of compounds which are closely related in terms of molecular reactivity and structure. This advantage can turn into a limitation at the point of analyzing the library composition.

The attempt attaching nucleobases to the abasic site on DNA backbone showed no product formation in the absence of a DNA-template. However, under same conditions the addition of a DNA-template into the reaction enabled the attachment of the nucleobases on the abasic site. The correct nucleobase amongst four nucleobases was selectively chosen by the DNA template through Watson-Crick base pairing and stacking interactions. Four imine products were formed but the one with the correct hydrogen bonding with the template was the most stable one, so the most dominant one. When a new template was added, the change in the ratios of the products in the library showed the adaptive nature of the library. This further indicates the role of the template in the selection process of the nucleobases. The attachment of guanine in the presence of an appropriate template proceeded with good yields and good selectivity. Only small amounts of mistemplated product was observed. Attachment of cytosine, adenine and thymine in presence of their templating bases, showed tendency in the formation of the favourable product, however, the selectivity was not as high as the attachment of guanine. Mistemplated products were observed in higher proportions during the incorporation of adenine, cytosine and thymine. The highest selectivity was observed for the guanine

incorporation and this has been attributed to the greater numbers of hydrogen bonds. The lowest selectivity was observed for the thymine incorporation probably due to the formation of only two hydrogen bonds with the templating base. Since the cytosine and adenine incorporated products were eluted in a close distance to each other, it was difficult to determine their selectivities. A better selectivity can be predicted for the cytosine than adenine due to the number of hydrogen bonds. Stacking interactions play also a role in the selectivity besides the hydrogen bonds. Purine bases were incorporated with better yield and greater selectivity than pyrimidines (G>C>A>T).

Following Le Chateliers`s principle for the library in dynamic equilibrium, the starting concentration of the thymine was increased because thymine was the least selectively incorporated nucleobase. The increased starting concentrations of thymine nucleobase aldehyde resulted in an increased change in the ratio of thymine incorporated product. On the other hand, the ratio of mistemplated thymine products was also increased. In future studies, the starting concentration of the bases could be optimized to improve the selectivity of the incorporation.

An interesting result was obtained from a reaction in which a DNA template that had an abasic site at the templating position. In this case **P2**$_{CHO}$ was incorporated in better yields. Those results had been attributed to the stacking interactions of phenantroline.[135]

Prior to this thesis, two similar studies were carried out using imine exchange reaction to fill the abasic sites on PNA using nucleobase-aldehydes by LIU and co-workers and by BRADLEY and co-workers.[97,115] Although the imine chemistry employed in this thesis is the same with the previously published works, herein the use of a DNA backbone with amine group for base filling approach instead of PNA backbone presents a new approach for DCC applications to oligonucleotides. In their works MALDI-MS was used for the analysis which enabled the quantification of the selectivities of the nucleobases by comparing the intensities of the products. BRADLEY and co-workers extended the application to the genetic analysis.[115] They were able to analyze the sequence of the complementary DNA template through selective incorporation of nucleobases on the PNA abasic positions.

The results obtained from their published works, provided further confirmation to the results presented in this thesis for the selectivities for four nucleobases. Guanine and cytosine were incorporated more selectively than either adenine and thymine. Furthermore, purine bases were incorporated more selectively than pyrimidines due to the greater stacking interactions. In their work formation of mistemplated products was observed in very small amounts. However, in this

thesis the proportions of the mistemplated products in the composition of the library were observed in significant ratios.

For future studies, the ability of base-filling can be extended on a DNA backbone that has two or more neighbouring blank positions. But a better optimization for the here applied HPLC method would be necessary. The dynamic base-filling reactions on DNA/DNA duplex can be extended to genetic analysis by a direct read-out with MALDI-MS. Furthermore, oligonucleotides with thiol functional groups on the backbone can be used to investigate another reversible reaction like thioester exchange process based on dynamic combinatorial chemistry.

The dynamic chemistry assay described here can be applied using labelled nucleobase-aldehydes and their subsequent analysis by fluorescence detection. On the other hand, not only natural nucleobases but novel nucleobases can be also screened through dynamic base-filling reactions

4 DNA-BASED CATALYSIS

The incorporation of transition metal complexes into DNA is an important objective for the development of DNA-based hybrid catalysts. The metal complexes can bind to DNA via noncovalent and covalent attachment. So far, the covalent incorporation of the transition metal complexes into DNA sequence was mostly considered at the 5'- or 3'-end or internally, either at the nucleobase or at the ribose 2'-position.[136,137] *In this chapter, the post-synthetic, covalent incorporation of the phenantroline (phen) ligand to the acyclic backbone of DNA is described. By anchoring an achiral 1,10-phenantroline-copper(II) complex into dsDNA, we aimed to generate a novel DNA-based catalyst in order to investigate its performance in the copper(II)-catalyzed Diels-Alder reaction in water.*

4.1 CONCEPT OF DNA-BASED HYBRID CATALYSIS

Apart from template-directed reactions, another application of DNA is the use of double-stranded DNA as a stereochemical control element in enantioselective reactions.[19,138] In this role of DNA as stereocontrol element, DNA does not behave directly as a catalyst but provides a chiral environment in asymmetric reactions.[19] This catalytic ensemble requires the use of an achiral metal ligand together with DNA. The catalytically active transition metal ligand is non-covalently or covalently anchored to the DNA double helix for the assembly of DNA-based hybrid catalysis. Although the ligand is achiral, the corresponding metal complex with DNA is chiral. Thus, in a catalytic process, the metal coordinated ligand provides the catalytic activity and the DNA provides the enantioselectivity by its secondary coordination sphere. With this approach, the catalytic reaction takes place in, or very closed to the chiral DNA helix structure. The chirality is transferred from the DNA to the catalyzed reaction and enables the preferred formation of one of the enantiomers of the reaction products in excess.

Among applications of asymmetric reactions, a series of DNA-based catalysis has been developed, which use a hybrid catalyst composed of dsDNA and a copper(II) complex.[121,139,140] The catalytic activity was investigated in a copper catalyzed Diels-Alder reaction in water.[141–144] The application shows that the use of DNA-based hybrid catalysts leads to high enantioselectivity, whereas in the absence of DNA, the corresponding products are obtained as racemats.

Recently, a DNA-based asymmetric catalysis approach was introduced by ROELFES and co-workers.[143] In their modular assembly three oligonucleotides are used (Fig. 48a): The first oligonucleotide is functionalized with 2,2'- bipyridine at the 5'-end phosphate group (Oligo 1); the second oligonucleotide (Oligo 2) is an unfunctionalized oligonucleotide and the third oligonucleotide is the template strand complementary to both oligonucleotides (Oligo 1 and Oligo 2). Using their chiral catalyst, the copper catalyzed Diels-Alder reaction between α,β-unsaturated 2-acylpyridine (aza-chalcone) and cyclopentadiene was investigated (Fig. 48b). The reaction between **30** and **31** (Fig. 48) gives four products: two enantiomeric endo products (**32**) and two enantiomeric exo (**33**) products. In absence of the DNA-based catalyst, the reaction products were racemic however with the use of their DNA-based catalytic approach, moderate to good enantiomeric excess (*ee*) was achieved: 71% conversion of **31** to endo and exo products and 93% *ee* for the major isomer (endo). Therefore, it is clear that the enantioselectivity of the reaction came from DNA. However, the mechanism behind that, the induction of the DNA and its control over the enantioselectivity is not fully understood and remains a challenge.

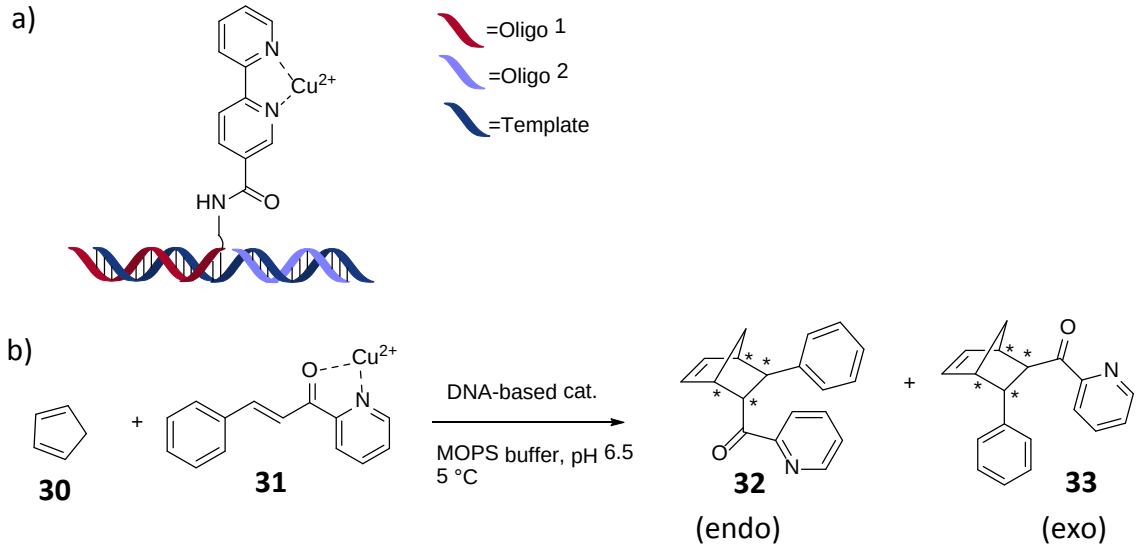

MOPS= 3-(*N*-morpholino)propansulfonic acid

Figure 48: a) Schematic representation of the assembly of the DNA-based catalysts used in the work of ROELFES and co-workers.[143] b) Diels-Alder reaction between aza-chalcone (**31**) and cyclopentadiene (**30**) to afford the endo product (**32**) and exo product (**33**).

4.2 POST-SYNTHETIC INCORPORATION OF PHENANTROLINE TO OLIGONUCLEOTIDES

The first part of this thesis (Chapter 3) describes the incorporation of a D-threoninol-based acylic linker into the oligonucleotide strand in order to generate a ribose free, acyclic site in the backbone and its subsequent application in dynamic combinatorial chemistry. The presence of the reactive amino group on the backbone of the modified oligonucleotide enables its further functionalization by tethering appropriate functional molecules such as metal ligands. Metal ligands can be post-synthetically tethered, with a carboxyl group irreversibly or with an aldehyde group reversibly, to the amino group on the modified oligonucleotide. During the dynamic chemistry process which was applied in the first part of this thesis, the reversible attachment of the aldehyde modified phenantroline (**P2**$_{CHO}$) on the modified oligonucleotide **ON1** in the presence of a complementary template strand was described. The template-directed incorporation of the phenantroline ligand to the specific position on the DNA was recalled here in Figure 49. The covalent attachment of the metal ligand (**P2**$_{CHO}$) through reductive amination has been accomplished by post-synthetic functionalization. After succesful incorporation of the phenantroline ligand (**P2**$_{CHO}$) to the **ON1**, the single stranded **ON1+P** was separated from unreacted strand (**ON1**) and its complementary strand (**T**p) by AE-HPLC.

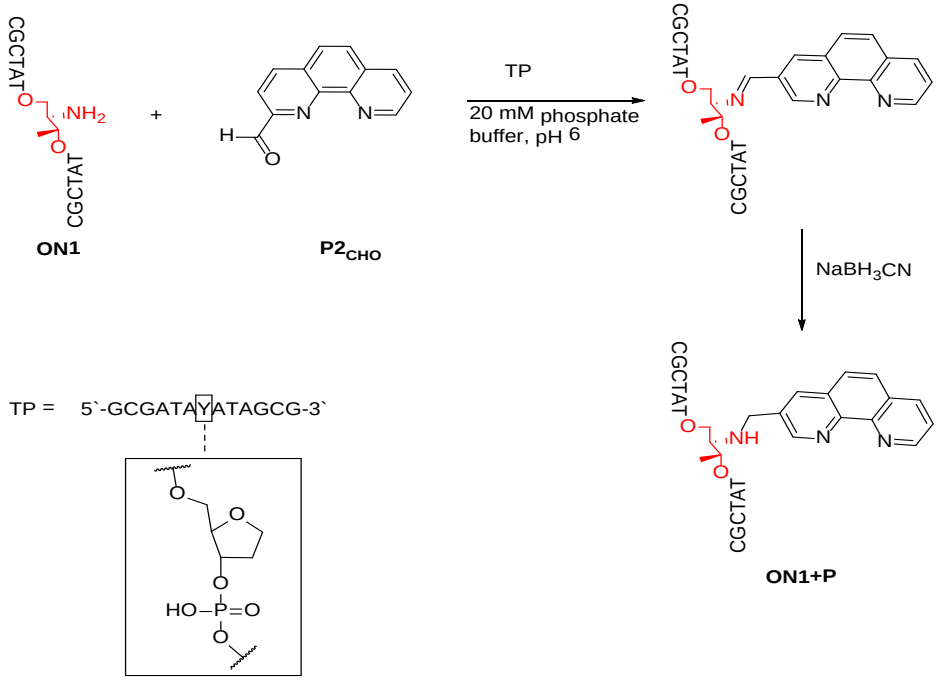

Figure 49: The template-directed attachment of the phenantroline-aldehyde ligand to the amino group on the **ON1** through reductive amination. $\mathbf{T}_P$ is the complementary template strand with an abasic site opposite to amine functionality.

4.3 Assembly of DNA-Based Metal Complex

In order to design a DNA-based catalysis, a metal ligand is post-synthetically attached to the DNA via a covalent linkage. Subsequent hybridization in the presence of a metal salt allows the DNA-based catalysis (Fig. 50).

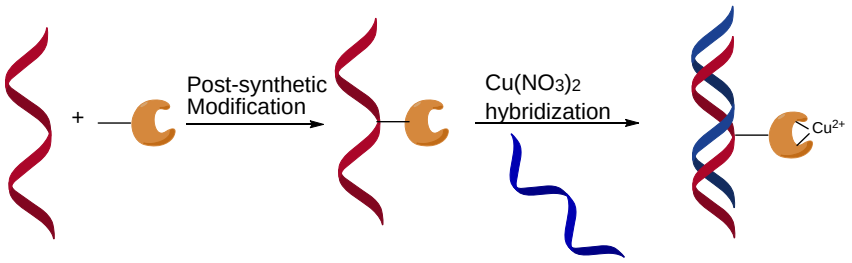

Figure 50: Schematic representation of the assembly of the DNA-based catalyst.[redrawn from [145]]

The copper coordinated DNA-based system was assembled by thermal annealing of the equimolar amounts of **ON1+P** and its complementary strand (**T**p) in the presence of copper(II) salt as shown in Figure 51. The aqueous solutions of **ON1+P** (12 nmol) and **T**p (12 nmol) were mixed together and freeze-dried. To the freeze-dried mixture of the oligonucleotides, a solution of copper(II) nitrate trihydrate ($Cu(NO_3)_2 \cdot 3H_2O$) (12 nmol) in annealing buffer (10 mM Tris, pH 7) was added. The solution was heated up to 80 °C and then cooled down slowly to room temperature. Hybridization in the presence of the metal ion gave rise to the formation of the duplex DNA and the catalytically active metal complex is positioned internally. After the annealing process, the double-stranded **ON1+P** (ds**ON1+P**) was passed through a gel filtration column in order to remove excess of copper salts. The ds**ON1+P** coordinated with copper metals was proven in its single-stranded form by ESI mass spectrometry.

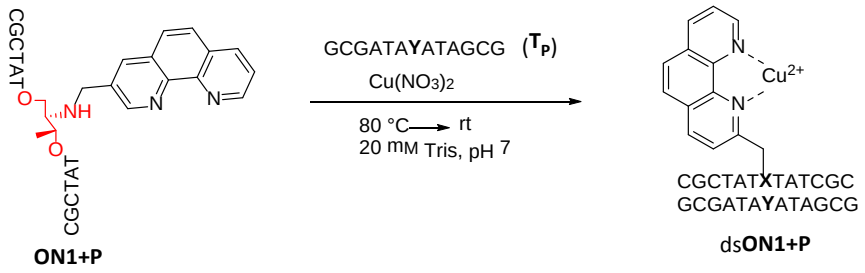

Figure 51: Synthesis of the assembly of the DNA-based catalyst, ds**ON1+P**.

After annealing, the melting temperature was determined for ds**ON1+P** (Fig. 52) and showed that the system remained hybridized. The melting temperature of the duplex was determined as 33.8 °C.

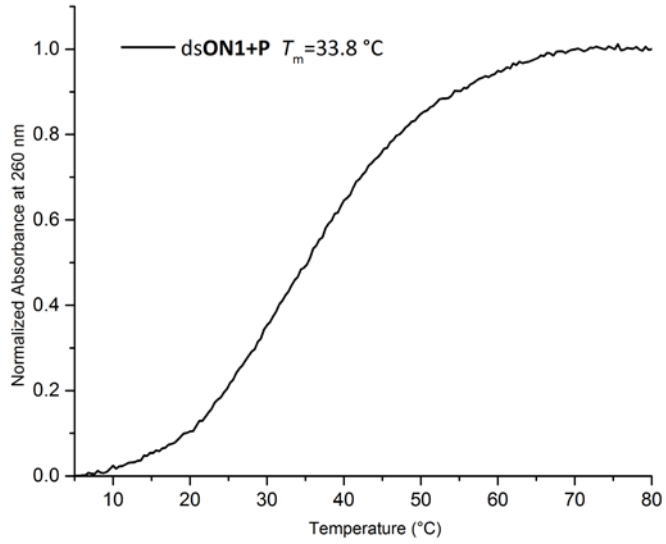

Figure 52: Melting curve for the DNA-based phenantroline catalyst coordinated with copper (ds**ON1+P**). (2,5 μM ds-DNA, 10 mM sodium phosphate buffer, pH 7, 100 mM NaCl).

For the DNA-based 1,10-phenantroline-copper(II) complex (ds**ON1+P**), circular dichroism (CD) measurements showed a positive ellipticity maximum at 275 nm and negative minimum at around 250 nm with a crossover around 260 (Fig. 53). This corresponds to the typical B-DNA structure and suggests the modification did not change the structure of DNA assembly.

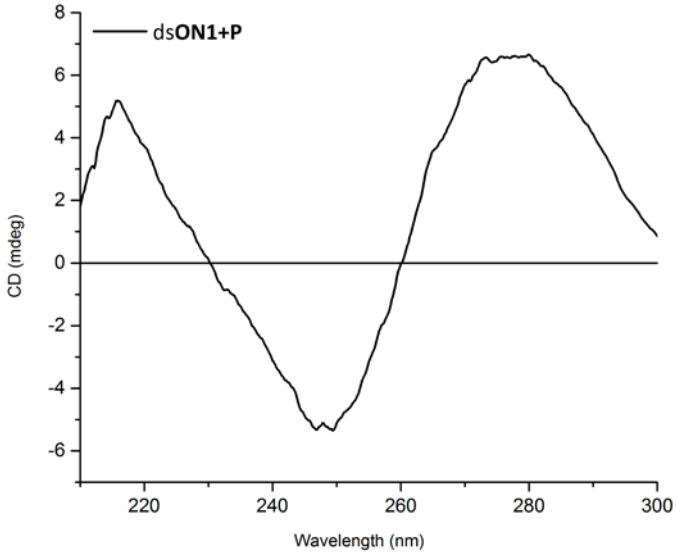

Figure 53: CD spectrum for the DNA-based phenantroline catalyst (ds**ON1+P**). (5 μM ds-DNA, 10 mM sodium phosphate buffer, pH 7, 100 mM NaCl).

4.4 APPLICATION OF DNA-BASED CATALYSIS IN DIELS-ALDER REACTION

Herein, the catalytic performance of ds**ON1+P** was tested in a Diels-Alder reaction between aza-chalcone (**31**) and cyclopentadiene (**30**) under same conditions as described in literature known applications (Fig. 48).[142,143]

In an initial experiment, the reaction was carried out in absence of the DNA-based catalyst, ds**ON1+P**. The aza-chalcone in acetonitrile (**31**) (120 nmol) and the excess of cyclopentadiene (**30**) (1.20 mmol) were mixed in MOPS buffer (20 mM, pH 6.5) in the presence of $Cu(NO_3)_2$ (12 nmol, 10 mol%). Reaction was perfomed at 5 °C. The reaction mixture was observed at various time scales by HPLC and results are given in Figure 53. After one day, the peak for aza-chalcone (**31**) was still there and the formation of the endo and exo products (**32**-**33**) was observed only in small amounts (Fig. 53a). After three days, the peak for aza-chalcone (**31**) was decreased and the formation of a new peak for the products (**32-33**) was obtained (Fig. 53b). Hereafter, further experiments between aza-chalcone and cyclopentadiene were performed with a reaction time of three days. The conversion of **31** (81%) into products (**32-33**) with a reaction time of three days was determined by a comparison of the HPLC peak areas of the product and the starting material (Table 6). The peak for the products **32-33** was collected and analyzed by chiral HPLC in order to determine the diastereoselectivity (endo:exo) and enantiomeric excess (*ee*) according to literature (Table 6).[143,146]

No product formation was observed in a reaction between aza-chalcone and cyclopentadiene in absence of copper showed the essential role of Cu^{2+} as Lewis acid in this reaction (Fig. 53c).

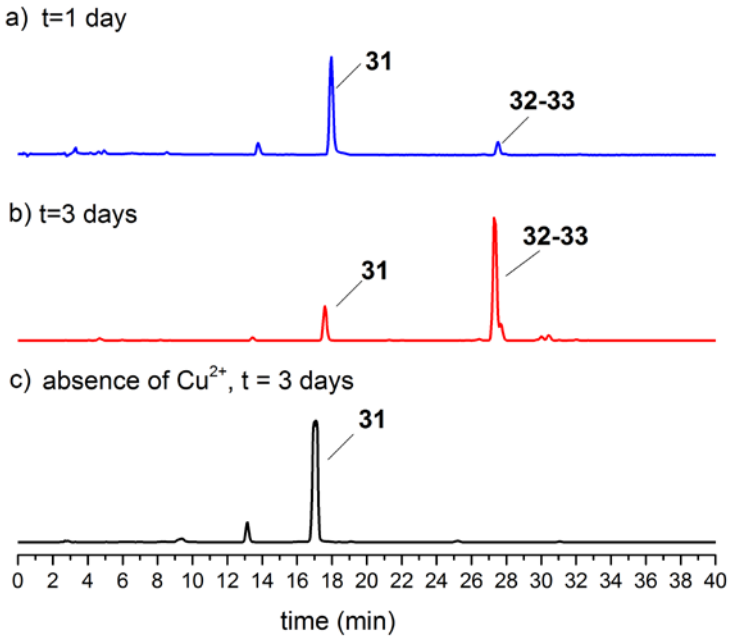

Figure 53: Representative RP-HPLC profiles of the Diels-Alder reaction between aza-chalcone (**31**) and cyclopentadiene (**30**) in order to afford endo and exo products (**32**-**33**). Solvent System (A4) H_2O, 0.1% TFA; (B4) MeOH, 0.1%TFA. Gradient 50-100% B4**.** a) Diels-Alder reaction after one day in the presence of $Cu(NO_3)_2$; b) Diels-Alder reaction after three days in the presence of $Cu(NO_3)_2$; c) Diels-Alder reaction after three days in the absence of $Cu(NO_3)_2$.

In the next step, the same reaction was carried out in the presence of DNA-based catalyst (ds**ON1+P**) (12 nmol, 10 mol%) by mixing azachalcone (120 nmol) and excess of cyclopentadiene (1.20 mmol) in MOPS buffer (20 mM, pH 6.5). Reaction was perfomed at 5 °C in order to keep the double-stranded oligonucleotide in its hybridized form. After three days, the reaction mixture was analysed by RP-HPLC (Fig. 54). The conversion of the aza-chalcone (**31**) to the endo and exo products (**32**-**33**) by a comparison of the HPLC peak areas was calculated as 60% (Fig. 54). The use of DNA-based catalyst (ds**ON1+P**) resulted with a low conversion (60%) than that of the $Cu(NO_3)_2$ catalyzed reaction (Table 6).

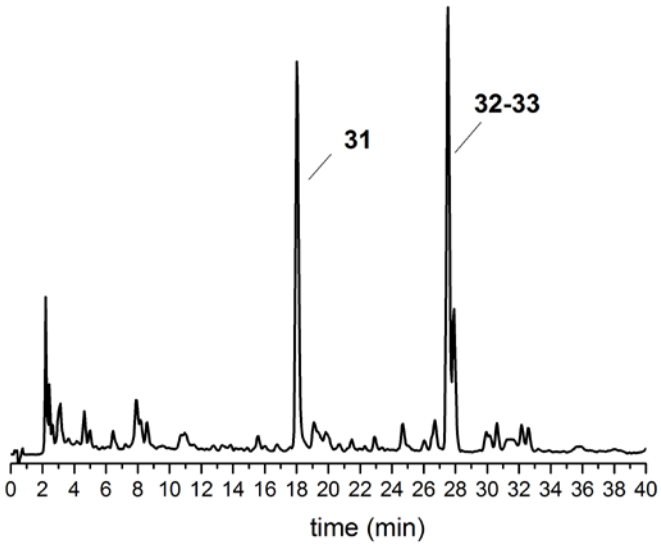

Figure 54: Representative RP-HPLC profiles after Diels-Alder reaction between aza-chalcone (**31**) and cyclopentadiene (**30**) in order to afford endo and exo products (**32**-**33**). Diels-Alder reaction after three days in the presence of ds**ON1+P**. Solvent System (A4) H_2O, 0.1% TFA; (B4) MeOH, 0.1%TFA. Gradient 50-100% B4**.**

The eluted peaks for the products **32**-**33** were collected and analyzed by chiral HPLC in order to determine the diastereoselectivity (endo:exo) and enantiomeric excess (*ee*). However, the use of DNA-based hybrid catalyst (ds**ON1+P**) itself did not show the predicted enantioselectivity in the reaction.

Table 6: Diels-Alder reactions catalyzed by $Cu(NO_3)_2$ or DNA-Cu^{2+} complex.

Catalyst	Conversion[a] (%)	endo:exo[a]	*ee*[b]
$Cu(NO_3)_2$	81	93:7	0
ds**ON1+P**	60	93:7	0

[a] Determined by RP-HPLC peak areas of aza-chalcone (**31**) and the products (**32-33**).
[b] Determined by chiral HPLC peak areas of endo and exo product.

4.5 DISCUSSION

The covalent attachment of the phenantroline based metal ligand to the backbone of the DNA resulted in the formation of a DNA-based catalyst. This DNA-based catalytic system was used in a Cu^{2+} catalyzed Diels-Alder reaction in water. Although 60% conversion was obtained, no enantioselectivity in the product of the reaction was observed. Inspite of the results obtained here, further studies are necessary to obtain enantioselectivities in asymmetric reactions.

Most challenging but time-consuming part in this work was the design of the DNA-based metal complex including the covalent attachment of the ligand to the oligonucleotide and its coordination to the copper. Even though one application of the DNA-based metal complex in Diels-Alder reaction was shown, more studies and efforts should be made for catalytic applications in future studies.

5. SUMMARY

With the growing field of DNA technology there is an increasing demand for new modifications of DNA, which improve its versatility and promote the DNA as a fundamental scaffold for a wide field of applications like catalysis, encoding processes and supramolecular functionalized structures.

The research described in this thesis includes the preparation of a modified oligonucleotide and is then focused on the functionalization of this modified oligonucleotide by a dynamic combinatorial chemistry approach. For the modification of the oligonucleotide, the ribose unit of the backbone in the native structure of DNA was replaced by D-threoninol. In order to achieve this purpose, in the first step D-threoninol (**1**) was successfully converted to the phosphoramidite monomer **4** with an orthogonal protected amino group (Fig. 55). The corresponding phosphoramidite monomer **4** was necessary in order to make it suitable for automated DNA synthesis. It was successfully incorporated into the central position of a 13mer oligonucleotide by using automated solid phase synthesis.

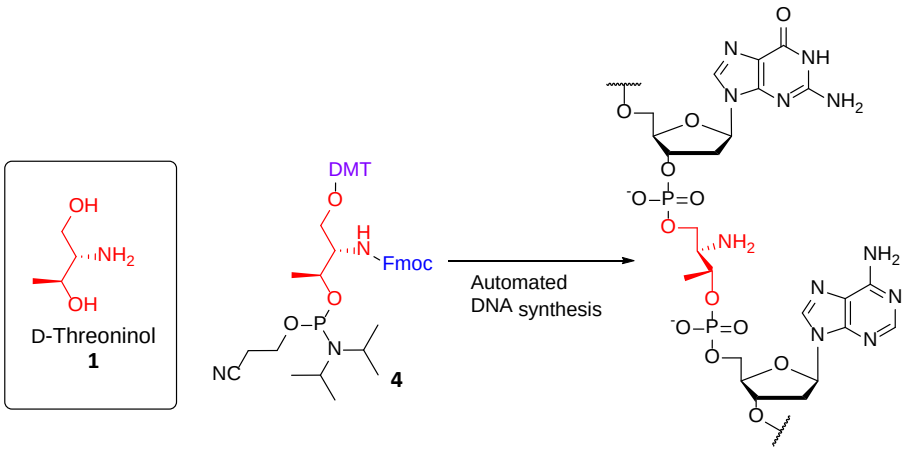

Figure 55: Phosphoramidite monomer **4** was incorporated into oligonucleotides via automated synthesis on a solid support.

The advantage of the reactive amino group on the backbone of the modified oligonucleotide was that any functional molecule of interest functionalized as an aldehyde can be easily tethered into the oligonucleotide post-synthetically. In this work the natural nucleobases were synthesized with aldehyde groups (Fig. 56) to allow them to reversibly react with the free amino group on the modified oligonucleotide.

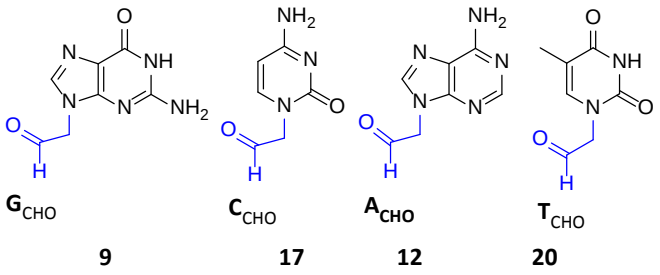

Figure 56: A set of aldehyde modified nucleobases, $\mathbf{G}_{CHO}$, $\mathbf{C}_{CHO}$, $\mathbf{A}_{CHO}$, $\mathbf{T}_{CHO}$.

This thesis is an example for the dynamic combinatorial chemistry approach applied to oligonucleotides demonstrating the selective attachment of aldehyde-modified nucleobase units to the abasic site of the double-stranded-oligonucleotide. This was achieved by allowing the modified oligonucleotide to react with four nucleobases through reversible imine formation in the presence of a complementary template strand. In the presence of four nucleobases, four possible imine products were obtained in the dynamic library but one of them was more dominant with respect to others. The correct nucleobase which paired with the nucleotide of the template strand according to Watson-Crick base pairing had the strongest binding to the template and was the dominant one in the library (Fig. 57). However, the composition of the library did not necessarily consist of the singly most strongly bound product, but rather reflected a combination of products by arranging the whole system. It was interesting to see that when a new template was added, the library reorganized itself by amplifying the most stable product at the expense of others. The results demonstrated the adaptive and flexible nature of the dynamic library. The dynamic library was proven to be responsive to the external influences that alter the relative thermodynamic stabilities of the library members.

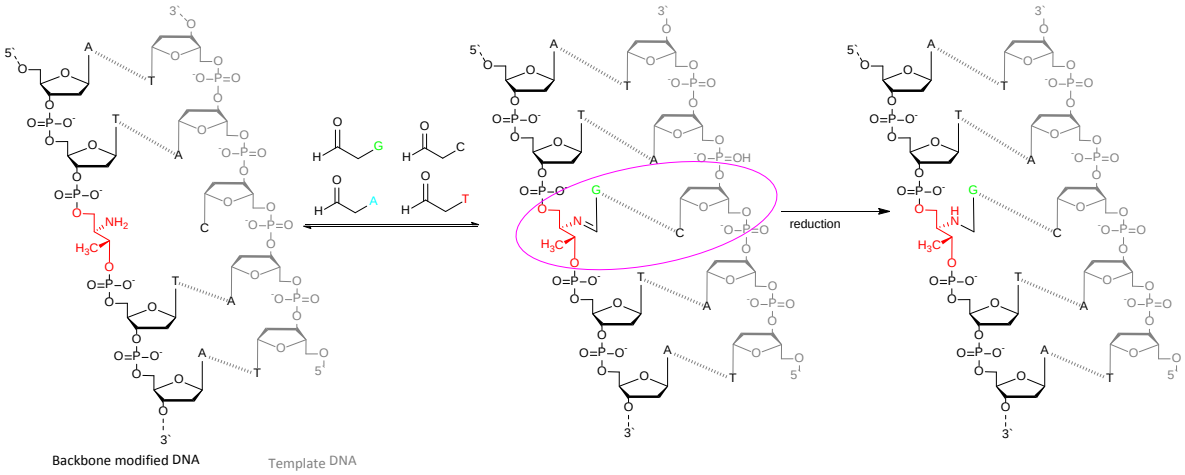

Figure 57: Schematic representation of the model system used in this work in order to functionalize the backbone modified oligonucleotide through dynamic chemistry approach. The selection of a guanine nucleobase through a complementary template strand including cytosine in its sequence. **G** for guanine, **C** for cytosine, **A** for adenine and **T** for thymine.

The composition of the dynamic library was investigated by anion exchange-HPLC and subsequent ESI-MS analysis. The number of hydrogen bonds and the stacking interactions played an important role in the selectivity of the nucleobases. The higher selectivity was observed for the guanine and cytosine than adenine and thymine due to their higher number of hydrogen bonds. Furthermore, purine bases were incorporated with better yield and greater selectivity than pyrimidines (G>C and A>T).

Not only nucleobases but also a metal ligand with π-surface was attached to the same modified oligonucleotide in order to gain a new function to the DNA. To achieve this purpose 1,10-phenantroline was functionalized as an aldehyde **29** (Fig. 58). Afterwards, the phenantroline ligand **29** was successfully attached to the amine of the modified oligonucleotide in presence of the template strand. In future works, various phenantroline-based ligands with extended π-surfaces can be prepared in order to attach them to the backbone of the modified oligonucleotide. Dynamic combinatorial chemistry is a promising approach for the selection and screening of the best bound ligand.

Furthermore, the phenantroline attached oligonucleotide was annealed with its complementary strand in the presence of copper ions in order to generate a DNA-based metal complex ds**ON1+P**. Finally, this DNA-based metal complex was used as catalyst in an application for an enantioselective Diels-Alder reaction. In presence of Cu(II) catalyst ($Cu(NO_3)_2$), the Diels-Alder reaction between a diene and dienophile gave products in racemic fashion. In a second reaction, the DNA-based hybrid catalyst ds**ON1+P** instead of free copper salts was used in order to obtain the products with enantiomeric stereoselectivity. However, the use of DNA-based hybrid catalyst ds**ON1+P** did not show the predicted enantioselectivity in the reaction. The aim of designing an efficient enantioselective DNA-based catalyst was not completed due to time limitation, but it represents the further outlook of this work.

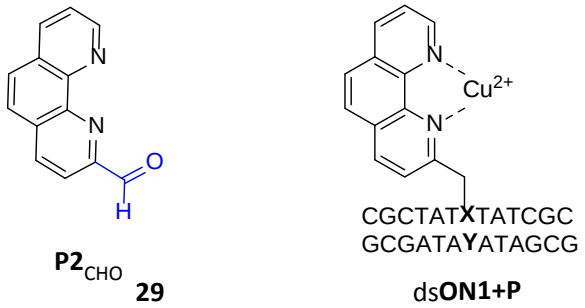

P2$_{CHO}$ **29** ds**ON1+P**

Figure 58: Aldehyde substituted phenantroline, **P2**$_{CHO}$ (left)and DNA-based metal complex, ds**ON1+P** (right).

6. EXPERIMENTAL PART

6.1 MATERIALS AND GENERAL INFORMATION

Reagents Unless otherwise stated, reagents were supplied by *Fluka* (Taufkirchen, Germany), *Sigma-Aldrich* (Taufkirchen, Germany), *Acros-Organics* (Geel, Belgium), *Merck* (Darmstadt, Germany), *ABCR* (Karlsruhe, Germany), *Fischer Scientific* (Nidderau, Germany) and *Alfa Aesar* (Karlsruhe, Germany) as analytical grade and used without further purification.

Solvents Solvents for flash chromatography (ethyl acetate, pentane, methanol, dichloromethane) were distilled prior to use. Dry solvents were supplied by *Acros-Organics* (Geel, Belgium), *Sigma-Aldrich* (Taufkirchen, Germany) *or Fluka* (Taufkirchen, Germany). Dry solvents were stored over molecular sieves (4 Å). Acetonitrile (HPLC-grade) was obtained from *VWR International.* Ultra pure water (*Milli-Q* water) generated using water purification device *Simplicity* (*Millipore*, Bedford, UK).

Reactions All air and water sensitive reactions were performed under inert atmosphere using standard schlenk technique. Prior to the moisture sensitive reactions the glassware apparatus was dried by heating under vacuum followed by cooling to room temperature and flushed with dry argon. This process was repeated for three times. Microwave reactions for acid hydrolysis were performed using a *Discover* microwave (MW) with a reaction cavity (*CEM*).

Freeze-drying Freeze-drying (lyophilization) of compounds from aqueous solutions containing was performed using a *Christ-Alpha-2-4* lyophilizer attached to a high vacuum pump. For lyophilization of small amounts in *Eppendorf* caps, an evacuable *Christ RCV-2-18* ultracentrifuge connected to the lyophilization device was used. All solutions were frozen with liquid nitrogen before being attached to the lyophilizer.

6.2 CHROMATOGRAPHY

Thin Layer Chromatography (TLC)

TLC was performed on aluminium-backed *Merck* silica gel 60 F254 plates (layer thickness: 0.20 mm). The spots were detected by fluorescence quenching at 254 nm. Non-fluorescence quenching compounds were detected using a ninhydrine solution in ethanol (3.0 g ninhydrine, 100 mL ethanol). Aldehyde and acetal products were visualized using 2,4-dinitrophenylhydrazine solution (60 mL H_2SO_4, 80 mL H_2O, 200 mL 95% ethanol).

Flash Column Chromatography

The chromatographic separations were carried out by the fritted glass column using Merck silica gel 60 (particle size: 40-60 μm) at 0.4-1.0 bar pressure. The columns were packed with wet silica gel. The quantity of silica gel was in relation with the weight of the substance to be purified (70-100 fold weight excess). All compounds were either adsorbed on silica gel before loading or loaded as a concentrated solution in the same solvent used as an eluent. Eluents are mentioned in each individual protocol in Chapter 6.6.

Reverse Phase-High Performance Liquid Chromatography (RP-HPLC)

Reverse Phase (RP)-HPLC analysis were performed on different devices: (*i*) a *Pharmacia Äkta basic* (*GE Healthcare*, London, UK) with a pump type *P-900*, variable wavelength detector *UV-900; (ii)* a *JASCO* system (*Jasco*, Groß-Umstadt, Germany) equipped with two pumps *PU-2080Plus*, a diode array multi wavelength detector *MD2010Plus* a 3-line degasser *DG-208053*. UV absorption for oligonucleotides was detected at 260 nm.

Oligonucleotides were analyzed using the following columns using flow rates 1 mL/min for analytic purification and 3 mL/min for semi-preparative purification: *Macherey Nagel* Column, *EC 250/4.6 Nucleodur 100-5 C18ec* (analytic), *Macherey Nagel* Column, *VP 250/10 Nucleodur 100-5 C18ec* (semi-preparative). Oligonucleotides were eluted using buffer solutions. Buffer solutions were prepared by using *Milli-Q* water. As elution buffer a solvent system was employed; solvent A1 (0.1 M TEAA, pH 7.0) and solvent B1 (MeCN/TEAA (0.1 M, pH 7.0), 70:30) with a gradient of B1 from 5% to 60% over 30 min. The fractions containing desired product were collected and lyophilized.

The products of Diels-Alder reaction were analyzed using the following column using flow rate 1 mL/min for analytic purification: As eluents a solvent system was employed; solvent A4 (H2O, 0.1% TFA) and solvent B4 (MeOH, 0.1% TFA) with a gradient of B4 from 50% to 100% over 30 min.

The enantiomeric excess was determined by chiral HPLC using a Daicel CHIRALCEL OD column (250 × 4.6 mm) with the eluents hexane/2-propanol (98/2), flow 0.5 mL/min. Retention times: t_R = 14.1, 15.9 (exo isomer); t_R = 18.5, 22.9 (endo isomer).

Anion Exchange-High Performance Liquid Chromatography (AE-HPLC)

Anion Exchange (AE)-HPLC analysis were performed on a micro HPLC, a *JASCO* system equipped with two pumps *PU-2080Plus*, a diode array multi wavelength detector *MD2010Plus*, a column thermostat *CO-2060Plus* and an autosampler unit *AS-2055Plus*. UV absorption for oligonucleotides was detected at 260 nm. Oligonucleotides were analyzed by using the *DNAPac PA200 4x5 mm*, *DIONEX* Ionexchange column with a flow rate 1 mL/min for analytic purification. Oligonucleotides were eluted using buffer solutions. Buffer solutions were prepared by using *Milli-Q* water. As elution buffer two different solvent systems were employed. The first solvent system was solvent A2 (20 mM Tris-Cl, pH 8.0) and solvent B2 (20 mM Tris-Cl, 1.25 M NaCl, pH 8.0) under denaturating conditions at 80° C with a gradient of B2 from 25% to 60% over 30 min. The second solvent system was solvent A3 (10 mM NaOH, pH 12) and solvent B3 (10 mM NaOH, 1.25 M NaCl, pH 12) under denaturating conditions with a gradient of B3 from 35% to 70% over 30 min. The fractions containing the desired product were collected and neutralized to pH 7.0 before lyophilization.

6.3 CHARACTERIZATION

Nuclear Magnetic Resonance Spectroscopy (NMR)

^{1}H-, ^{13}C- and ^{31}P- NMR spectra were recorded on a *Varian Unity 300* spectrometer, a *Varian Inova 500 or 600* or a *Bruker 300* or *400* spectrometer. Chemical shifts (δ) were reported in parts per million (TMS = ppm). The resonances of the rest protons of deuterated solvents were taken as internal standards. $CDCl_3$: 7.24 ppm (^{1}H-NMR) and 77.0 ppm (^{13}C-NMR), DMSO-D_6: 2.49 ppm (^{1}H-NMR) and 39.5 ppm (^{13}C-NMR). Abbreviations for signals are: s (singlet), d (doublet), t (triplet), q (quartet), m (multiplet), bs (broad singlet). Coupling constants $^{n}J_{X,Y}$ are given in Hertz (Hz), where *n* is the order of coupling. ^{13}C spectra were recorded as broadband decoupled ATP spectra. Data from [^{1}H,^{1}H]-COSY, HSQC and HMBC experiments were used to interpret the signals.

Mass Spectrometry (MS)

Electrospray-ionization mass spectras (ESI-MS) were obtained with a *Finnigan* instrument (type *LGC* or *TSQ 7000*) or *Bruker* spectrometers (*Apex-Q IV 7T* and *micrOTOF API*). High Resolution (HR) spectra were obtained with the *Bruker Apex-Q IV 7T* or the *Bruker micrOTOF*, respectively. Spectra were provided in the form of relative intensity vs. *m*/*z* plots, where *m* is the total mass of the molecule and *z* is the total charge of the molecule.

Ultraviolet Spectroscopy (UV/Vis)

Concentrations of oligonucleotides were calculated using UV spectrometer on (*i*) a *JASCO V-550 UV/VIS* spectrometer (Gross-Umstadt, Germany) (d=1 cm) while the sample cell was floated with nitrogen or (*ii*) with a *Thermo Scientific Nanodrop 2000c* (d=0.1 cm). Molecular absorption coefficients were calculated for the oligonucleotide sequence via summation of the monomer nucleobase absorption coefficients at 260 nm. Cytosine: $\varepsilon_{260\,nm}$= 7050 L·mol^{-1}·cm^{-1}, Guanine: $\varepsilon_{260\,nm}$= 12100 L·mol^{1}·cm^{-1}, Thymine: $\varepsilon_{260\,nm}$= 8400 L·mol^{-1} cm^{-1}, Adenine: $\varepsilon_{260\,nm}$= 15200 L·mol^{-1}·cm^{-1}.[147]

UV-Thermal Melting Analysis

Melting temperatures of oligonucleotide duplexes were determined on a *Jasco* V-550 UV/VIS system with a peltier heating accessory *Jasco ETC-505S/ETC-505T*. Measurements were carried out in a quartz cuvettes of 1 cm path length. 1:1 mixture of each strand (5 µM) was prepared in 10 mM phosphate buffer pH 7, 100 mM NaCl (500 µL total volume). The quartz cuvette was covered with silicon oil and tightly plugged. The change in absorbance at 260 nm was recorded on a range of 4-80 °C with a heating rate of 0.4 °C/min. Detailed experimental conditions are stated with the respective experiments. The value of the T_m was calculated from the first derivative of the melting curve and smoothed (*Savitzky-Golay*).

Circular Dichroism

CD spectra were recorded on a *Jasco-810* spectropolarimeter (Gross-Umstadt, Germany) equipped with a *Jasco PTC432S* temperature controller using the *Jasco Spectra Manager control* (*V 1.17.00*) and *application* (*V 1.53.00*) software package. The sample cell was floated with nitrogen. For CD spectra recording of double strand oligonucleotides, buffer conditions are stated with the respective experiments. For experiments 1 mm glass cuvette were used. The single strand oligonucleotide concentrations were adjusted to 5 µM. The spectra were recorded at 20 °C in a wavelength range of 350-190 nm with 1.0 nm bandwidth, using 1.0 s response and a scan speed of 50 nm/min. Five spectra were averaged. Spectra were background-corrected against blank buffer solution.

6.4 OLIGONUCLEOTIDE SYNTHESIS

Oligonucleotides were synthesized on DNA/RNA/LNA Synthesizer (K&A *Laborgeräte,* Schaafheim, Germany) using standard β-cyanoethyl phosphoramidite method.[27] Reagents for oligonucleotide syntheses (3% dichloroacetic acid in toluene, 5-benzylmercaptotetrazole, 0.02 M Iodine in THF/pyridine) were purchased from *EMP BIOTECH* (Berlin, Germany). Nucleoside phosphoramidite monomers were supplied by *Sigma-Aldrich* (Taufkirchen, Germany) with base labile protecting groups for the natural nucleobases (Ac for dC, Dmf for dG and Bz for dA). The Controlled Pore Glass (CPG) solid support attached by a succinimide linker at the 3'- end of 5'-protected deoxynucleoside (A, C, T or G) in 200 nmol were supplied by *Link Technologies* (Lanarkshine, UK). *Milli-Q* water was used in all syntheses and applications for oligonucleotides. For oligonucleotide synthesis the nucleoside phosphoramidite building blocks was dissolved in dry acetonitrile (1 g nucleoside in 20 mL acetonitrile). Complementary strands were purchased from *BIOMERS* (Ulm/Donau, Germany).

Desalting of Oligonucleotides In order to prepare oligonucleotides for ESI-MS, RP- and AE-HPLC purified oligonucleotides were desalted using *Sep-Pak®* C18 cartridges (*Waters*, Milford, USA). Initially, the cartridge was washed with 10 mL acetonitrile to wet the stationary phase. Conditioning was followed by an equilibration step using 10 mL TEAA buffer (0.1 M, pH 7.0). The oligonucleotide was dissolved in 1.5 mL TEAA buffer (0.1 M, pH 7.0) and then loaded very slowly onto the cartridge. After loading the sample, the cartridge was washed with *Milli-Q* water in order to remove salts while retaining the oligonucleotide. Elution of the more strongly bound oligonucleotide was performed by *Milli-Q*/acetonitrile (50:50, v/v).

Oligonucleotides were desalted after dynamic nucleobase incorporation reactions using *Centri·Pure N10* gel filtration columns (*emp Biotech*, Berlin, Germany). Initially, the column was equilibrated by loading it with 5 mL *Milli-Q* water. The oligonucleotide was dissolved in 1.0 mL *Milli-Q* water and then transferred to the column. After the sample was entered to the gel bed completely, an *Eppendorf* cap was placed under the column for the sample collection. Elution of the purified oligonucleotide was performed by 1.5 mL *Milli-Q* water.

6.5 DYNAMIC NUCLEOBASE INCORPORATION

Prior to the reactions, stock solutions of **ON1** and template strands were prepared by dissolving the strands in the same buffer used for the dynamic exchange reactions (20 mM sodium phosphate buffer, 1 M NaCl, pH 6). Stock solutions of the nucleobase aldehydes were prepared freshly in the same buffer as for oligonucleotides (20 mM sodium phosphate buffer, 1 M NaCl pH 6.0).

6.5.1 BASE-FILLING REACTIONS IN THE PRESENCE OF SINGLE NUCLEOBASE

ON1 (50.0 µL of a 200 µM stock solution, 10.0 nmol, 1.0 eq.), template strand (50.0 µL of a 200 µM stock solution, 10.0 nmol, 1.0 eq.), one of the four aldehyde-nucleobases (40.0 µL of a 7 mM stock solution, 280 nmol, 28 eq.) and buffer (120 µL of 20 mM phosphate buffer, pH 6, 1 M NaCl) were mixed in an *Eppendorf* cap and incubated at room temperature for three hours. For reduction $NaBH_3CN$ (50.0 µL of 1 M stock solution, 50.0 µmol) was added and shaking continued for one hour. The reaction mixture was passed through a gel filtration column (*Centri·Pure N10*) to remove excess of aldehydes and salts. After lyophilization of the samples, crude products were analyzed by AE-HPLC using solvent system A2 and B2 at 80 °C.

6.5.2 BASE-FILLING REACTIONS IN THE PRESENCE OF FOUR NUCLEOBASES AT EQUIMOLAR CONCENTRATIONS

ON1 (50.0 µL of a 200 µM stock solution, 10.0 nmol, 1.0 eq.), template strand (50.0 µL of a 200 µM stock solution, 10.0 nmol, 1.0 eq.), aldehyde-nucleobases $\mathbf{G_{CHO}}$, $\mathbf{C_{CHO}}$, $\mathbf{A_{CHO}}$, $\mathbf{T_{CHO}}$ (each in 40 µL of a 7 mM stock solution, 280 nmol, 28 eq.) were mixed and incubated at room temperature for three hours. For reduction $NaBH_3CN$ (50 µL of 1 M stock solution, eq.) was added and shaking continued for one hour. The reaction mixture was purified by gel filtration (*Centri·Pure N10* columns) to remove excess of aldehydes and salts. After lyophilization of the samples, crude products were analyzed using AE-HPLC under two different conditions: Solvent system A2 and B2, 80 °C or solvent system A3 and B3, pH 12.

6.5.3 Base-filling Reactions in the Presence of four nucleobases at Non-equimolar concentrations

Reactions were performed similarly as described in 5.5.2, with the following amounts of aldehydes: $\mathbf{G_{CHO}}$ (40.0 µL of a 7 mM stock solution, 280 nmol, 28 eq.), $\mathbf{C_{CHO}}$ (40.0 µL of a 9 mM stock solution, 364 nmol, 36 eq.), $\mathbf{A_{CHO}}$ (40.0 µL of a 13 mM stock solution, 504 nmol, 50 eq.), $\mathbf{T_{CHO}}$ (40.0 µL of a 23 mM stock solution, 924 nmol, 92 eq.).

6.5.4 Test of Reversibility

ON1 (50.0 µL of a 200 µM stock solution, 10.0 nmol, 1.0 eq.), template strand (50.0 µL of a 200 µM stock solution, 10.0 nmol, 1.0 eq.), aldehyde-nucleobases $\mathbf{C}_{CHO}$, $\mathbf{A}_{CHO}$, $\mathbf{T}_{CHO}$ (each in 40 µL of a 7 mM stock solution, 280 nmol, 28 eq.) were mixed and incubated at room temperature. After three hours $\mathbf{G}_{CHO}$ was added and incubated for further one hour. For reduction $NaBH_3CN$ (50 µL of 1 M stock solution, eq.) was added and shaking continued for one hour. The reaction mixture was purified by gel filtration (*Centri·Pure N10* columns) to remove excess of aldehydes and salts. After lyophilization of the samples, crude products were analyzed using AE-HPLC under two different conditions: Solvent system A2 and B2, 80 °C or solvent system A3 and B3, pH 12.

6.5.5 Phenantroline Incorporation with Abasic Template

ON1 (50.0 µL of a 200 µM stock solution, 10.0 nmol, 1.0 eq.), template strand (50.0 µL of a 200 µM stock solution, 10.0 nmol, 1.0 eq.), $\mathbf{P2}_{CHO}$ and aldehyde-nucleobases $\mathbf{G_{CHO}}$, $\mathbf{C_{CHO}}$, $\mathbf{A_{CHO}}$, $\mathbf{T_{CHO}}$ (each in 40 µL of a 7 mM stock solution, 280 nmol, 28 eq.) were mixed and incubated at room temperature for three hours. For reduction $NaCNBH_3$ (50 µL, 1 M) was added and shaking continued for one hours. The reaction mixture was purified by gel filtration (*Centri·Pure N10* columns) to remove excess of aldehydes and salts. After lyophilization of the samples, crude products were analyzed using AE-HPLC: Solvent system A2 and B2, 80 °C.

6.6 SYNTHESIS OF D-THREONINOL-BASED PHOSPHORAMIDITE MONOMER

6.6.1 *N*-[(Fluoren-9-ylmethoxy)-carbonyl]-D-threoninol (2)[117]

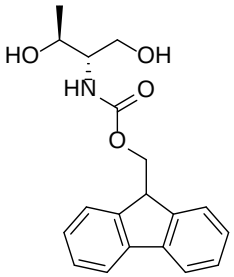

2

$C_{19}H_{21}NO_4$ [327.38]

D-Threoninol (**1**) (500 mg, 4.76 mmol, 1.00 eq.) was added to a stirring suspension of *N*-[[(fluoren-9-ylmethoxy)-carbonyl]oxy]-succinimide (Fmoc-OSu) (500 mg, 4.76 mmol, 1.00 eq.) in a mixture of aceton/water (1:1 v/v, 20 mL) containing sodium hydrogen carbonate (1.67 g, 4.76 mmol, 1.00 eq.). The reaction mixture was stirred overnight at room temperature. After removal of the solvent under reduced pressure, the crude product was taken up in dichloromethane (50 mL), washed with water (2 x 50 mL), dried over sodium sulfate, filtered and concentrated under reduced pressure. Purification by flash column chromatography (dichloromethane/methanol, 9:1) afforded **2** as a white solid (1.40 g, 4.28 mmol, 90%).

TLC R_f = 0.52 (dichloromethane/methanol, 9:1).

^{1}H-NMR (300 MHz, $CDCl_3$, RT): δ (ppm) = 1.18 (d, 3H, $^3J_{H,H}$ = 6.3 Hz, H-4), 2.47 (s, 2H, 2 x OH), 3.48-3.59 (m, 1H, H-2), 3.78 (d, 2H, $^3J_{H,H}$ = 3.7 Hz, H-1), 4.08-4.15 (m, 1H, H-3), 4.17 (t, 1H, $^3J_{H,H}$ = 6.6 Hz, Fmoc-CH), 4.35-4.50 (m, 2H, Fmoc-CH_2), 5.49 (d, 1H, $^3J_{H,H}$ = 8.3 Hz, NH), 7.25-7.32 (m, 2H, Fmoc-2,7-H), 7.33-7.40 (m, 2H, Fmoc-3,6-H), 7.58 (d, 2H, $^3J_{H,H}$= 7.3 Hz, Fmoc-1,8-H), 7.74 (d, 2H, $^3J_{H,H}$= 7.4 Hz, Fmoc-4,5-H).

^{13}C-NMR (126 MHz, $CDCl_3$, RT): δ (ppm) = 20.35 (1C, C-4), 47.27 (1C, Fmoc-CH), 55.98 (1C, C-3), 64.99 (1C, C-1), 66.72 (1C, Fmoc-CH_2), 68.85 (1C, C-2), 119.95 (2C, Fmoc-1,8-C), 125.00 (2C, Fmoc-2,7-C), 127.02 (2C, Fmoc-4,5-C), 127.69 (2C, Fmoc-3,6-C), 141.32 (2C, Fmoc-11,12-C), 143.81 (2C, Fmoc-1,8-C), 156.99 (1C, Fmoc-CO).

ESI-MS: *m/z* (rel.%) = 350.1 (26) $[M+Na]^+$, 677.3 (100) $[2M+Na]^+$.

HRMS (ESI): calcd. for $[C_{19}H_{21}NO_4Na]^+$ ($[M+Na]^+$): 350.1363; found: 350.1362.

6.6.2 O^1-(4,4'-Dimethoxytrityl)- *N*-[(fluoren-9-ylmethoxy)-carbonyl]-D-threoninol (3) [117]

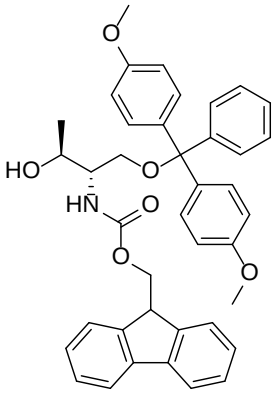

3

$C_{40}H_{39}NO_6$ [629.75]

Prior to the reaction, Fmoc-D-threoninol (**2**) (500 mg, 1.53 mmol, 1.00 eq.) was dried by coevaporation with dry pyridine (3 x 15 mL) and then dissolved in dry pyridine (15 mL) under argon. 4,4'-Dimethoxytritylchloride (569 mg, 1.68 mmol, 1.10 eq.), 4-(dimethylamino)-pyridine (DMAP) (9.35 mg, 0.08 mmol, 0.05 eq.) and triethylamine (0.3 mL, 2.14 mmol, 1.40 eq.) was added to this solution and was stirred at room temperature overnight. Pyridine was evaporated under reduced pressure and the crude product was taken up in dichloromethane and washed with water (3 x 50 mL). The organic phase was further washed with saturated sodium hydrogencarbonate solution (30 mL) and water (30 mL). The organic phase was dried over sodium sulfate, filtered and concentrated under reduced pressure. Purification by flash column chromatography (dichloromethane/methanol/triethylamine, 99:1:0.5) afforded **3** as a yellow oil (787 mg, 1.25 mmol, 82%).

TLC R_f = 0.63 (dichloromethane/methanol/triethylamine, 99:1:0.5).

^{1}H-NMR (300 MHz, $CDCl_3$, RT): δ (ppm) = 1.16 (d, 3H, $^3J_{H,H}$ = 6.3 Hz, H-4), 2.92 (s, 1H, OH), 3.20-3.41 (m, 2H, H-1), 3.64-3.71 (m, 1H, H-2), 3.73 (s, 6H, -OCH_3), 4.04-4.13 (m, 1H, H-3), 4.23 (t, 1H, $^3J_{H,H}$ = 7 Hz, Fmoc-CH), 4.30-4.47 (m, 2H, Fmoc-CH_2), 5.47 (d, 1H, $^3J_{H,H}$ = 8.3 Hz, NH), 6.76-6.84 (m, 4H, DMT-H), 7.18- 7.32 (m, 9H, DMT-H), 7.35-7.40 (m, 4H, Fmoc-2,7-H, Fmoc-3,6-H), 7.59-7.69 (m, 2H, Fmoc-1,8-H), 7.74-7.77 (m, 2H, Fmoc-4,5-H).

^{13}C-NMR (126 MHz, $CDCl_3$, RT): δ (ppm) = 20.14 (1C, C-4), 47.64 (1C, Fmoc-CH), 55.47 (2C, 2 x -OCH_3), 55.99 (1C, C-3), 64.97 (1C, C-1), 67.01 (1C, Fmoc-CH_2), 67.97 (1C, C-2), 86.79 (1C, DMT-C), 113.47 (4C, DMT-C), 120.21 (2C, Fmoc-1,8-C), 123.98 (2C, Fmoc-2,7-C), 125.38 (3C, Fmoc-4,5-C, DMT-C), 127.16 (2C, Fmoc-3,6-C), 127.34 (4C, DMT-C), 127.94 (2C, DMT-C), 128.22

(2C, DMT-C), 130.24 (2C, DMT-C), 141.57 (2C, Fmoc-11,12-C), 144.41 (2C, Fmoc-10,13-C), 144.43 (1C, DMT-C), 150.06 (1C, Fmoc-CO), 159.00 (2C, DMT-C).

ESI-MS: *m/z* (rel.%) = 652.3 (100) $[M+Na]^+$, 1281.5 (33) $[2M+Na]^+$.

HRMS (ESI): calcd. for $[C_{40}H_{39}NO_6Na]^+$ ($[M+Na]^+$): 652.2662, found: 652.2670.

6.6.3 O^1-(4,4'-Dimethoxytrityl)-*N*-[(fluoren-9-ylmethoxy)-carbonyl]-O^3-[2-cyanoethyl-*N,N* diisopropylaminophosphinyl]-D-threoninol (**4**)[117]

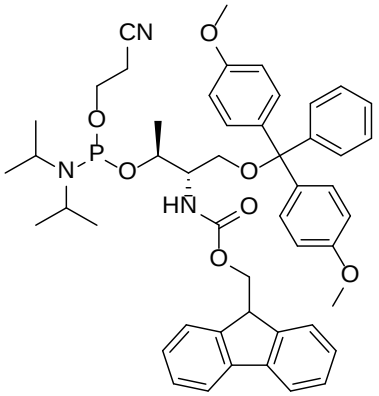

4

$C_{49}H_{56}N_3O_6P$ [813.98]

Prior to the reaction DMT-Fmoc-D-threoninol (**3**) (500 mg, 0.79 mmol, 1.00 eq.) was dried by coevaporation with dry pyridine (3 x 15 mL) and then dissolved in dry dichloromethane (15 mL) uder argon. *N,N*-Diisopropylethylamine (DIPEA) (0.20 mL, 1.20 mmol, 1.50 eq.) and 2-cyanoethyl-*N,N*-diisopropylphosphoramiditchloride (0.24 mL, 1.03 mmol, 1.30 eq.) was added at 0 °C dropwise while stirring. The reaction mixture was stirred for three hours at room temperature under argon and washed with addition of saturated sodium hydrogencarbonate solution (10 mL). The water phase was further washed with dichloromethane (3 x 10 mL). The combined organic phase was dried over sodium sulfate and the solvent was removed under reduced pressure. The crude product was subjected to column chromatography (*n*-pentane/ethyl acetate, 3:1). The desired fractions were collected and evaporated under reduced pressure. The purified product was dissolved in chloroform (1 mL) and precipitated in cold hexane at 0 °C (50 mL). The product was filtered, washed with cold hexane and dried under high vacuum to afford **4** as a white powder (268 mg, 0.33 mmol, 43%).

TLC R_f = 0.38 (*n*-Pentane/ethyl acetate, 3:1).

^{1}H-NMR (300 MHz, $CDCl_3$, RT): δ (ppm) = 1.09-1.19 (m, 12H, 2 x -CH($C\underline{H}_3$)$_2$), 1.23 (d, 3H, $^3J_{H,H}$ = 6.4 Hz, H-4), 2.36 (t, 2H, $^3J_{H,H}$ = 6.3 Hz, -CH_2CN), 3.15-3.23 (m, 2H, 2 x -C$\underline{H}$(CH_3)$_2$), 3.40-3.59 (m, 4H, H-1, -OC$\underline{H}_2CH_2$CN), 3.76 (s, 6H, 2 x -OCH_3), 3.83-3.93 (m, 1H, H-2), 4.18-4.27 (m, 1H, H-3), 4.27-4.37 (m, 1H, Fmoc-CH), 4.37-4.44 (m, 2H, Fmoc-CH_2), 5.08 (d, 1H, $^3J_{H,H}$ = 8.3 Hz, NH), 6.73-6.86 (m, 4H, DMT-H), 7.14-7.45 (m, 13H, Fmoc-2,7-H, Fmoc-3,6-H, DMT-H), 7.55-7.64 (m, 2H, Fmoc-1,8-H), 7.76 (d, 2H, $^3J_{H,H}$ = 7.4 Hz, Fmoc-4,5-H).

^{13}C-NMR (126 MHz, $CDCl_3$, RT): δ (ppm) = 19.42 (1C, C-4), 20.10 (1C, -$\underline{C}H_2CN$), 24.58 (4C, 2 x -CH($\underline{C}H_3)_2$), 43.06 (1C, Fmoc-CH), 47.28 (2C, 2 x -$\underline{C}H(CH_3)_2$), 55.15 (2C, 2 x -OCH_3), 56.23 (1C, C-3), 58.17 (1C, -O$\underline{C}H_2CH_2CN$), 63.02 (1C, C-1), 66.61 (1C, Fmoc-CH_2), 68.89 (1C, C-2), 86.05 (1C, DMT-CH), 113.01 (4C, DMT-CH_{Ar}), 117.59 (1C, CN), 119.89 (2C, Fmoc-1,8-C), 125.02 (2C, Fmoc-2,7-C), 126.98 (3C, Fmoc-4,5-C, DMT-C), 127.60 (2C, Fmoc-3,6-C), 127.74 (4C, DMT-C), 128.22 (2C, DMT-C), 130.05 (2C, DMT-C), 135.97 (2C, DMT-C), 141.24 (2C, Fmoc-11,12-C), 143.90 (2C, Fmoc-10,13-C), 144.75 (1C, DMT-C), 156.35 (1C, Fmoc-CO), 158.42 (2C, DMT-C).

^{31}P-NMR (121 MHz, $CDCl_3$, RT): δ (ppm) = 148.

ESI-MS: *m/z* (rel.%) = 830.4 (18) $[M+H]^+$, 852.4 (100) $[M+Na]^+$.

HRMS (ESI): calcd. for $[C_{49}H_{57}N_3O_6P]$ ($[M+H]^+$): 830.3929, found: 830.3929, calcd. for $[C_{49}H_{56}N_3O_7PNa]$ ($[M+Na]^+$): 852.3751, found: 852.3748.

6.7 SYNTHESIS OF NUCLEOBASE-ALDEHYDES

6.7.1 2-Amino-6-chloro-9-(2,2-diethoxyethyl)-purine (6)[115,124]

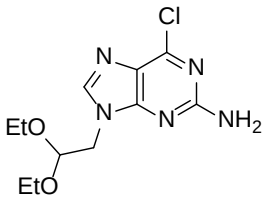

6

$C_{11}H_{16}ClN_5O_2$ [285.73]

A suspension of 2-amino-6-chloropurine (6.00 g, 35.4 mmol, 1.00 eq.), cesium carbonate (5.80 g, 17.7 mmol, 0.50 eq.) and bromoacetaldehyde diethyl acetal (8.20 mL, 53.1 mmol, 1.50 eq.) in dry *N,N'*-dimethylformamide (150 mL) was heated at 100 °C under stirring for 24 h. The reaction mixture was filtered when it is hot through celite and concentrated under reduced pressure. The residue was taken up in water (100 mL) and extracted with boiling chloroform (3 x 150 mL), filtered through celite and evaporated under reduced pressure. Before column chromatography the residue was taken up in methanol (150 mL) and was treated with silica gel and evaporated. Purification by flash column chromatography (dichloromethane/methanol, 95:5) afforded **6** as a white solid (6.00 g, 21.2 mmol, 60%).

TLC R_f = 0.35 (dichloromethane/methanol, 95:5).

^{1}H-NMR (300 MHz, $CDCl_3$, RT): δ (ppm) = 1.18 (t, 6H, $^3J_{H,H}$ =7.1 Hz, 2 x CH_3), 3.49 (dq, 2H, $^2J_{H,H}$ = 9.2 Hz, $^3J_{H,H}$ = 7.1 Hz, -OC$\underline{H}_2CH_3$), 3.72 (dq, 2H, $^2J_{H,H}$ = 9.2 Hz, $^3J_{H,H}$ = 7.1 Hz, -OC$\underline{H}_2CH_3$), 4.17 (d, 2H, $^3J_{H,H}$ = 5.2 Hz, NCH_2), 4.67 (t, 1H, $^3J_{H,H}$ = 5.2 Hz, $CH(OEt)_2$), 5.10 (s, 2H, NH_2), 7.85 (s, 1H, H-8).

^{13}C-NMR (126 MHz, $CDCl_3$, RT): δ (ppm) = 15.08 (2C, 2 x CH_3), 46.03 (1C, NCH_2), 63.65 (2C, 2 x O$\underline{C}H_2CH_3$), 99.93 (1C, $\underline{C}H(OEt)_2$), 124.66 (1C, C-5), 143.35 (1C, C-8), 150.96 (1C, C-6), 153.88 (1C, C-4), 159.16 (1C, C-2).

ESI-MS: *m/z* (rel.%): 286.1 (100) $[M+H]^+$, 308.1 (18) $[M+Na]^+$, 571.2 (17) $[2M+H]^+$, 593.2 (53) $[2M+Na]^+$.

HRMS (ESI): calcd. for $[C_{11}H_{17}ClN_5O_2]^+$ ($[M+H]^+$): 286.1065, found: 286.1071; calcd. for $[C_{11}H_{15}ClN_5O_2]^-$ ($[M-H]^-$): 284.0920, found: 284.0918.

6.7.2 2-(Guanin-9-yl)-ethanal hydrate trifluoroacetate (**9**)[115]

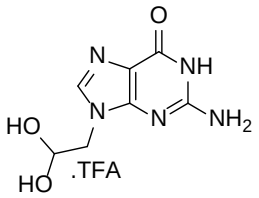

9

$C_7H_7N_5O2$ [193.17]

2-Amino-6-chloro-9-(2,2-diethoxyethyl)-purine (10.0 mg, 35.0 mmol) was dissolved in TFA/H_2O (1:2 v/v, 0.50 mL) and heated at 100 °C in the microwave for 30 min. After removal of TFA, it was lyophilized to give 2-(guanin-9-yl)-ethanal hydrate trifluoroacetate (**9**) as a blue solid (7 mg, 35 mmol, 90%).

TLC R_f = 0.07 (dichloromethane/methanol, 90:10).

^{1}H-NMR (300 MHz, D_2O, RT): δ (ppm) = 4.35 (d, 2H, $^3J_{H,H}$=4.7 Hz, NCH_2), 5.47 (t, 1H, $^3J_{H,H}$=4.7 Hz, C<u>H</u>$(OH)_2$), 8.78 (s, 1H, H-8).

^{13}C-NMR (126 MHz, D_2O, RT): δ (ppm) = 52.10 (1C, NCH_2), 89.39 (1C, $(CHOH)_2$), 111.08 (1C, C-5), 120.11 (1C, CF_3), 141.11 (1 C, C-8), 153.13 (1C, C-4), 157.79 (1C, C-2), 158.35 (1C, C-6), 165.34 (1C, <u>C</u>OCF_3)

ESI-MS: *m/z* (rel.%): 194.07 (72) $[M+H]^+$, 212.08 (100) $[M+H_3O]^+$.

HRMS (ESI): calcd. for aldehyde $[C_7H_6N_5O_2]^-$ ($[M-H]^-$): 192.0527, found: 192.0523.

6.7.3 9-(2,2-Diethoxyethyl)-adenine (**11**)

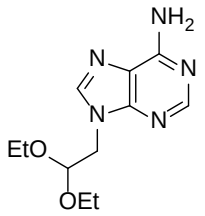

11

$C_{11}H_{17}N_5O_2$ [251.29]

A mixture of adenine (1.00 g, 7.40 mmol, 1.00 eq.), dry potassium carbonate (1.00 g, 7.4 mmol, 1.00 eq.) and bromoacetaldehyde diethyl acetal (1.10 mL, 7.40 mmol, 1.00 eq.) in dry *N,N'*-dimethylformamide (20 mL) was heated at 110 °C under stirring for 24 h. The reaction mixture was concentrated under reduced pressure. The residue was taken up in water (30 mL) and extracted with ethyl acetate (3 x 50 mL). The combined organic phase was washed with brine and dried over sodium sulfate. Purification by flash column chromatography (dichloromethane/methanol, 90:10) afforded **11** as a white solid (1.10 g, 4.44 mmol, 60%).

TLC R_f = 0.50 (dichloromethane/methanol, 90:10).

^{1}H-NMR (300 MHz, $CDCl_3$, RT): δ (ppm) = 1.14 (t, 6H, $^3J_{H,H}$ = 7 Hz, 2 x CH_3), 3.47 (dq, 2H, $^2J_{H,H}$ = 9.5 Hz, $^3J_{H,H}$ = 7 Hz, OCH_2CH_3), 3.72 (dq, 2H, $^2J_{H,H}$ = 9.5 Hz, $^3J_{H,H}$ = 7 Hz, OCH_2CH_3), 4.26 (d, 2H, $^3J_{H,H}$ = 5.5 Hz, NCH_2), 4.70 (t, 1H, $^3J_{H,H}$ = 5.5 Hz, $CH(OEt)_2$), 5.96 (s, 2H, NH_2), 7.89 (s, 1H, H-2), 8.33 (s, 1H, H-8).

^{13}C-NMR (126 MHz, $CDCl_3$, RT): δ (ppm) = 15.18 (2C, 2 x CH_3), 46.27 (1C, NCH_2), 63.91 (1C, O<u>C</u>H_2CH3), 100.31 (1C, $CH(OEt)_2$), 119.17 (1C, C-5), 141.81 (1C, C-8), 150.19 (1C, C-4), 152.54 (1C, C-2), 155.21 (1C, C-6).

ESI-MS: *m/z* (rel. %): 252.2 (100) $[M+H]^+$.

HRMS (ESI): calcd. for $[C_{11}H_{18}N_5O_2]^+$ ($[M+H]^+$): 252.1455, found: 252.1455; calcd. for $[C_{11}H_{16}N_5O_2]^-$ ($[M-H]^-$): 250.1309, found: 250.1306.

6.7.4 2-(Adenin-9-yl)-ethanal hydrate trifluoroacetate (**12**)

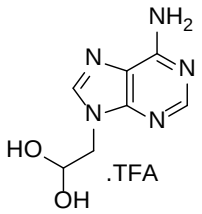

12
$C_7H_7N_5O$ [177.17]

9-(2,2-Diethoxyethyl)-adenine (10.0 mg, 40.0 mmol) was dissolved in TFA/H_2O (1:1 v/v, 0.50 mL) and heated at 100 °C in the microwave for 30 min. After removal of TFA it was lyophilized to give **12** as a white solid (7 mg, 40.0 mmol, quantitative).

TLC R_f = 0.50 (dichloromethane/methanol, 90:10).

^{1}H-NMR (300 MHz, D_2O, RT): δ (ppm) = 4.45 (d, 2H, $^3J_{H,H}$ = 4.7 Hz, NCH_2), 5.47 (t, 1H, $^3J_{H,H}$ = 4.7 Hz, $CH(OH)_2$), 8.40 (s, 1H, H-2), 8.47 (s, 1H, H-8).

^{13}C-NMR (126 MHz, D_2O, RT): δ (ppm) = 51.84 (1C, NCH_2), 90.02 (1C, $(CH(OH)_2$), 117.78 (1C, CF_3), 120.10 (1C, C-5), 147.02 (1C, C-8), 148.05 (1C, C-4), 151.52 (1C, C-2), 152.50 (1C, C-6), 165.31 (1C, $\underline{C}OCF_3$).

ESI-MS: *m/z* (rel. %): 178.1 (9) $(M+H)^+$, 210.1 (100) $(M+Na)^+$.

HRMS (ESI): calcd. for aldehyde $[C_7H_8N_5O]^+$ ($[M+H]^+$): 178.0723, found: 178.0725; calcd. for $[C_7H_6N_5O]^-$ ($[M-H]^-$): 176.0578, found: 176.0579.

6.7.5 4-*N*-Acetylcytosine (**14**) [115]

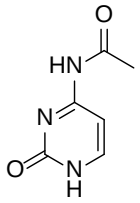

14
$C_6H_7N_3O_2$ [153.14]

A suspension of cytosine (1.00 g, 9.00 mmol) in acetic anhydride (10 mL) and glacial acetic acid (2 mL) was refluxed overnight under nitrogen. The reaction mixture was cooled down to room temperature and the insoluble product was filtered and collected. It was washed with cold ethanol (10 mL), followed by diethyl ether (10 mL) and dried to afford derivative **14** as a white solid (1.20 g, 8.00 mmol, 88%).

TLC R_f = 0.35 (dichloromethane/methanol, 90:10).

^{1}H NMR (300 MHz, $CDCl_3$, RT): δ (ppm) = 2.08 (s, 3H, CH_3), 7.07 (d, 1H, $^3J_{H,H}$ = 7 Hz, H-5), 7.78 (d, 1H, $^3J_{H,H}$ = 7 Hz, H-6), 13.30 (s, 1H, H-1).

^{13}C NMR (126 MHz, $CDCl_3$, RT): δ (ppm) = 24.25 (1C, CH_3), 94.34 (1C, C-5), 146.90 (1C, C-6), 155.93 (1C, C-2), 162.95 (1C, C-4), 170.56 (1C, $\underline{C}OCH_3$).

ESI-MS: *m/z* (rel.%): 154.1 (25) $[M+H]^+$, 176.1 (100) $[M+Na]^+$.

HRMS (ESI): calcd. for $[C_6H_8N_3O_2]^+$ ($[M+H]^+$): 154.0611, found: 154.0612; calcd. for $[C_6H_7N_3O_2Na]^+$ ($[M+Na]^+$): 176.0430, found: 176.0435.

6.7.6 4-*N*-Acetyl-1-(2,2-diethoxyethyl)-cytosine (**15**)

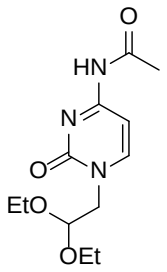

15

$C_{12}H_{19}N_3O_4$ [269.30]

A mixture of 4-*N*-acetylcytosine (3.60 g, 23.4 mmol, 1.00 eq.), dry potassium carbonate (3.32 g, 23.4 mmol, 1.00 eq.) and bromoacetaldehyde diethyl acetal (3.8 mL, 23.4 mmol, 1.00 eq.) in dry *N,N'*-dimethylformamide (60 mL) was heated at 130 °C under stirring for 24 h. The resulting dark brown reaction mixture was filtered when it is hot through celite and concentrated under reduced pressure. The residue was taken up in water (100 mL) and extracted with ethyl acetate (3 x 150 mL). The combined organic phase was washed with brine (100 mL), dried over sodium sulfate, filtered and concentrated under reduced pressure. Purification by flash column chromatography (dichloromethane/methanol, 95:5) afforded derivative **15** as a yellow solid (3.80 g, 14.0 mmol, 60%).

TLC R_f = 0.50 (dichloromethane/methanol, 95:5).

^{1}H-NMR (300 MHz, $CDCl_3$, RT): δ (ppm) = 1.24 (t, 6H, $^3J_{H,H}$ = 7 Hz, 2 x -$OCH_2C\underline{H}_3$), 2.03 (s, 3H, $COC\underline{H}_3$), 3.42 (dq, 2H, $^2J_{H,H}$ = 9 Hz, $^3J_{H,H}$ = 7 Hz, $OC\underline{H}_2CH_3$), 3.62 (dq, 2 H, $^2J_{H,H}$ = 9 Hz, $^3J_{H,H}$ = 7 Hz, -$OC\underline{H}_2CH_3$), 3.80 (d, 2H, $^3J_{H,H}$ = 5.5 Hz, NCH_2), 4.72 (t, 1H, $^3J_{H,H}$ = 5.5 Hz, $C\underline{H}(OEt)_2$), 7.12 (d, 1H, $^3J_{H,H}$ = 7 Hz, H-5), 7.68 (d, 1H, $^3J_{H,H}$ = 7 Hz, H-6), 10.78 (s, 1H, NH).

^{13}C-NMR (126 MHz, $CDCl_3$, RT): δ (ppm) = 15.63 (2C, 2 x CH_3), 54.1 (1C, NCH_2), 64.71 (1C, -$O\underline{C}H_2CH_3$), 97.23 (1C, C-5), 100.8 (1C, $\underline{C}H(OEt)_2$), 152.4 (1 C, C-6), 158.16 (1C, C-2), 164.11 (1C, C-4), 172.8 (1C, CO).

ESI-MS: *m/z* (rel.%): 270.2 (100) $[M+H]^+$.

HRMS (ESI): calcd. for $[C_{12}H_{20}N_3O_4]^+$ ($[M+H]^+$): 270.1448, found: 270.1450; calcd. for $[C_{12}H_{19}N_3O_4Na]^+$ ($[M+Na]^+$): 292.1268, found:292.1272.

6.7.7 1-(2,2-Diethoxyethyl)-cytosine (**16**)

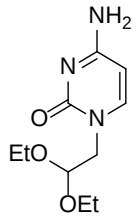

16

$C_{10}H_{17}N_3O_3$ [227.26]

A solution of 4-*N*-acetyl-1-(2,2-diethoxyethyl)-cytosine **8** (0.50 g, 1.8 mmol) in methanolic ammonia (2 M, 10 mL) was stirred at room temperature for 92 h. The reaction mixture was concentrated under reduced pressure to a white solid. Purification by column chromatography (dichloromethane/methanol, 95:5) afforded derivative **16** as a white product (0.296 g, 1.26 mmol, 70%).

TLC R_f = 0.20 (dichloromethane/methanol, 90:10).

^{1}H-NMR (300 MHz, $CDCl_3$, RT): δ (ppm) = 1.15 (t, 6H, $^3J_{H,H}$ = 7 Hz, 2 x -$OCH_2C\underline{H}_3$), 3.52 (dq, 2H, $^2J_{H,H}$ = 9.5 Hz, $^3J_{H,H}$ = 7 Hz, -$OC\underline{H}_2CH_3$), 3.72 (dq, 2H, $^2J_{H,H}$ = 9.5 Hz, $^3J_{H,H}$ = 7 Hz, -$OC\underline{H}_2CH_3$), 3.80 (d, 2H, $^3J_{H,H}$ = 5.4 Hz, NCH_2), 4.72 (t, 1H, $^3J_{H,H}$ = 5.4 Hz, $C\underline{H}(OEt)_2$), 5.81 (d, 1H, $^3J_{H,H}$ = 7.2 Hz, H-5), 7.48 (d, 1H, $^3J_{H,H}$ = 7.2 Hz, H-6).

^{13}C-NMR (126 MHz, $CDCl_3$, RT): δ (ppm) = 15.63 (2C, 2 x CH_3), 53.52 (1C, NCH_2), 64.91 (1C, -$O\underline{C}H_2CH_3$), 95.23 (1C, C-5), 101.47 (1C, $\underline{C}H(OEt)_2$), 148.75 (1C, C-6), 159.16 (1C, C-2), 168.11 (1C, C-4).

ESI-MS: *m/z* (rel.%): 228.1 (100) $[M+H]^+$, 455.3 (82) $[M+Na]^+$.

HRMS (ESI): calcd. for $[C_{10}H_{18}N_3O_3]^+$ ($[M+H]^+$): 228.1343, found: 228.1346; calcd. for $[C_{10}H_{17}N_3O_3Na]^+$ ($[M+Na]^+$): 250.12, found: 250.1163.

6.7.8 2-(Cytosin-1-yl)-ethanal hydrate trifluoroacetate (**17**)

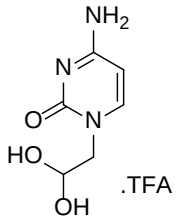

17
$C_6H_7N_3O_2$ [153.14]

1-(2,2-Diethoxyethyl)cytosine (**16**) (20.0 mg, 0.08 mmol) was dissolved in TFA/H_2O (1:1 v/v, 1.00 mL) and was heated at 100 °C in the microwave for 30 min. After removal of TFA it was lyophilized to give yellow oil. Purification by flash column chromatography (dichloromethane/methanol, 75:25) afforded derivative **10** as a white solid (10.7 mg, 0.07 mmol, 90%).

TLC R_f = 0.45 (dichloromethane/methanol, 75:25).

^{1}H NMR (300 MHz, D_2O, RT): δ (ppm) = 3.97 (d, 2H, $^3J_{H,H}$ = 5.1 Hz, CH_2), 5.34 (t, 1H, $^3J_{H,H}$ = 5.1 Hz, C<u>H</u>$(OH)_2$), 6.22 (d, 1H, $^3J_{H,H}$ = 7.7 Hz, H-5), 7.87 (d, 1H; $^3J_{H,H}$ = 7.7 Hz, H-6).

^{13}C NMR (126 MHz, D_2O, RT): δ (ppm) = 53.31 (1C, NCH_2), 88.40 (1C, $(CH(OH)_2$), 95.20 (1C, C-5), 116.58 (1C, CF_3), 148.30 (1C, C-6), 159.9 (1C, C-2), 165.34 (1C, <u>C</u>OCF_3), 168.34 (1C, C-4).

ESI-MS: *m/z* (rel. %): 154.1 (100) $[M+H]^+$, 172.1 (25) $[M+H_3O]^+$.

HRMS (ESI): calcd. for $[C_6H_8N_3O_2]^+$ ($[M+H]^+$): 154.0611, found: 154.0613.

6.7.9 1-(2,2-Diethoxyethyl)-thymine (**19**)

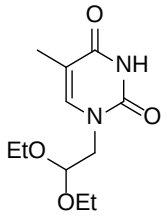

19

$C_{11}H_{18}N_2O_4$ [242.28]

A mixture of thymine (1.00 g, 8.10 mmol, 1.00 eq.), dry potassium carbonate (1.10 g, 8.1 mmol) and bromoacetaldehyde diethyl acetal (1.22 mL, 8.1 mmol, 1.00 eq.) in dry *N,N'*-dimethylformamide was heated at 110 °C under stirring for 24 h. The reaction mixture was concentrated under reduced pressure. The residue was taken up in water (30 mL) and extracted with ethyl acetate (3 x 50 mL). Purification by column chromatography (dichloromethane/methanol, 95:5) afforded derivative **19** as a yellow product (0.78 g, 3.24 mmol, 55%).

TLC R_f = 0.30 (dichloromethane/methanol, 95:5).

^{1}H-NMR (300 MHz, $CDCl_3$, RT): δ (ppm) = 1.11 (t, 6H, $^3J_{H,H}$ = 7.2 Hz, 2 x CH_3), 1.83 (d, 3H, $^3J_{H,H}$ = 1.2 Hz, C=CCH_3), 3.46 (dq, 2H, $^2J_{H,H}$ = 9.6 Hz, $^3J_{H,H}$ = 7.2 Hz, -O$CH_2$$CH_3$), 3.68 (dq, 2H, $^2J_{H,H}$ = 9.6 Hz, $^3J_{H,H}$ = 7.2 Hz, -O$CH_2$$CH_3$), 4.56 (t, 1H, $^3J_{H,H}$ = 5.4 Hz, $CH(OEt)_2$), 7.04 (q, 1H, $^3J_{H,H}$ = 1.2 Hz, C=CH), 10.04 (bs, 1H, NH).

^{13}C NMR (126 MHz, $CDCl_3$, RT): δ (ppm) = 12.72 (1C, C=$\underline{C}H_3$), 15.10 (2C, 2 x CH_3), 50.66 (1C, NCH_2), 64.08 (2C, 2 x O$\underline{C}H_2CH_3$), 100.20 (1C, $\underline{C}H(OEt)_2$), 109.72(1C, $\underline{C}$=CH_3), 141.95 (1C, C-6), 151.30 (1C, C-2), 164.68 (1C, C-4).

ESI-MS: *m/z* (rel. %): 243.1 (62) $[M+H]^+$, 265.1 (100) $[M+Na]^+$.

HRMS (ESI): calcd. for $[C_{11}H_{19}N_2O_4]^+$ ($[M+H]^+$): 243.1339, found: 243.1339; calcd. for $[C_{11}H_{18}N_2O_4Na]^+$ ($[M+H]^+$): 265.1159, found: 265.1158.

6.7.10 2-(2,4-Dihydroxy-5-methylpyrimidin-1-yl)-ethanal hydrate (**20**)

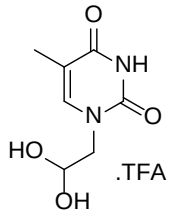

20
$C_7H_8N_2O_3$ [168.15]

1-(2,2-Diethoxyethyl)-thymine (10.0 mg, 0.04 mmol) was dissolved in TFA/H_2O (1:1 v/v, 0.5 mL) and heated at 100 °C in the microwave for 30 min. After removal of TFA it was lyophilized to give **14** (6.73 mg, 0.04 mmol, 90%) as a yellow solid.

TLC R_f = 0.30 (dichloromethane/methanol, 95:5).

^{1}H-NMR (300 MHz, D_2O, RT): δ (ppm) = 1.91 (s, 3H, CH_3), 3.86 (d, 2H, $^3J_{H,H}$ = 5.2 Hz, CH_2), 5.30 (t, 1H, $^3J_{H,H}$ = 5.2 Hz, $CH(OH)_2$), 7.49 (s, 1H, C=CH).

^{13}C-NMR (126 MHz, D_2O, RT): δ (ppm) = 13.81 (1C, C=$\underline{C}H_3$), 55.71 (1C, NCH_2), 89.98 (1C, $\underline{C}H(OEt)_2$), 112.99 (1C, C-5), 146.38 (1C, C-6), 155.02 (1C, C-2), 169.53 (1C, C-4).

ESI-MS: *m/z* (rel.%): 169.1 (100) $[M+H]^+$.

HRMS (ESI): calcd. for aldehyde $[C_7H_9N_2O_3]^+$ ($[M+H]^+$): 169.0608, found: 169.0609; calcd. for $[C_7H_7N_2O_3]^-$ ($[M-H]^-$): 167.0462, found: 167.0460.

6.8 SYNTHESIS OF PHENANTROLINE-ALDEHYDES

6.8.1 2,9-Dimethyl-1,10-phenantroline *N*-oxide dehydrate (**22**) [148]

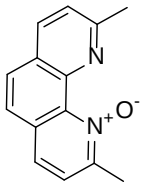

22
$C_{14}H_{12}N_2O$ [224.26]

A stirred solution of 2,9-dimethyl-1,10-phenantroline (1.00 g, 4.8 mmol) in glacial acetic acid (6 mL) and heated to 60 °C under reflux. Then hydrogen peroxide (0.93 mL, 30%) was added and heated further 3 hours under reflux. The reaction mixture was cooled down at room temperature. The mixture was added to sodium carbonate solution in order to bring the pH in neutral range. The resulting mixture was extracted with dichloromethane, dried over magnesium sulfate and evaporated under reduced pressure to afford derivative **22** as a black solid (1.06 g, 4.75 mmol, 99%).

^{1}H NMR (300 MHz, $CDCl_3$, RT): δ (ppm) = 2.74 (s, 3H, 2-phenCH_3), 2.89 (s, 3H, 9-phenCH_3), 7.46 (d, 1H, $^3J_{H,H}$ = 8.1 Hz, H-3), 7.48 (d, 1 H, $^3J_{H,H}$ = 8.1 Hz, H-8), 7.59-7.63 (m, 2H, H-5, H-6), 7.67 (d, 1H, $^3J_{H,H}$ = 8.1 Hz, H-4), 8.07 (d, 1H, $^3J_{H,H}$ = 8.2 Hz, H-7).

^{13}C NMR (126 MHz, $CDCl_3$, RT): δ (ppm) = 19.55 (1 C, 2C-CH_3), 26.11 (1 C, 2C-CH_3), 123.31 (2 C, C5, C6), 123.35 (1C, C8), 123.86 (1C, C3), 125.43 (1C, C4b), 127.83 (1C, C4), 131.69 (1C, C4a), 135.77 (1C, C7), 136.09 (1C, C10a), 142.20 (1C, C10b), 150.13 (1C, C2), 158.60 (1C, C9).

ESI-MS: *m/z* (*rel.*%): 225.1 (100) $(M+H)^+$, 447.2 (30) $(2M-H)^-$.

HRMS (ESI): calcd. for $[C_{14}H_{13}N_2O]^+$ ($[M+H]^+$): 225.1022, found: 225.1026; calcd. for $[C_{14}H_{11}N_2O]^+$ ($[M-H]^-$): 223.0877, found: 223.0873.

6.8.2 2-(Acetoxymethyl)-9-methyl-1,10-phenantroline (**23**)[148]

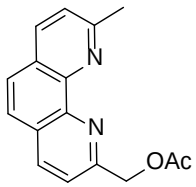

23
$C_{16}H_{14}N_2O_2$ [266.30]

To a solution of 2,9-dimethyl-1,10-phenantroline *N*-Oxide dihydrate (0.50 g, 2.2 mmol) in dichloromethane, acetic anhydride (2 mL) was added. Dichloromethane was removed under reduced pressure and the solution was refluxed for 1 hour. The solvent was removed under reduced pressure and the residue was taken in chloroform, washed with saturated aqueous sodium carbonate Na_2CO_3, dried over magnesium sulfate and again concentrated under reduced pressure. The crude residue was eluted through a short Al_2O_3 column with dichloromethane/ethylacetate to afford the derivative **23** (0.53 g, 2.00 mmol, 90%).

^{1}H NMR (300 MHz, $CDCl_3$, RT): δ (ppm) = 2.22 (s, 3H, CO_2CH_3), 2.97 (s, 3H, 9-phenCH_3), 5.66 (s, 2H, CH_2) 7.52 (d, 1H, $^3J_{H,H}$ = 8.1 Hz, H-3), 7.54 (d, 1 H, $^3J_{H,H}$ = 8.1 Hz, H-8), 7.69-7.74 (m, 2H, H-5, H-6), 7.77 (d, 1H, $^3J_{H,H}$ = 8.1 Hz, H-4), 8.28 (d, 1H, $^3J_{H,H}$ = 8.2 Hz, H-7).

^{13}C NMR (126 MHz, $CDCl_3$, RT): δ (ppm) = 20.95 (1 C, $COCH_3$), 25.70 (1C, CH_3), 67.7 (1C, CH_2), 120.86 (1C, C8), 123.4 (1C, C3), 123.7 (1C, 6C), 125.2 (1C, 5C), 126.4 (1C, C4b) 127.9 (1C, C4a), 136.1 (1C, C4), 136.9 (1C, C7), 145.0, (1C, C10a), 145.1 (1C, C10b), 156.3 (1C, C2), 159.5 (1C,C9) 170.6 (1C, CO).

ESI-MS: *m/z* (rel.%): 267.1 (100) $(M+H)^+$, 289.1 (12) $(M+Na)^+$.

HRMS (ESI): calcd. for $[C_{16}H_{15}N_2O_2]^+$ ($[M+H]^+$): 267.1128, found: 267.1132; calcd. for $[C_{16}H_{14}N_2O_2Na]^+$ ($[M+Na]^+$): 289.0947, found: 289.0947.

6.8.3 2-(Hydroxymethyl)-9-methyl-1,10-phenantroline (**24**)[148]

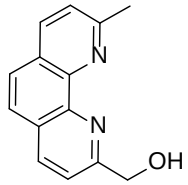

24

$C_{14}H_{12}N_2O$ [224.26]

A suspension of 2-(Acetoxymethyl)-9-methyl-1,10-phenantroline (0.65 g, 2.44 mmol) and anhydrous K_2CO_3 (600 mg) in anhydrous ethanol (15 mL) was stirred for 4 hours. The mixture was concentrated under reduced pressure and the residue was extracted with dichloromethane. The organic layer was evaporated under reduced pressure to afford the derivative **24** (0.47 g, 2.12 mmol, 87%).

^{1}H NMR (300 MHz, DMSO, RT): δ (ppm) = 2.93 (s, 3H, 9-phenCH_3), 5.11 (s, 2H, CH_2), 7.49 (d, 1H, $^3J_{H,H}$ = 8.1 Hz, H-3), 7.51 (d, 1 H, $^3J_{H,H}$ = 8.1 Hz, H-8), 7.62 (d, 1H, $^3J_{H,H}$ = 8.1 Hz, H-4), 7.71 (d, 2H, $^3J_{H,H}$ = 8.4 Hz, H-5, H-6), 8.21 (d, 1H, $^3J_{H,H}$ = 8.2 Hz, H-7).

^{13}C NMR (126 MHz, DMSO, RT): δ (ppm) = 24.93 (1C, CH_3), 64.82 (1C, CH_2), 119.93 (1C, C3), 123.06 (1C, C8), 125.20 (1C, 6C), 125.28 (1C, 5C), 125.56 (1C, C4b), 126.33 (1C, C4a), 136.04 (1C, C7), 136.09 (1C, C4), 144.48 (1C, C10a), 144.53 (1C,C10b), 157.87 (1C, C9), 161.76 (1C, C2).

ESI-MS: *m/z* (rel.%): 225.1 (100) $(M+H)^+$, 247.1 (23) $(M+Na)^+$, 471.2 (43) $(2M+Na)^+$.

HRMS (ESI): calcd. for $[C_{14}H_{13}N_2O]^+$ ($[M+H]^+$): 225.1022, found:225.1022; calcd. for $[C_{14}H_{12}N_2ONa]^+$ ($[M+Na]^+$): 247.0842, found: 247.0836.

6.8.4 9-Methyl-1,10-phenantroline-2-carbaldehyde (**25**)

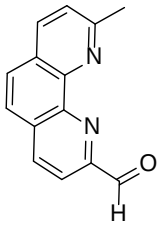

25
$C_{14}H_{10}N_2O$ [222.25]

A solution of oxalyl chloride (0.6 mL, 2.33 mmol, 1.60 eq.) in dry dichloromethane (0.2 mL) under argon was cooled to -78 °C. A mixture of DMSO (0.18 mL, 2.33 mmol) in dichloromethane (1.50 mL) was slowly added and it was stirred further 15 minutes at -78 °C. 2-(Hydroxymethyl)-9-methyl-1,10-phenantroline (0.34 g, 1.5 mmol, 1.00 eq.) in dichloromethane (3 mL) was slowly added to this mixture and was stirred for 30 minutes. Triethylamine (1.8 mL) was added to that mixture. After the addition was completed, the reaction mixture was warmed up to room temperature and 30 minutes later water (20 mL) was added. The organic phase was separated and the water phase was extracted with dichloromethane. The combined organic phases were washed with brine, dried with magnesium sulfate and concentrated. Purification by column chromatography (dichloromethane/methanol, 98:2) afforded **25** as a yellow solid (0.07 g, 0.3 mmol, 20%).

^{1}H NMR (300 MHz, DMSO, RT): δ (ppm) = 2.82 (s, 3H, 9-phenCH_3), 7.71 (d, 1H, $^3J_{H,H}$ = 8.1 Hz, H-3), 7.73 (d, 1H, $^3J_{H,H}$ = 8.1 Hz, H-8), 8.08 (d, 2H, $^3J_{H,H}$ = 8.4 Hz, H-5, H-6), 8.22 (d, 1H, $^3J_{H,H}$ = 8.1 Hz, H-4), 8.69 (d, 1H, $^3J_{H,H}$ = 8.2 Hz, H-7), 10.12 (s, 1H, CHO) .

^{13}C NMR (126 MHz, DMSO, RT): δ (ppm) = 25.03 (1C, CH_3), 120.74 (1C, C3), 129.76 (1C, C8), 131.20 (1C, 6C), 131.98 (1C, 5C), 132.56 (1C, C4b), 133.33 (1C, C4a), 143.04 (1C, C7), 143.09 (1C, C4), 151.64 (1C, C10a), 151.75 (1C,C10b), 163.87 (1C, C9), 167.76 (1C, C2), 194.21 (1C, CHO).

ESI-MS: *m/z* (rel. %): 223.1 (100) $(M+H)^+$, 245.1 (23) $(M+Na)^+$.

HRMS (ESI): calcd. for $[C_{14}H_{11}N_2O]^+$ ($[M+H]^+$): 223.0866, found: 223.0867; calcd. for $[C_{14}H_{10}N_2ONa]^+$ ($[M+Na]^+$): 245.0685, found: 245.0682.

6.8.5 2-Methyl-1,10-phenantroline (**28**)[149]

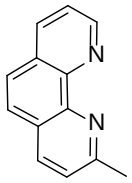

28
$C_{13}H_{10}N_2$ [194.24]

8-aminoquinoline (2.00 g, 14.0 mmol, 1.00 eq.) and sodium iodide (22 mg, 0.15 mmol) were heated at 110 °C in 70% sulfuric acid H_2SO_4 (3 mL) to allow the complete dissolution of the solids. After complete dissolution of the solids, the cratonaldehyde (1.00 mL, 14 mmol, 1.00 eq.) was added under nitrogen atmosphere over 5 h at 110 °C, maintaining a continuous stirring. After a further hour at 110 °C the black color reaction mixture was allowed to cool at room temperature and slowly poured into 1 M sodium carbonate Na_2CO_3 solution (70 mL) until the final pH was around 8. The aqueous solution was extracted with dichloromethane (2 × 40 mL) and the combined organic layers were extracted with 37% hydrochloric acid HCl. The acidic solution was neutralized by the addition of concentrated sodium hydroxide NaOH solution and extracted with dichloromethane (3 × 50 mL). The organic layers were combined and the solvent evaporated under reduced pressure. The product was purified by column chromatography on silica gel (dichloromethane/methanol, 95:5) and dried over magnesium sulfate affording the corresponding 2-methyl-1,10-phenantroline (1.68 g, 8.68 mmol, 62%).

^{1}H-NMR (300 MHz, $CDCl_3$, RT): δ (ppm) = 2.95 (s, 3H, CH_3), 7.52 (d, 1H, $^3J_{H,H}$ = 8.2 Hz, H-3), 7.55 (dd, 1H, $^3J_{H,H}$ = 8.1 Hz, 4.3 Hz, H-8), 7.71-7.80 (m, 2H, H-5, H-6), 8.14 (d, 1H, $^3J_{H,H}$ = 8.1 Hz, H-4), 8.25 (dd, 1H, $^3J_{H,H}$ = 8.1 Hz, 1.5 Hz, H-7), 9.21 (dd, 1H, $J_{H,H}$ = 4.3 Hz, 1.6 Hz, H-9).
^{13}C-NMR (126 MHz, $CDCl_3$, RT): δ (ppm) = 37.2 (1C, CH_3), 122.65 (1C, C8), 123.65(1C, C3), 125.32 (1C, C6), 126.37 (1C, C5), 126.54 (1C, C4b), 128.65 (1C, C4a), 136.04 (1C, C7), 136.09 (1C, C4), 145.7 (1C, C10a), 146.0 (1C, C10b), 150.02 (1C,C9), 159.46 (1C, C2).
ESI-MS: *m/z* (rel. %): 195.1 (100) $(M+H)^+$, 411.2 (45) $[2M+Na]^+$.
HRMS (ESI): calcd. for $[C_{13}H_{11}N_2]^+$ ($[M+H]^+$): 195.0917, found: 195.0910; calcd. for $[C_{13}H_{10}N_2Na]^+$ ($[M+Na]^+$): 217.0736, found: 217.0737.

6.8.6 1,10-Phenantroline-2-carbaldehyde (**29**)

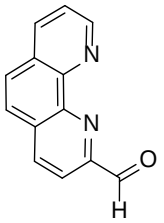

29
$C_{13}H_8N_2O$ [208.22]

The seleniumdioxide (SeO_2) (0.60 g, 5.46 mmol, 2.10 eq.) was dissolved in dioxane (19 mL) and water (0.5 mL) and heated under reflux. 2-methyl-1,10-phenantroline (0.50 g, 2.60 mmol, 1.00 eq.) was dissolved in dioxane (12 mL) and added quickly to the refluxing mixture. The mixture is refluxed for 15 minutes and then decanted from selenium through filtering it when it is hot into a large flask. The solvent was evaporated and the residue was given in water to extract it with chloroform. The organic layer was evaporated under reduced pressure and dried over Na_2SO_4 to afford derivative **29** as a brown solid (0.38 g, 1.82 mmol, 70%).

^{1}H NMR (300 MHz, DMSO, RT): δ (ppm) = 7.84 (d, 1H, $^3J_{H,H}$ = 8.1 Hz, H-3), 7.86 (d, $^3J_{H,H}$ = 8.1 Hz, 1H, H-8), 8.09-8.25 (m, 2H, H-5, H-6), 8.56 (d, 1H, $^3J_{H,H}$ = 8.1 Hz, H-4), 8.71 (dd, $J_{H,H}$ = 8.1 Hz, 1.5 Hz, 1H, H-7), 9.18 (dd, 1H, $J_{H,H}$ = 4.3 Hz, 1.6 Hz, H-9), 10.30 (s, 1H, CHO).

ESI-MS: *m/z* (rel. %): 223.1 (100) $(M+H)^+$, 209.1 (58) (M+Na).

HRMS (ESI): calcd. for $[C_{13}H_9N_2O]^+$ ($[M+H]^+$): 209.0709, found: 209.0711; calcd. for $[C_{13}H_8N_2ONa]^+$ ($[M+Na]^+$): 231.0529, found: 231.0529.

6.9 OLIGONUCLEOTIDES

OLIGO **ON1**

5'-C-G-C-T-A-T-**X**-T-A-T-C-G-C-3'

$C_{120}H_{159}N_{41}O_{76}P_{12}$ [3763.49]

HPLC: (DNAPac PA200 4x5mm, DIONEX Ionexchange, Gradient: 25-60% B2 in 30min. [B2 = 20 mM Tris-Cl, 1.25 M NaCl, pH 8.0, 80° C]): t_R = 7.3 min.

ESI-MS *m*/*z*: 3761.67 [M], deconvulated spectrum.

OLIGO **ON1+G**

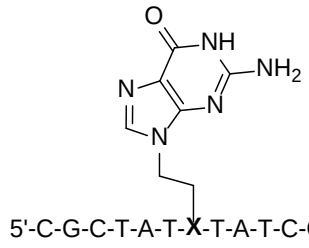

5'-C-G-C-T-A-T-**X**-T-A-T-C-G-C-3'

$C_{127}H_{166}N_{46}O_{77}P_{12}$ [3940.66]

HPLC: (DNAPac PA200 4x5mm, DIONEX Ionexchange, Gradient: 25-60% B2 in 30min. [B2 = 20 mM Tris-Cl, 1.25 M NaCl, pH 8.0, 80° C]): t_R = 9.6 min.

ESI-MS *m*/*z*: 3938.73 [M], 3960.72 [M+Na-H], 3982.70 [M+2Na-2H], deconvulated spectrum.

OLIGO **ON1+C**

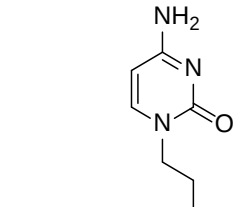

5'-C-G-C-T-A-T-**X**-T-A-T-C-G-C-3'

$C_{126}H_{166}N_{44}O_{77}P_{12}$ [3900.63]

HPLC: (DNAPac PA200 4x5mm, DIONEX Ionexchange, Gradient: 25-60% B2 in 30min. [B2 = 20 mM Tris-Cl, 1.25 M NaCl, pH 8.0, 80° C]): t_R = 9.0 min.

ESI-MS *m/z*: 3898.73 [M], 3920.71 [M+Na-H], 3936.68 [M+K-2H], deconvulated spectrum.

OLIGO **ON1+A**

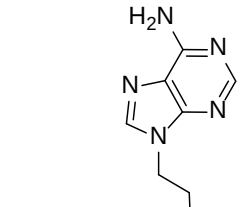

5'-C-G-C-T-A-T-**X**-T-A-T-C-G-C-3'

$C_{127}H_{166}N_{46}O_{76}P_{12}$ [3924.66]

HPLC: (DNAPac PA200 4x5mm, DIONEX Ionexchange, Gradient: 25-60% B2 in 30min. [B2 = 20 mM Tris-Cl, 1.25 M NaCl, pH 8.0, 80° C]): t_R = 9.2 min.

ESI-MS *m/z*: 3922.74 [M], 3944.72 [M+Na-H], 3966.70 [M+2Na-2H], deconvulated spectrum.

OLIGO **ON1+T**

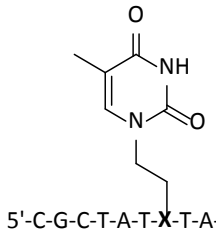

5'-C-G-C-T-A-T-**X**-T-A-T-C-G-C-3'

$C_{127}H_{167}N_{43}O_{78}P_{12}$ [3915.64]

HPLC: (DNAPac PA200 4x5mm, DIONEX Ionexchange, Gradient: 25-60% B2 in 30min. [B2 = 20 mM Tris-Cl, 1.25 M NaCl, pH 8.0, 80° C]): t_R = 9.3 min.

ESI-MS *m/z*: 3913.72 [M], 3935.70 [M+Na-H], 3957.68 [M+2Na-2H], deconvulated spectrum.

OLIGO **ON1+P**

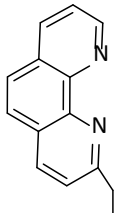

5'-C-G-C-T-A-T-X-T-A-T-C-G-C-3'

$C_{133}H_{167}N_{43}O_{76}P_{12}$ [3955.71]

HPLC: (DNAPac PA200 4x5mm, DIONEX Ionexchange, Gradient: 25-60% B2 in 30min. [B2 = 20 mM Tris-Cl, 1.25 M NaCl, pH 8.0, 80° C]): t_R = 5.8 min.

ESI-MS *m/z*: 3953.74 [M], deconvulated spectrum.

ABBREVIATIONS

A	adenine
Ac	acetyl
AcOH	acetic acid
AE	anion exchange
approx.	approximately
aq	aqueous
ATP	adenosine 5'-triphosphate
bp	base pair(s)
br s	broad singlet (NMR assignment)
Bz	benzoyl
C	cytosine
calcd.	calculated
cat.	catalytic
conc.	concentrate
d	doublet (NMR assignment)
DCC	dynamic combinatorial chemistry
DCL	dynamic combinatorial library
DCM	dichloromethane
dd	doublet of doublets (NMR assignment)
dATP	2'-deoxyadenosine 5'-triphosphate
dCTP	2'-deoxycytidine 5'-triphosphate
dGTP	2'-deoxyguanosine 5'-triphosphate
DiPEA	*N,N*-diisopropylethylamine
DMAP	4-dimethylaminopyridine
DMF	*N,N*-dimethylformamide
DMSO	dimethylsulfoxide
DNA	2'-deoxyribonucleic acid
dNTP	2'-deoxynucleotide 5'-triphosphate
dq	doublet of quartets (NMR assignment)
dsDNA	double-stranded 2'-deoxyribonucleic acid
dTTP	2'-deoxythymidine 5'- triphosphate
EDTA	ethylenediaminetetraacetic acid

EI	electron impact
eq	equivalent(s)
ES	electrospray
Et	ethyl
F	fluorophore
FA	formic acid
Fmoc	fluorenylmethoxycarbonyl
G	guanine
h	hour(s)
HPLC	high performance liquid chromatography
HRMS	high resolution mass spectrometry
I	relative peak intensity
J	NMR coupling constant (preceding superscript number denotes the number of bonds separating coupled nuclei)
kb	kilobases (i.e. thousand bases)
LCMS	liquid chromatography mass spectrometry
LNA	locked nucleic acid
m	multiplet (NMR assignment)
MALDI	matrix-assisted laser desorption/ionization
Me	methyl
min	minute(s)
Mmt	monomethoxytrityl
mp	melting point
mRNA	messenger RNA
MS	mass spectrometry
m/z	mass-to-charge ratio
NMR	nuclear magnetic resonance
nt	nucleotide
PAGE	polyacrylamide gel electrophoresis
PBS	phosphate buffered saline
PCR	polymerase chain reaction
PEG	polyethylene glycol
PG	protecting group
PNA	peptide nucleic acid

PPi	pyrophosphate
ppm	parts per million
q	quartet (NMR assignment)
RNA	ribonucleic acid
R*f*	thin layer chromatography retention factor (R*f* = (distance travelled by analyte) /(distance travelled by solvent))
rNMP	ribonucleoside monophosphates
rNTP	ribonucleoside triphosphates
rRNA	ribosomal RNA
RT	room temperature
s	singlet (NMR assignment)
sat.	saturated
SNP	single nucleotide polymorphism
ssDNA	single-stranded 2'-deoxyribonucleic acid
T	thymine
t	triplet (NMR assignment)
TFA	trifluoroacetic acid
THF	tetrahydrofuran
TLC	thin layer chromatography
T_m	duplex melting temperature
TOF	time-of-flight
t_R	retention time
Tris	tris(hydroxymethyl)aminomethane
tRNA	transfer RNA
U	uracil
UV	volume/volume ratio
w/v	weight/volume ratio
δ	chemical shift
v	frequency

BIBLIOGRAPHY

[1] J. D. Watson, F. H. C. Crick, *Nature* **1953**, *171*, 737–738.

[2] E. Kool, J. Morales, K. Guckian, *Angew. Chem. Int. Ed.* **2000**, *39*, 990–1009.

[3] P. Yakovchuk, E. Protozanova, M. D. Frank-Kamenetskii, *Nucleic Acids Res.* **2006**, *34*, 564–574.

[4] Y.-P. Pang, J. L. Miller, P. A. Kollman, *J. Am. Chem. Soc.* **1999**, *121*, 1717–1725.

[5] D. B. Smithrud, T. B. Wyman, F. Diederich, *J. Am. Chem. Soc.* **1991**, *113*, 5420–5426.

[6] K. M. Guckian, B. A. Schweitzer, R. X.-F. Ren, C. J. Sheils, D. C. Tahmassebi, E. T. Kool, *J. Am. Chem. Soc.* **2000**, *122*, 2213–2222.

[7] J. M. Berg, J. L. Tymoczko, L. Stryer, in *Biochem. Textb.*, **2006**, p. 1120.

[8] N. C. Seeman, *Nature* **2003**, *421*, 427–431.

[9] N. C. Seeman, *Angew. Chemie Int. Ed.* **1998**, *37*, 3220–3238.

[10] N. C. Seeman, *Mol. Biotechnol.* **2007**, *37*, 246–257.

[11] J. S. Cohen, *Oligodeoxynucleotides: Antisense Inhibitors of Gene Expression*, Macmillan Press, **1989**.

[12] J. Kurreck, *Eur. J. Biochem.* **2003**, *270*, 1628–1644.

[13] C. Wilson, A. D. Keefe, *Curr. Opin. Chem. Biol.* **2006**, *10*, 607–614.

[14] C. Wojczewski, K. Stolze, J. W. Engels, *Synlett* **1999**, *1999*, 1667–1678.

[15] N. C. Seeman, *Chem. Biol.* **2003**, *10*, 1151–1159.

[16] P. W. K. Rothemund, *Nature* **2006**, *440*, 297–302.

[17] K. Tanaka, A. Tengeiji, T. Kato, N. Toyama, M. Shionoya, *Science* **2003**, *299*, 1212–13.

[18] J. Gao, C. Strässler, D. Tahmassebi, E. T. Kool, *J. Am. Chem. Soc.* **2002**, *124*, 11590–11591.

[19] S. K. Silverman, *Angew. Chem. Int. Ed.* **2010**, *49*, 7180–7201.

[20] Z. J. Gartner, R. Grubina, C. T. Calderone, D. R. Liu, *Angew. Chem. Int. Ed.* **2003**, *42*, 1370–1375.

[21] D. Summerer, A. Marx, *Angew. Chem. Int. Ed.* **2002**, *41*, 89–90.

[22] Z. J. Gartner, D. R. Liu, *J. Am. Chem. Soc.* **2001**, *123*, 6961–6963.

[23] U. Asseline, *Curr. Org. Chem.* **2006**, *10*, 491–518.

[24] Q. Gu, C. Cheng, R. Gonela, S. Suryanarayanan, S. Anabathula, K. Dai, D. T. Haynie, *Nanotechnology* **2006**, *17*, R14–R25.

[25] K. Keren, M. Krueger, R. Gilad, G. Ben-Yoseph, U. Sivan, E. Braun, *Science* **2002**, *297*, 72–75.

[26] R. K. Saiki, D. H. Gelfand, S. Stoffel, S. J. Scharf, R. Higuchi, G. T. Horn, K. B. Mullis, H. A. Erlich, *Science* **1988**, *239*, 487–491.

[27] S. L. Beaucage, M. H. Caruthers, *Tetrahedron Lett.* **1981**, *22*, 1859–1862.

[28] R. T. Pon, *Tetrahedron Lett.* **1991**, *32*, 1715–1718.

[29] M. V Kvach, D. A. Tsybulsky, A. V Ustinov, I. A. Stepanova, S. L. Bondarev, S. V Gontarev, V. A. Korshun, V. V Shmanai, *Bioconjug. Chem.* **2007**, *18*, 1691–1696.

[30] M. Adamczyk, C. M. Chan, J. R. Fino, P. G. Mattingly, *J. Org. Chem.* **2000**, *65*, 596–601.

[31] S. I. Khan, A. E. Beilstein, M. T. Tierney, M. Sykora, M. W. Grinstaff, *Inorg. Chem.* **1999**, *38*, 5999–6002.

[32] M. H. Lyttle, T. G. Carter, D. J. Dick, R. M. Cook, *J. Org. Chem.* **2000**, *65*, 9033–9038.

[33] S. L. Beaucage, R. P. Iyer, *Tetrahedron* **1993**, *49*, 1925–1963.

[34] S. M. Freier, K. H. Altmann, *Nucleic Acids Res.* **1997**, *25*, 4429–4443.

[35] A. T. Krueger, H. Lu, A. H. F. Lee, E. T. Kool, *Acc. Chem. Res.* **2007**, *40* , 141–150.

[36] E. T. Kool, *Acc. Chem. Res.* **2002**, *35*, 936–943.

[37] A. J. A. Cobb, *Org. Biomol. Chem.* **2007**, *5*, 3260–3275.

[38] S. H. Weisbrod, A. Marx, *Chem. Commun.* **2008**, 5675–5685.

[39] S. Jäger, G. Rasched, H. Kornreich-Leshem, M. Engeser, O. Thum, M. Famulok, *J. Am. Chem. Soc.* **2005**, *127*, 15071–15082.

[40] A. Nadler, J. Strohmeier, U. Diederichsen, *Angew. Chem. Int. Ed.* **2011**, *50*, 5392–5396.

[41] F. Seela, M. Zulauf, *Chem. Eur. J.* **1998**, *4*, 1781–1790.

[42] H. Weizman, Y. Tor, *J. Am. Chem. Soc.* **2001**, *123*, 3375–3376.

[43] G. V. Bobkov, S. N. Mikhailov, A. Van Aerschot, P. Herdewijn, *Tetrahedron* **2008**, *64*, 6238–6251.

[44] M. Kimoto, R. Kawai, T. Mitsui, S. Yokoyama, I. Hirao, *Nucleic Acids Res.* **2009**, *37*, e14.

[45] I. Hirao, M. Kimoto, *Proc. Jpn. Acad. Ser. B. Phys. Biol. Sci.* **2012**, *88*, 345–367.

[46] M. S. Christensen, C. M. Madsen, P. Nielsen, *Org. Biomol. Chem.* **2007**, *5*, 1586–1594.

[47] N. K. Christensen, T. Bryld, M. D. Sørensen, K. Arar, J. Wengel, P. Nielsen, *Chem. Commun.* **2004**, 282–283.

[48] K. Groebke, J. Hunziker, W. Fraser, L. Peng, U. Diederichsen, K. Zimmermann, A. Holzner, C. Leumann, A. Eschenmoser, *Helv. Chim. Acta* **1998**, *81*, 375–474.

[49] K. Haraguchi, N. Shiina, Y. Yoshimura, H. Shimada, K. Hashimoto, H. Tanaka, *Org. Lett.* **2004**, *6*, 2645–2648.

[50] N. Oka, T. Wada, K. Saigo, *J. Am. Chem. Soc.* **2003**, *125*, 8307–8317.

[51] P. S. Miller, J. Yano, E. Yano, C. Carroll, K. Jayaraman, P. O. P. Ts'o, *Biochemistry* **1979**, *18*, 5134–5143.

[52] C. A. Stein, Y. C. Cheng, *Science* **1993**, *261*, 1004–1012.

[53] J. K. Chen, R. G. Schultz, D. H. Lloyd, S. M. Gryaznov, *Nucleic Acids Res.* **1995**, *23*, 2661–2668.

[54] L. Zhang, A. Peritz, E. Meggers, *J. Am. Chem. Soc.* **2005**, *127*, 4174–4175.

[55] K. Murayama, Y. Tanaka, T. Toda, H. Kashida, H. Asanuma, *Chem. Eur. J.* **2013**, *19*, 14151–14158.

[56] H. Kashida, K. Murayama, T. Toda, H. Asanuma, *Angew. Chem. Int. Ed.* **2011**, *50*, 1285–1288.

[57] M. Egholm, O. Buchardt, L. Christensen, C. Behrens, S. M. Freier, D. A. Driver, R. H. Berg, S. K. Kim, B. Norden, P. E. Nielsen, *Nature* **1993**, *365*, 566–568.

[58] T. Fujii, H. Kashida, H. Asanuma, *Chem. Eur. J.* **2009**, *15*, 10092–10102.

[59] H. Asanuma, Y. Hara, A. Noguchi, K. Sano, H. Kashida, *Tetrahedron Lett.* **2008**, *49*, 5144–5146.

[60] H. Kashida, T. Fujii, H. Asanuma, *Org. Biomol. Chem.* **2008**, *6*, 2892–2899.

[61] H. Kashida, X. Liang, H. Asanuma, *Curr. Org. Chem.* **2009**, *13*, 1065–1084.

[62] N. Usman, C. D. Juby, K. K. Ogilvie, *Tetrahedron Lett.* **1988**, *29*, 4831–4834.

[63] P. S. Nelson, M. Kent, S. Muthini, *Nucleic Acids Res.* **1992**, *20*, 6253–6259.

[64] F. Vandendriessche, K. Augustyns, A. Van Aerschot, R. Busson, J. Hoogmartens, P. Herdewijn, *Tetrahedron* **1993**, *49*, 7223–7238.

[65] L. Zhang, E. Meggers, *J. Am. Chem. Soc.* **2005**, *127*, 74–75.

[66] K. Yamana, M. Takei, H. Nakano, *Tetrahedron Lett.* **1997**, *38*, 6051–6054.

[67] H. Asanuma, T. Toda, K. Murayama, X. Liang, H. Kashida, *J. Am. Chem. Soc.* **2010**, *132*, 14702–14703.

[68] V. Kumar, K. R. Gore, P. I. Pradeepkumar, V. Kesavan, *Org. Biomol. Chem.* **2013**, 5853–5865.

[69] D. Graham, A. Grondin, C. McHugh, L. Fruk, W. E. Smith, *Tetrahedron Lett.* **2002**, *43*, 4785–4788.

[70] F. Amblard, J. H. Cho, R. F. Schinazi, *Chem. Rev.* **2009**, *109*, 4207–4220.

[71] O.Jochim, *Dissertation*, Georg-August-University Goettingen, **2014**.

[72] Y. Ura, J. M. Beierle, L. J. Leman, L. E. Orgel, M. R. Ghadiri, *Science* **2009**, *325*, 73–77.

[73] P. Seneci, S. Miertus, *Mol. Divers.* **2000**, *5*, 75–89.

[74] M. H. Fonseca, B. List, *Curr. Opin. Chem. Biol.* **2004**, *8*, 319–326.

[75] F. Balkenhohl, C. von dem Bussche-Hünnefeld, A. Lansky, C. Zechel, *Angew. Chem. Int. Ed.* **1996**, *35*, 2288–2337.

[76] N. K. Terrett, *Combinatorial Chemistry*, Oxford Chemistry Masters, **1998**.

[77] J.-M. Lehn, *Chem. Eur. J.* **1999**, *5*, 2455–2463.

[78] S. J. Rowan, S. J. Cantrill, G. R. L. Cousins, J. K. M. Sanders, J. F. Stoddart, *Angew. Chem. Int. Ed.* **2002**, *41*, 898–952.

[79] O. Ramström, J.-M. Lehn, *Nat. Rev. Drug Discov.* **2002**, *1*, 26–36.

[80] B. L. Miller, *Dynamic Combinatorial Chemistry: In Drug Discovery, Bioorganic Chemistry, and Materials Science*, John Wiley & Sons, **2009**.

[81] A. Herrmann, *Chem. Soc. Rev.* **2014**, *43*, 1899–1933.

[82] S. Otto, R. L. E. Furlan, J. K. M. Sanders, *Drug Discov. Today* **2002**, *7*, 117–125.

[83] P. T. Corbett, J. Leclaire, L. Vial, K. R. West, J.-L. Wietor, J. K. M. Sanders, S. Otto, *Chem. Rev.* **2006**, *106*, 3652–3711.

[84] C. D. Meyer, C. S. Joiner, J. F. Stoddart, *Chem. Soc. Rev.* **2007**, *36*, 1705–1723.

[85] C. Godoy-Alcántar, A. K. Yatsimirsky, J.-M. Lehn, *J. Phys. Org. Chem.* **2005**, *18*, 979–985.

[86] V. Goral, M. I. Nelen, A. V Eliseev, J. M. Lehn, *Proc. Natl. Acad. Sci. U. S. A.* **2001**, *98*, 1347–1352.

[87] T. Bunyapaiboonsri, O. Ramström, S. Lohmann, J. M. Lehn, L. Peng, M. Goeldner, *ChemBioChem* **2001**, *2*, 438–444.

[88] I. Huc, J.-M. Lehn, *Proc. Natl. Acad. Sci.* **1997**, *94*, 2106–2110.

[89] A. F. Abdel-Magid, K. G. Carson, B. D. Harris, C. A. Maryanoff, R. D. Shah, *J. Org. Chem.* **1996**, *61*, 3849–3862.

[90] Z. J. Gartner, M. W. Kanan, D. R. Liu, *Angew. Chem. Int. Ed.* **2002**, *41*, 1796–1800.

[91] D. T. Hickman, N. Sreenivasachary, J.-M. Lehn, *Helv. Chim. Acta* **2008**, *91*, 1–20.

[92] B. Klekota, B. L. Miller, *Tetrahedron* **1999**, *55*, 11687–11697.

[93] P. Dydio, P.-A. R. Breuil, J. N. H. Reek, *Isr. J. Chem.* **2013**, *53*, 61–74.

[94] B. L. Miller, *Top. Curr. Chem.* **2012**, *322*, 107–137.

[95] U. Diederichsen, *ChemBioChem* **2009**, *10*, 2717–2719.

[96] L. E. Orgel, R. Lohrmann, *Acc. Chem. Res.* **1974**, *7*, 368–377.

[97] J. M. Heemstra, D. R. Liu, *J. Am. Chem. Soc.* **2009**, *131*, 11347–11349.

[98] R. Naylor, P. T. Gilham, *Biochemistry* **1966**, *5*, 2722–2728.

[99] T. Inoue, G. F. Joyce, K. Grzeskowiak, L. E. Orgel, J. M. Brown, C. B. Reese, *J. Mol. Biol.* **1984**, *178*, 669–676.

[100] G. von Kiedrowski, *Angew. Chem. Int. Ed.* **1986**, *25*, 932–935.

[101] X. Li, Z. Y. J. Zhan, R. Knipe, D. G. Lynn, *J. Am. Chem. Soc.* **2002**, *124*, 746–747.

[102] Y. Xu, N. B. Karalkar, E. T. Kool, *Nat. Biotechnol.* **2001**, *19*, 148–152.

[103] D. M. Rosenbaum, D. R. Liu, *J. Am. Chem. Soc.* **2003**, *125*, 13924–13925.

[104] J. J. Chen, X. Cai, J. W. Szostak, *J. Am. Chem. Soc.* **2009**, *131*, 2119–2121.

[105] G. F. Joyce, *Cold Spring Harb. Symp. Quant. Biol.* **1987**, *52*, 41–51.

[106] T. Wu, L. E. Orgel, *J. Am. Chem. Soc.* **1992**, *114*, 5496–5501.

[107] F. Diederich, *Templated Organic Synthesis*, John Wiley & Sons, **2008**.

[108] J. T. Goodwin, D. G. Lynn, *J. Am. Chem. Soc.* **1992**, *114*, 9197–9198.

[109] X. Li, D. R. Liu, *Angew. Chem. Int. Ed.* **2004**, *43*, 4848–4870.

[110] J. Niu, R. Hili, D. R. Liu, *Nat. Chem.* **2013**, *5*, 282–292.

[111] Z.-Y. J. Zhan, D. G. Lynn, *J. Am. Chem. Soc.* **1997**, *119*, 12420–12421.

[112] B. A. Schweitzer, E. T. Kool, *J. Org. Chem.* **1994**, *59*, 7238–7242.

[113] P. J. Unrau, D. P. Bartel, *Nature* **1998**, *395*, 260–263.

[114] J. M. Heemstra, D. R. Liu, **n.d.**

[115] F. R. Bowler, J. J. Diaz-Mochon, M. D. Swift, M. Bradley, *Angew. Chem. Int. Ed.* **2010**, *49*, 1809–1812.

[116] Y. Brudno, D. R. Liu, *Chem. Biol.* **2009**, *16*, 265–276.

[117] M. A. Reynolds, T. A. Beck, R. I. Hogrefe, A. McCaffrey, L. J. Arnold, M. M. Vaghefi, *Bioconjug. Chem.* **1992**, *3*, 366–374.

[118] K. Fukui, M. Morimoto, H. Segawa, K. Tanaka, T. Shimidzu, *Bioconjug. Chem.* **1996**, *7*, 349–355.

[119] K. Fukui, K. Iwane, T. Shimidzu, K. Tanaka, *Tetrahedron Lett.* **1996**, *37*, 4983–4986.

[120] H. Asanuma, T. Takarada, T. Yoshida, D. Tamaru, X. Liang, M. Komiyama, *Angew. Chem. Int. Ed.* **2001**, *40*, 2671–2673.

[121] X. Liang, H. Asanuma, H. Kashida, A. Takasu, T. Sakamoto, G. Kawai, M. Komiyama, *J. Am. Chem. Soc.* **2003**, *125*, 16408–16415.

[122] H. Kashida, K. Murayama, T. Toda, X. Liang, H. Asanuma, *Collect. Symp. Ser.* **2011**, *12*, 116–124.

[123] M. T. Doel, A. S. Jones, N. Taylor, *Tetrahedron Lett.* **1969**, *10*, 2285–2288.

[124] P. Doláková, M. Masojídková, A. Holý, *Nucleos. Nucleot. Nucl.* **2003**, *22*, 2145–2160.

[125] W. Li, J. Li, Y. Wu, N. Fuller, M. A. Markus, *J. Org. Chem.* **2010**, *75*, 1077–1086.

[126] S. Kammer, A. Kelling, H. Baier, W. Mickler, C. Dosche, K. Rurack, A. Kapp, F. Lisdat, H.-J. Holdt, *Eur. J. Inorg. Chem.* **2009**, *2009*, 4648–4659.

[127] R. S. Kumar, S. Arunachalam, V. S. Periasamy, C. P. Preethy, A. Riyasdeen, M. A. Akbarsha, *Eur. J. Med. Chem.* **2008**, *43*, 2082–2091.

[128] S. M. Langenegger, R. Häner, *Helv. Chim. Acta* **2002**, *85*, 3414–3421.

[129] S. M. Langenegger, R. Häner, *Chem. Biodivers.* **2004**, *1*, 259–264.

[130] L. A. Loeb, B. D. Preston, *Annu Rev Genet* **1986**, *20*, 201–230.

[131] J. Lhomme, J. F. Constant, M. Demeunynck, *Biopolymers* **1999**, *52*, 65–83.

[132] S. Smirnov, T. J. Matray, E. T. Kool, C. de los Santos, *Nucleic Acids Res.* **2002**, *30*, 5561–5569.

[133] T. J. Matray, E. T. Kool, *J. Am. Chem. Soc.* **1998**, *120*, 6191–6192.

[134] S. M. Langenegger, R. Häner, *ChemBioChem* **2005**, *6*, 848–851.

[135] A. Sigel, B. P. Operschall, H. Sigel, *J. Biol. Inorg. Chem.* **2014**, *19*, 691–703.

[136] C. H. B. Chen, D. S. Sigman, *J. Am. Chem. Soc.* **1988**, *110*, 6570–6572.

[137] J. Gallagher, C. H. Chen, C. Q. Pan, D. M. Perrin, Y. M. Cho, D. S. Sigman, *Bioconjug. Chem.* **1996**, *7*, 413–420.

[138] S. K. Silverman, *Org. Biomol. Chem.* **2004**, *2*, 2701–2706.

[139] D. Coquière, B. L. Feringa, G. Roelfes, *Angew. Chem. Int. Ed.* **2007**, *46*, 9308–9311.

[140] C. Wang, Y. Li, G. Jia, S. Lu, Y. Liu, C. Li, *Acta Chim. Sin.* **2013**, *71*, 36–39.

[141] J. Oelerich, G. Roelfes, *Chem. Sci.* **2013**, *4*, 2013–2017.

[142] G. Roelfes, A. J. Boersma, B. L. Feringa, *Chem. Commun.* **2006**, 635–637.

[143] N. S. Oltra, G. Roelfes, *Chem. Commun.* **2008**, 6039–6041.

[144] G. Roelfes, B. L. Feringa, *Angew. Chem. Int. Ed.* **2005**, *44*, 3230–3232.

[145] H. S. A. Sigel, *Interplay between Metal Ions and Nucleic Acids*, Springer Science & Business Media, **2012**.

[146] C. Wang, G. Jia, J. Zhou, Y. Li, Y. Liu, S. Lu, C. Li, *Angew. Chem. Int. Ed.* **2012**, *51*, 9352–9355.

[147] M. J. Cavaluzzi, P. N. Borer, *Nucleic Acids Res.* **2004**, *32*, e13.

[148] G. R. Newkome, K. J. Theriot, V. K. Gupta, F. R. Fronczek, G. R. Baker, *J. Org. Chem.* **1989**, *54*, 1766–1769.

[149] F. Ferretti, F. Ragaini, R. Lariccia, E. Gallo, S. Cenini, *Organometallics* **2010**, *29*, 1465–1471.

Acknowledgements

Everything comes to an end. Recalling the past four years in Göttingen, I would like to express my acknowledgements to the following people for their help and support:

First of all, I would like to thank my supervisor Prof. Dr. Ulf Diederichsen for giving me the opportunity to complete my Ph.D. thesis in his research group, for which I am forever grateful. I'd like to thank him for his support and guidance throughout the work of this thesis, for scientific freedom and for the financial support.

I am also grateful for the financial support provided by the *Ministry for Science and Culture of the State of Lower Saxony* within the framework of the Catalysis for Sustainable Synthesis (CaSuS). I also appreciate the interesting lectures that have been held during the workshops.

I would like to thank Prof. Dr. Lutz Ackermann for co-referring this thesis.

I would like to thank all people, with whom I have worked together in the Diederichsen's group, for all their help. Special thanks to my colleagues in Lab. 108 for the nice working atmosphere, past and present, Dr. Tatiana Baranova, Dr. Annika Groschner, Dr. André Nadler, Dr. Stefanie Scholz, Frank Stein, Dominik Herkt, Marta Gascon Moya, Florian Rüping, Ulrike Rost, Hanna Radzey, Dr. Samit Guha, Janine Wegner, Julia Schneider, Dennis Pahlke and Markus Wiegand.

Every beginning is difficult. Special thanks goes for Dr. Oleg Jochim, Dr. Tatiana Baranova and Selda Kabatas for their support in my first year. Thanks for your scientific support and also making my settling-in period a comfortable one.

Special thanks goes for Ulrike Rost, Florian Czerny, Janine Wegner, Hanna Radzey, Muheeb Sadek and Julia Schneider. You have made my stay in Göttingen a creative and memorable one. I shall always remember all the times we spent together. In addition, I am very thankful to Geralin Höger, Anastasiya Myanovska, Dennis Pahlke and Markus Wiegand for all our enjoyable conversations. I thank to Harita Rao and Fernanda Antonia Pereira for their support and friendship. I have really enjoyed the Indian and Brasilian kitchen.

I express my special thanks to Juliane Gräfe, Angela Heinemann, Dr. Hanna Steininger and Aoife Neville for their help in solving various organizational problems.

I express my special thanks to Pawan Kumar, Selda Kabatas, Harita Rao, Janine Wegner, Barbara Hubrich and Aoife Neville for proofreading of this thesis.

Words are too less to express my thanks to Selda Kabatas. Dear Selda, you have always been a very nice colleague and a good friend who is inspiring and motivating. It was really a pleasure knowing you these years and thanks a lot for your help and support.

Finally, I would like to thank my family. I cannot imagine my life without the love from my parents and my brother. Thank you mom and dad for moral and material support and giving me the liberty to choose what I desire.